Reviews in Mineralogy & Geochemistry
Vol. 57, pp. 307-401, 2005

Apatite – An Adaptive Framework Structure

**Tim White, Cristiano Ferraris,
Jean Kim and Srinivasan Madhavi**

*School of Materials Science and Engineering
Nanyang Technological University
N 4.1-01-30, Nanyang Avenue
Singapore 639798*

This chapter was written in commemoration of the 60th anniversary of the publication "The atomic structure of fluor-apatite and its relation to that of tooth and bone material." by CA Beevers and DB McIntyre (1946) Mineralogical Magazine 27:254-257.

INTRODUCTION

Apatite, the most common phosphate mineral, is generally described by the formula $Ca_5(PO_4)_3(OH,F,Cl)$ or, more completely with regard to its usual description in $P6_3/m$ symmetry, by the unit cell content $[Ca_4][Ca_6][(PO_4)_6][OH,F,Cl]_2$. An earlier volume of the *Reviews* series (Kohn et al. 2002) has dealt with the mineralogy and crystallography of apatite *sensu stricto* (Hughes and Rakovan 2002) and the diverse compounds that adopt apatite or apatite-like structures (Pan and Fleet 2002; Huminicki and Hawthorne 2002). In addition, apatite compilations have appeared at regular intervals (Wychoff 1965; McConnell 1973; Nriagu and Moore 1984; Brown and Constantz 1994; Elliott 1994) as the breadth of apatite chemistry has expanded and the level of understanding of its importance with respect to the mineral, materials, environmental, and biological sciences increased. It is not therefore, the purpose of this chapter to restate these excellent reviews, but rather, to focus on microporosity in apatites, a feature which allows ion conduction and exchange, and that is proving to be an important consideration for fashioning synthetic analogues of these minerals in technologically advantageous ways.

The notion of apatite as an industrially significant microporous mineral is not new. In 1944, V. M. Goldschmidt who had studied apatite deposits in Scandinavia and at that time had found refuge from war-ravaged Europe at the Macaulay Institute of Soil Research, Aberdeen (Kauffman 1997; McIntyre 2004) persuaded C. A. Beevers to undertake a new refinement of fluorapatite. The results collected in the seminal paper of Beevers and McIntyre (1946), lead not only to the most accurate crystallographic data available at that time, but also provided the first overview of $[Ca_4][Ca_6][(PO_4)_6][F]_2$, noting that it was composed of CaO_6 columns linked together with PO_4 groups to form "a hexagonal network like a honeycomb with channels extending right through the structure in the *c* direction" (Fig. 1). More generally, it was recognized that the one-dimensional tunnel structure was determined primarily by "the calcium and phosphate arrangement, which is likely to be a strong and stable one." Into these tunnels were inserted the remaining calcium and fluorine. In comparing the hydroxyl and fluorapatites it was observed that OH^-, being slightly larger than F^-, leads to the former structure being expanded compared to the latter. Thus, Beevers and McIntyre identified the three critical elements of the microporous description of apatites namely: (1) the structure can be considered a tunnel structure with walls composed of corner-connected CaO_6 and PO_4 polyhedra as relatively invariant units; (2) filling of these tunnels by Ca and anions (OH, F)

1529-6466/05/0057-0010$10.00 DOI: 10.2138/rmg.2005.57.10

leads to characteristic adjustments that best satisfy bond-length requirements; and (3) even slight changes in the ionic radii of the tunnel atoms lead to expansion or contraction of the tunnel. On this basis, it was surmised that the "very critical fit" of the fluorine and hydroxyl ions was responsible for the greater stability of fluorapatite, consistent with the observation that bone could take up fluorine selectively even from dilute solutions. The possibility of reducing dental caries by increasing fluorine content was thus established and provided the fundamental underpinning for water fluorination technology.

While the microporous description of apatites pioneered by Beevers and McIntyre was largely overlooked for many years, it has become increasingly significant as apatites of various chemistries are investigated for assorted applications in chemical synthesis, clean energy and environmental remediation. For example, the so-called "lacunary" apatites are prospective fuel cell electrolytes, while lead apatites are potential photocatalysts, and radiation resistant phosphate apatites may be useful for retaining nuclear wastes. Although apatites have one-dimensional channels, as distinct from the three-dimensional channels in classic zeolites, they do display several zeolitic features including: a framework which can be tuned to accommodate different tunnel contents; an ability to accept large cations of different valance through the introduction of framework counter ions; and reversible ion exchange for some anions and cations. Fluorapatite can be described formally using microporous nomenclature (McCusker et al. 2001) as

$$| Ca^{II[6]}F^{I[3]} | [Ca^{II[7]}P^{V[4]}O^{II[4]}]_p \{1[4^{12}12^2]\}$$

Unlike zeolites however, completely empty channels have not yet been reported. Most recently, it has been recognized, in both natural and synthetic materials, that intergrowth of tunnels of different size at the nanoscale is possible, a feature with important technology performance implications. This article will focus on the description of apatites as microporous compounds, systematize the correlation of chemistry and tunnel geometry, and summarizes the crystal chemical foundation of several contemporary apatite-based technologies.

DESCRIPTIVE CRYSTALLOGRAPHY

While the general formula for apatites can be written as $[A_4][A_6][(BO_4)_6][X]_2$ the variants $[A_4][A_6][(BO_3)_6][X]_2$ and $[A_4][A_6][(BO_5)_6][X]_2$ occur less commonly (White and Dong 2003). Historically, apatite has generally been regarded as a "difficult" structure from the perspective of descriptive crystallography as, with the exception of the $BO_3/BO_4/BO_5$ units, its polyhedra appear irregular and relationships to other structures including glaserite (Moore and Araki 1977) and perovskite (Dong et al. 2005b) are not obvious. In addition, while many apatites are hexagonal, there is increasing recognition that monoclinic varieties are not unusual (Elliott et al. 1973). Nonetheless, it is well known that in comparing structures and for relating structure to properties, reference to idealized models is invaluable (Andersson 1978). For this reason, several alternate descriptions of apatite have appeared in an effort to make the structure accessible to comparative crystal chemistry.

Stuffed alloy representation

The description of many crystal structures can be simplified by considering the atomic arrangements as anion-stuffed alloy structures (O'Keeffe and Hyde 1985). Apatite is no exception, and the correspondence between the topology of the Ca_5P_3 cation array of $Ca_5(PO_4)_3F$ with the Mn_5Si_3 (D 8_8) alloy type (Wondratschek et al. 1964; Vegas et al. 1991) or Ca_5P_3F with Mo_5Si_3C (Schriewer and Jeitschko 1993) is well known. An illustration of Mn_5Si_3 and fluorapatite $[Ca(1)_4][Ca(2)_6][(PO_4)_6][F]_2$ emphasizing the cation arrangement is shown in Figure 2. The core unit is a $Ca(2)_6$ octahedron which is capped on every edge by

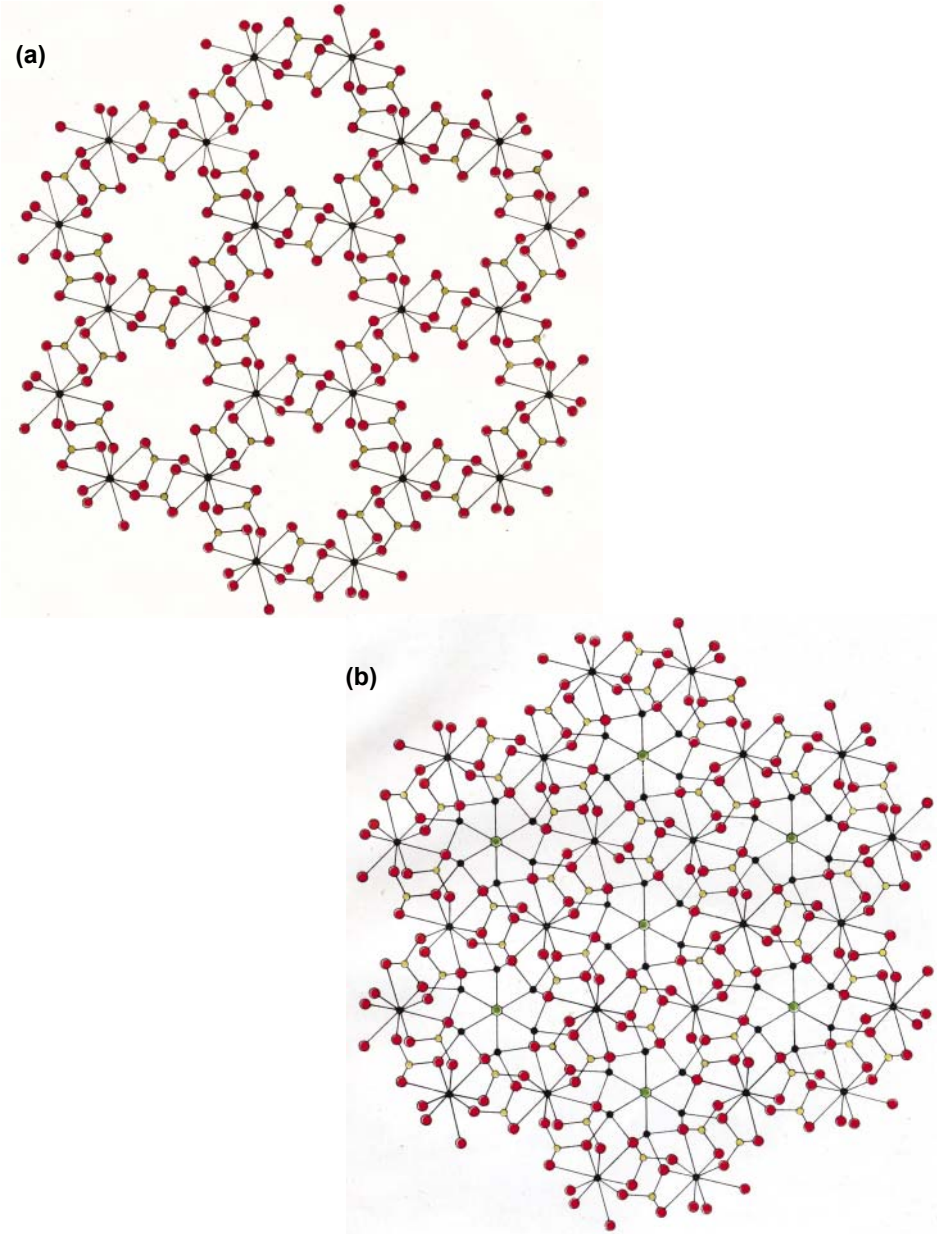

Figure 1. The original color illustrations of fluorapatite as presented by Beevers and McIntyre (1946). In their own words: (a) "[The] linkage of the Ca-O columns by the PO_4 groups produces a hexagonal network like a honeycomb with channels extending right through the structure in the *c*-direction," and (b) "The walls of these channels are lined with oxygen atoms, the arrangement being such that in the wall of each channel there are six 'caves' per unit length. Into these caves calcium atoms will just fit, one Ca going about half-way into each. Thus, about half the area of each Ca is left exposed on the inside of the channels and the F atoms just fit between the group of the three Ca's at one level." [Reproduced with permission of the Mineralogical Society, from Beevers and McIntyre (1946), *Mineralogical Magazine*, Vol. XXVII, Fig. 4 Plate XVII and Fig. 5 Plate XVIII, p. 254-257.]

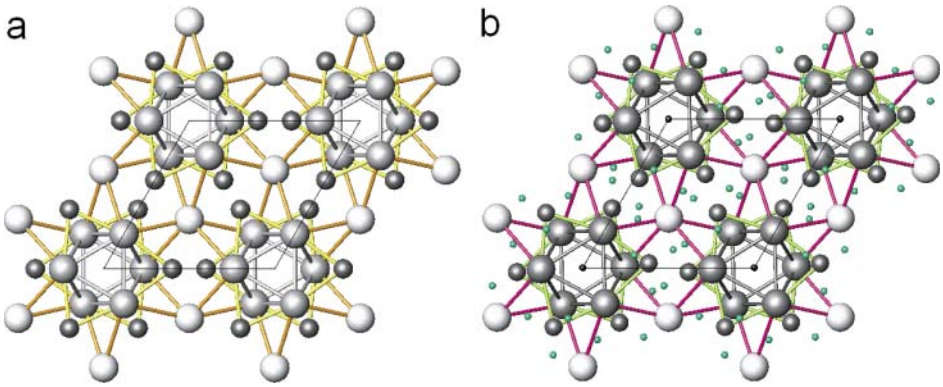

Figure 2. (a) The structure of Mn_5Si_3 emphasizing the Mn_6 octahedra that are capped on every edge by Mn or Si. (b) Fluorapatite represented similarly showing $Ca(1)_4(Ca(2)_6P_6$ capped octahedra with the interstices occupied by oxygen and fluorine.

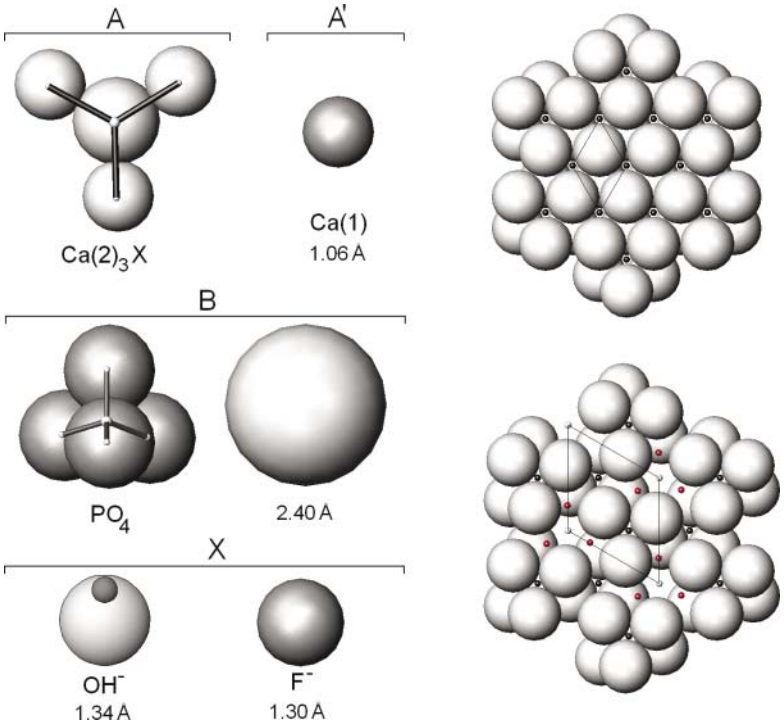

Figure 4. Representation of hydroxyapatite as close packed phosphate "spheres." The PO_4 tetrahedra are simplified as spheres of approximate radius 2.40 Å. Perfect close packing (upper right) is disrupted by the introduction of $Ca(2)_3OH$ units that cause rotation of the spheres (lower right), but the Ca(1) atoms are a better fit to the octahedral phosphate interstices.

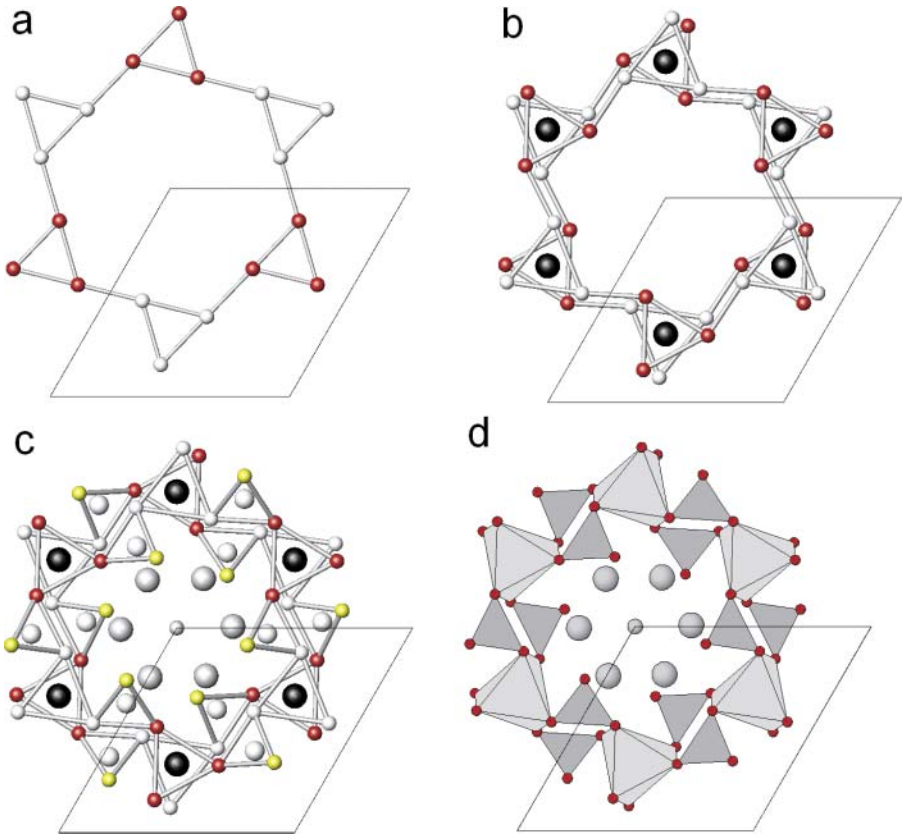

Figure 6. Fluorapatite can be derived by stacking triangular anion nets along *c*. (a) The prototype net of O(1) and O(2) triangles connected through their apices. (b) In fluorapatite alternate triangles are twisted about [001] to create metaprisms that contain Ca(1) atoms. (c) The O(3) atoms are inserted between the O(1)-(2) nets to create the tetrahedral interstices for P. The apatite framework is now complete. Into the tunnel framework Ca(2) and F atoms are introduced, with the twisting between the $O(1)_3$ and $O(2)_3$ triangles adjusted to best accommodate the $Ca(2)O_6F$ co-ordination sphere. (d) The structure, in polyhedral representation, emphasizing the $Ca(1)O_6$ metaprisms and PO_4 tetrahedra.

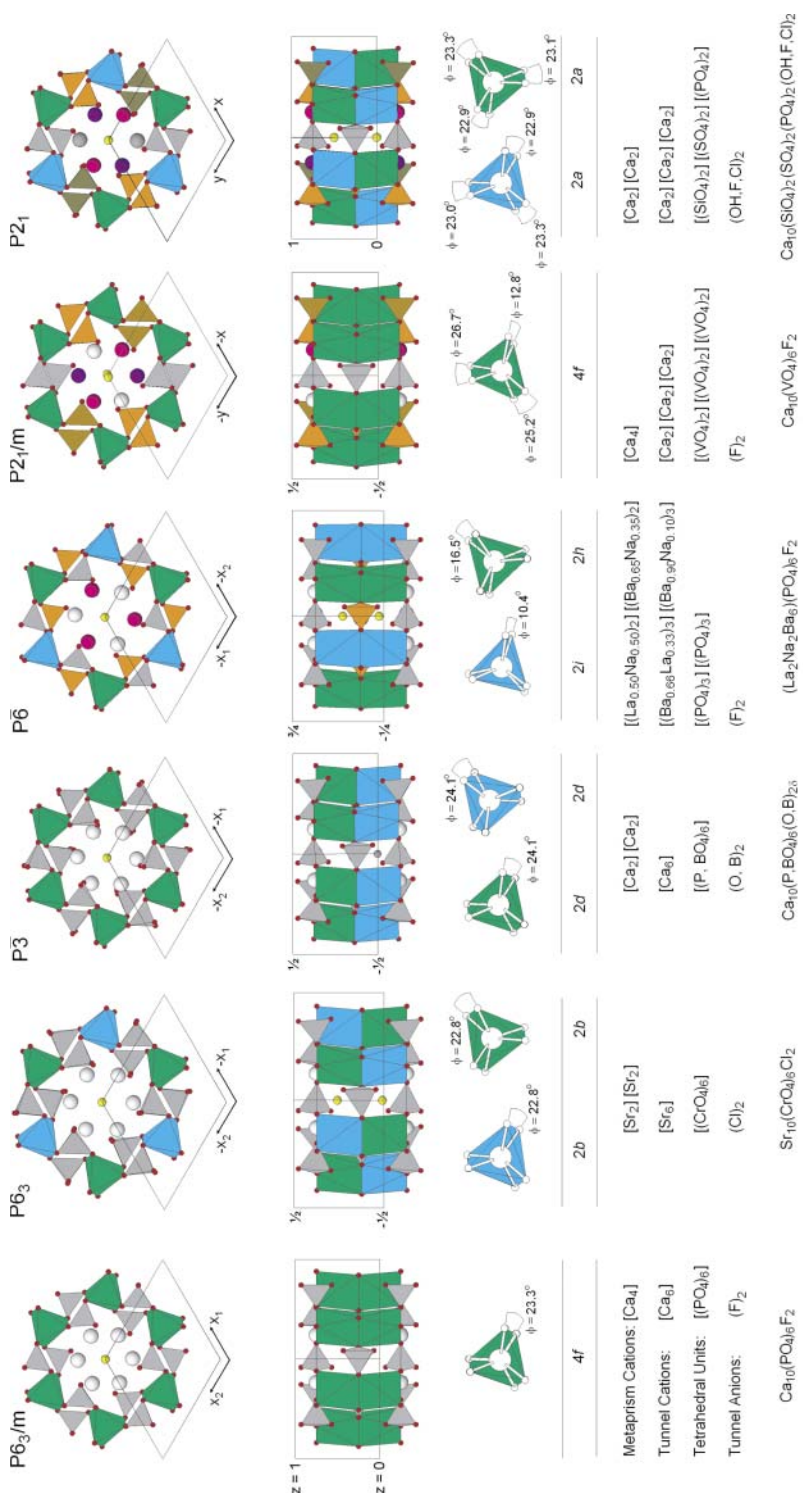

	4*f*	2*b*	2*b*	2*d*	2*d*	2*i*	2*h*	4*f*	2*a*	2*a*
Metaprism Cations:	$[Ca_4]$	$[Sr_2][Sr_2]$		$[Ca_2][Ca_2]$		$[(La_{0.50}Na_{0.50})_2][(Ba_{0.65}Na_{0.35})_2]$	$[Ca_4]$		$[Ca_2][Ca_2]$	
Tunnel Cations:	$[Ca_6]$	$[Sr_6]$		$[Ca_6]$		$[(Ba_{0.66}La_{0.33})_3][(Ba_{0.90}Na_{0.10})_3]$	$[Ca_2][Ca_2][Ca_2]$		$[Ca_2][Ca_2][Ca_2]$	
Tetrahedral Units:	$[(PO_4)_6]$	$[(CrO_4)_6]$		$[(P,BO_4)_6]$		$[(PO_4)_3][(PO_4)_3]$		$[(VO_4)_2][(VO_4)_2][(VO_4)_2]$		$[(SiO_4)_2][(SiO_4)_2][(PO_4)_2]$
Tunnel Anions:	$(F)_2$	$(Cl)_2$		$(O,B)_2$		$(F)_2$		$(F)_2$		$(OH,F,Cl)_2$
	$Ca_{10}(PO_4)_6F_2$	$Sr_{10}(CrO_4)_6Cl_2$		$Ca_{10}(P,BO_4)_6(O,B)_{2\delta}$		$(La_2Na_2Ba_6)(PO_4)_6F_2$		$Ca_{10}(VO_4)_6F_2$		$Ca_{10}(SiO_4)_2(SO_4)_2(PO_4)_2(OH,F,Cl)_2$

Figure 14. Polyhedral drawings of representative apatites in the six principle apatite space groups emphasizing the cation ordering schemes of the AO_6 metaprisms and BO_4 tetrahedra. In passing from $P6_3/m$ to $P2_1$, the number of unique cation acceptors sites increases to accommodate more complex chemistries or less symmetrical polyhedral distortions. For all symmetries, the metaprism twist angle can be used as a measure of tunnel expansion or collapse as a function of its content. In the case of the monoclinic apatites, the metaprisms have three distinct twist angles; however, their average is a suitable proxy for the single values observed at higher symmetries when investigating crystal chemical trends.

Ca(1) or P (Nyman and Andersson 1979). The entire construction is completed by joining these $Ca(1)_4Ca(2)_6P_6$ capped octahedra through their faces along [001] and by the Ca(1) apices in (001). The anions (oxygen and fluorine) are then introduced into the interstices between the cations. While the positions of the anions are variable, those of the cations are essentially fixed, although there is slight rotation of P as compared to Si about [001].

The equivalence of alloy cation arrays and apatite oxides has been explored in detail by Vegas and Jansen (2002) who compiled a list of 14 corresponding intermetallic and apatite structures (Table 1). A further advantage of the stuffed alloy description is that the D 8_8 alloy structure having $P6_3/mcm$ symmetry may be taken as the aristotype of the apatite family, with all other members adopting maximal non-isomorphic subgroups as shown in Figure 3.*

Table 1. Equivalency between apatite cation lattices and known alloys [after Vegas and Jansen 2002)].

Apatite-like Compounds	*Cation Array*	*Alloy Equivalent*
$Ca_5(AsO_4)_3Cl$	Ca_5As_3	Ca_5As_3
$Sr_5(AsO_4)_3Cl$	Sr_5As_3	Sr_5As_3
$Ba_5(AsO_4)_3Cl$	Ba_5As_3	Ba_5As_3
$Ba_5(AsO_4)_2(SO_4)S$	Ba_5As_2S	Ba_5As_3
$Y_5(SiO_4)_3N$	Y_5Si_3	Y_5Si_3
$CaNd_4(SiO_4)_3O$	$CaNd_4Si_3$	Nd_5Si_3
$CdNd_4(SiO_4)_3O$	$CdNd_4Si_3$	Nd_5Si_3
$La_{4.67}(SiO_4)_3O$	$La_{4.67}Si_3$	La_5Si_3
$CaLa_4(SiO_4)_3O$	$CaLa_4Si_3$	La_5Si_3
$Ce_{4.67}(SiO_4)_3O$	$Ce_{4.67}Si_3$	Ce_5Si_3
$Sm_{4.67}(SiO_4)_3O$	$Sm_{4.67}Si_3$	Sm_5Si_3
$MnSm_4(SiO_4)_3O$	$MnSm_4Si_3$	Sm_5Si_3
$Gd_{4.67}(SiO_4)_3O$	$Gd_{4.67}Si_3$	Gd_5Si_3
$Dy_{4.67}(SiO_4)_3O$	$Dy_{4.67}Si_3$	Dy_5Si_3

Close-packed metalloid units

Another simplification was developed by Elliott (1973) who considered that, to a first approximation, the structure of hydroxyapatite could be conveyed by considering the PO_4^{3-} radicals as spheres (diameter ~2.40 Å) arranged in hexagonal close packing (*hcp*), with interstitial insertion of the remaining cations and anions (Fig. 4: color figure on page 310). The basis for this approach was that in *hcp* continuous channels are formed along [001] (as in apatite) into which Ca(1) may be inserted to form the columns noted earlier, while OH and Ca(2) jointly occupy the remaining channels. Thus, in an ideal *hcp* compound $A_3B_3 \equiv [A][A']_2[B]_3$ where A and A′ are interstitials and B are the close-packed components, the equivalent description for $Ca_5(PO_4)_3(OH)$ hydroxyapatite will be $[Ca(2)_3(OH)][Ca(1)]_2[PO_4]_3$.

Introduction of ions [Ca(1)] and ionic entities $[Ca(2)_3(OH)]$ in the channels leads to the phosphate ions no longer being close packed. However, while Ca(1) is a near fit to the

* It should be noted that the non-isomorphic subgroups do not include $P2_1/b$ that has been assigned to chlorapatite (Mackie et al. 1972) amongst others. This is because $P6_3/m$ symmetry is broken by the need to accommodate order correlation of chlorine and X-anion vacancies between apatite channels. Such structures are perhaps best considered intergrowths of commensurate and incommensurate lattices (Alberius-Henning et al. 1999b).

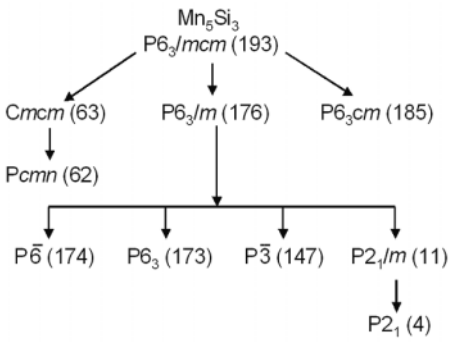

Figure 3. Symmetry relationships of apatite hettotypes derived from the Mn_5Si_3 aristotype. [Used with permission of the International Union of Crystallography (http://journals.iucr.org/) from White and Dong (2003) *Acta Crystallographica*, Vol. B59, Fig. 3, p. 3.]

octahedral phosphate interstice, $Ca(2)_3OH$ can only be accommodated through rotation of the $Ca(1)(PO_4)_6$ columns (Fig. 4). It then becomes apparent that the *a* lattice constant will be determined by the extent of rotation of the columns, but the *c* constant will be determined by the size of the A interstitial. Consequently, and as observed experimentally, variation in the *c*/*a* ratio is primarily controlled by contraction and dilation of *a* in response to the effective size of the A component. Following this logic it is possible to use the cell constants of cadmium, calcium, strontium and lead fluor-, hydroxy, chlor- and brom-apatites to extrapolate to the *c*/*a* ratio of a hypothetical material containing an X anion of zero radius as shown in Figure 5, leading to values of 0.806–0.831, which bracket the ideal geometrical ratio of 1.633/2 = 0.817. Because the X anion is not the only disrupting influence of perfect phosphate close-packing the approach to *hcp* by back-extrapolation is also limited by the size of the A(2) cation, as evidenced by the reduction in slope, and poorer packing in the X = 0 limit, in passing from smaller cadmium to larger lead. In addition, the recognition that phosphate (or indeed any BO_4 unit) is an intrinsically stable entity in apatite allows other crystal chemical observations to be readily explained, including the fact that non-disruptive X ion exchange in single crystal material is commonly observed.

Derivation from triangular anion nets

While many workers have noted the "irregularity" of the anion arrangement in apatites and the difficulty in describing the structure using cation-centered polyhedra, it is feasible, following from the idealized representation of Povarennykh (1972) to derive a prototype from a triangular network of oxygen. In this method, the starting point are regular anion triangles [O(1) and O(2) in $P6_3/m$ fluorapatite] connected through a single vertex as shown in Figure 6a (color figure on page 311). These layers occur at z = ¼ and ¾ but in real apatites do not superimpose in the [001] projection precisely. Rather, in each layer, alternate oxygen triangles twist slightly in (001) to produce interstices in which A(1) atoms reside at z = 0 and ½ (Fig. 6b). Tetrahedral interstices are formed by the introduction of O(3) atoms above and below the O(1) + O(2) layers that accommodate B cations at z = ¼ and ¾. The tunnel structure is now evident. Finally, A(2) and X atoms are introduced (Fig. 6c). Depiction of this model in polyhedral terms (Fig. 6d) highlights the corner connectedness of the metaprisms and tetrahedra, and the location of relatively more mobile and reactive tunnel species, reminiscent of the description by Beevers and McIntyre (1946). Several corollaries follow from this derivation.

First, if apatites are derived from triangular networks through twisting the O(1) and O(2) triangles to produce metaprisms, it is then possible to conceive of two possible prototypes. In one, the rotation between triangles in successive layers is 0° yielding an idealized structure containing $A(1)O_6$ trigonal prisms, while in the second, the rotation is set at 60° that generates $A(1)O_6$ octahedra (Fig. 7). The intermediate structure with a rotation of 30° generates an $A(1)O_6$ metaprism (a polyhedron intermediate between a trigonal prism and an octahedron) and a structure clearly resembling fluorapatite (Fig. 6d). Second, as the tunnel walls are defined by the shortest, and therefore strongest, metal-oxygen bond lengths their integrity is maintained throughout. It is also apparent that the tunnel volume is largest and smallest when

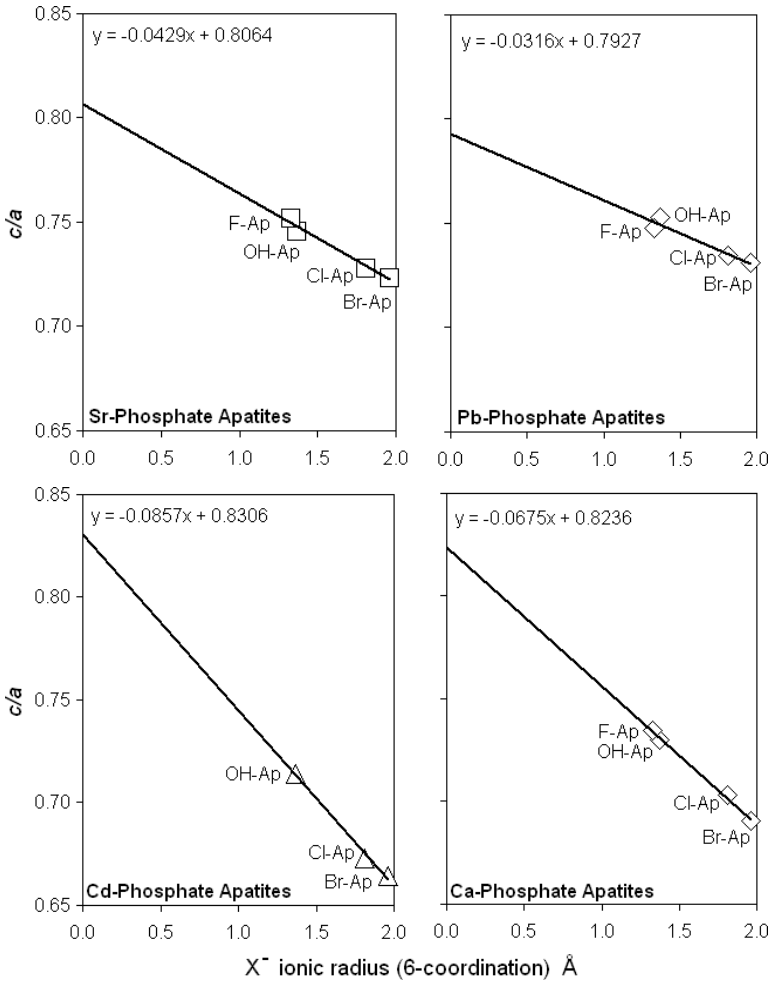

Figure 5. Based upon the closest packing phosphate model, back extrapolation to a hypothetical apatite containing no X anions leads to *c/a* ratios close to the theoretical value of 0.817. Apatites with larger A cations such as lead remain slightly expanded even with complete "removal" of the X atoms.

the rotation angles are 0° and 60° respectively. Finally, because metaprism rotation controls tunnel diameter, adjustments can be made spontaneously in response to changes in chemistry and tunnel filling.

Formally, the deviation of apatites from the prototypes can be described by a single parameter—the metaprism twist angle (ϕ)—which is defined as the (001) projected angle of O(layer 1)-A-O(layer 2). The degree of twist is controlled by the relative sizes of the wall and tunnel atoms, which in turn is related to chemistry. For example, in the simple chemical series $Cd_{10}(PO_4)_6(OH)_2$, $Cd_{10}(PO_4)_6Cl_2$ and $Cd_{10}(PO_4)_6Br_2$, ϕ becomes progressively more acute as the tunnel expands to accommodate the larger X anion (Fig. 8). While this trend illustrates the essential capacity of the twist angle to monitor apatite crystal chemistry, it is also evident that even in compositionally complex apatites ϕ can be an exquisitely sensitive probe for the detection of unexpected departures from stoichiometry or thermodynamic equilibrium.

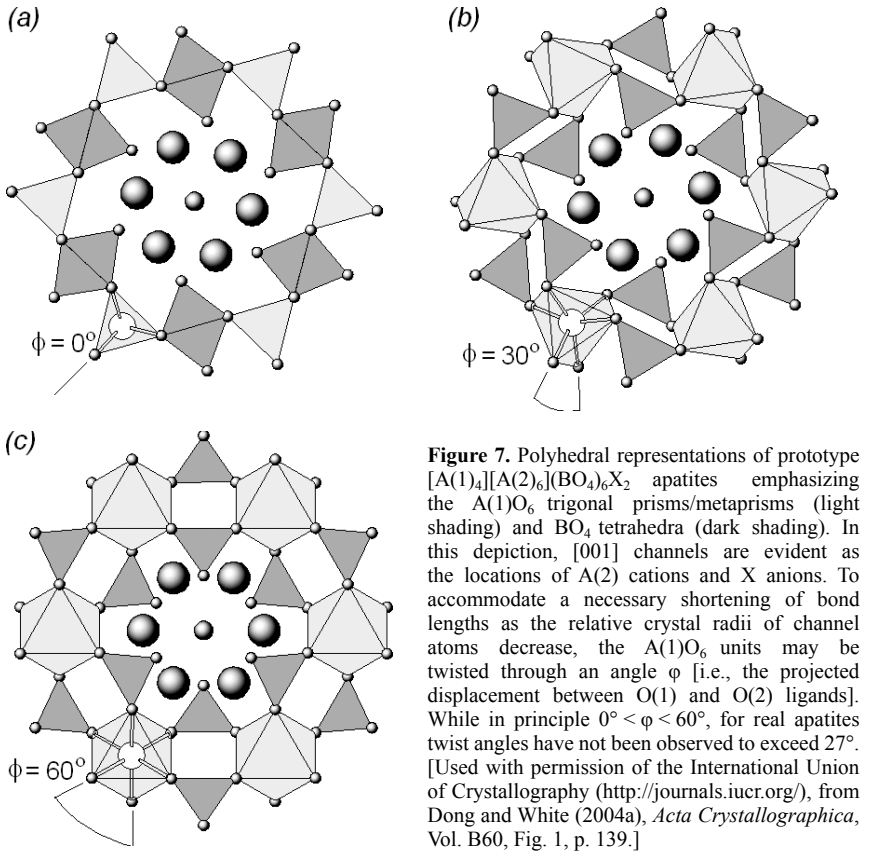

Figure 7. Polyhedral representations of prototype $[A(1)_4][A(2)_6](BO_4)_6X_2$ apatites emphasizing the $A(1)O_6$ trigonal prisms/metaprisms (light shading) and BO_4 tetrahedra (dark shading). In this depiction, [001] channels are evident as the locations of A(2) cations and X anions. To accommodate a necessary shortening of bond lengths as the relative crystal radii of channel atoms decrease, the $A(1)O_6$ units may be twisted through an angle φ [i.e., the projected displacement between O(1) and O(2) ligands]. While in principle $0° < \varphi < 60°$, for real apatites twist angles have not been observed to exceed 27°. [Used with permission of the International Union of Crystallography (http://journals.iucr.org/), from Dong and White (2004a), *Acta Crystallographica*, Vol. B60, Fig. 1, p. 139.]

CRYSTAL CHEMICAL SYSTEMATICS

It has been long known that attempting a systematic consideration of apatite crystal chemistry from literature data is problematical due to incomplete crystallographic and compositional characterization of materials. In this regard, the critical remarks of Felsche (1972) and McConnell (1973) remain germane to the present day. Essentially the difficulty of seeking a methodical arrangement of data arises from three potential sources of error:

1. *Composition*: It is generally true that even in contemporary crystallographic determinations and refinements independent verification of crystal composition is not undertaken. While misinterpretation is less likely in single crystal studies, modern research is often reliant on powder methods, particularly Rietveld analysis, as large single crystals are unavailable. However, poor agreement has been observed where chemical analyses and refined occupancies are compared (e.g., Wilson et al. 2003; Dong et al. 2005a).
2. *Equilibration*: There are often quite substantial discrepancies in the unit cell constants of apatites with the same nominal composition. Aside from the issue of bulk composition, the cell parameters will be influenced by cation partitioning over the available crystallographic sites. Moreover, even in moderately complex apatites the approach to equilibrium may require several weeks annealing close to the solidus (Dong and White 2004a).

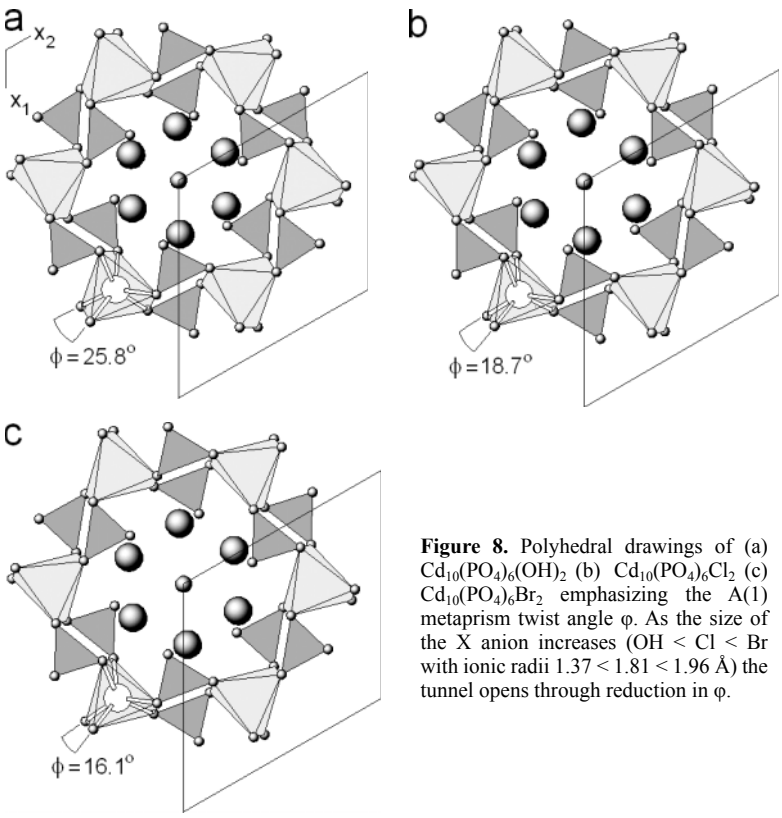

Figure 8. Polyhedral drawings of (a) $Cd_{10}(PO_4)_6(OH)_2$ (b) $Cd_{10}(PO_4)_6Cl_2$ (c) $Cd_{10}(PO_4)_6Br_2$ emphasizing the A(1) metaprism twist angle φ. As the size of the X anion increases (OH < Cl < Br with ionic radii 1.37 < 1.81 < 1.96 Å) the tunnel opens through reduction in φ.

3. *Partitioning*: Without the benefit of complete structure refinement, neither the distribution of atoms over cation acceptor sites, nor the confirmation of space group is possible. While the majority of apatites have been assigned $P6_3/m$, reports of lower symmetry analogues whose formation is intimately linked to composition and equilibration are becoming more common.

It is with these caveats that the following discussion should be considered. While a comprehensive data set has been assembled (Appendix A), the quality of individual entries will vary, however it is anticipated that the general trends synthesized below will nonetheless remain valid. In certain instances, materials subsets are considered in detail to demonstrate methods for detecting less reliable crystallographic refinements.

X anion ordering

The structural feature of apatites that has been most thoroughly, and reliably, studied has been the location of the X anion as a function of its size with respect to the surrounding A(2) cations (e.g., Mackie et al. 1972; Hata et al. 1979; Hashimoto and Matsumoto 1998; Kim et al. 2000). In the case of $Ca_{10}(PO_4)_6F_2$ the fluorine neatly fits within a $Ca(2)_3$ triangle, but substitution by OH^-, Cl^- and Br^- leads to consecutively greater displacements out of the triangular plane. In $P6_3/m$ this displacement leads to degeneracy of the 2*a* (0, 0, ¼) position as it splits into 4*e* (0, 0, *z*) symmetry to accommodate filled and vacant interstices. While the distribution of larger anions is often regarded as statistical, it has been observed that equilibrated materials or minerals can exhibit ordering both along and between anion-vacancy strings in the tunnels

to yield superstructures. For example, Bauer and Klee (1993) have shown that chlorapatite $Ca_{10}(PO_4)_6Cl_2$ can adopt $P2_1/b$ symmetry and a doubled *b*-axis (a = 9.643 Å, b = 19.279 Å, c = 6.766 Å, γ = 120.01°). More complex incommensurate ordering schemes have also been identified. In $Cd_{10}(PO_4)_6Br_2$, an incommensurate superstructure (R: P-3(00γ) a = 16.932 Å, b = 16.932 Å, c = 6.451 Å) has been reported with modulation wave vector $\mathbf{q} = 0.778\mathbf{c}^*$ (Alberius-Henning et al. 2000). The germanate $La_{9.33}(GeO_4)_6O_2$ has $\mathbf{q} = 1.6\text{-}1.7\mathbf{c}^*$ (Berastegui et al. 2002), and the instances of long range X-site ordering are being reported more frequently.

Correlation of cell parameters and ionic radii

A general classification of the fluor- and chlorapatites and their stability fields as a function of A and B cation radii was devised by Kreidler and Hummel (1970). The principles set out remain essentially correct; metalloids can adopt 4+, 5+ and 6+ valence states and have sizes ranging from S^{6+} (0.12 Å) to V^{5+} (0.355 Å) with appropriate charge compensation by A^+/A^{2+} cations with radii from Cd^{2+} (1.03 Å) to Ba^{2+} (1.38 Å). For larger metalloids (i.e., V and As) monoclinic symmetry may be favored. However, end members containing Al^{3+}, Sb^{5+}, W^{6+}, Mo^{6+}, Ta^{5+} and Nb^{5+} are not stable. Since this early work, it has been established that limited substitution of many of these metalloids is possible. The major outstanding question at that time was the possible role of manganese, but it has now been demonstrated unequivocally from single crystal studies that manganese can be accommodated in either the A or B site, and $Mn_{10}(PO_4)_6Cl_{1.8}(OH)_{0.2}$ (Engel et al. 1975b) and $Ba_{10}(MnO_4)_6Cl_2$ (Reinen et al. 1986) have been prepared.

Ito (1968) conducted an investigation of remarkable scope for the $A_4REE_6(SiO_4)_6(OH)_2$ hydroxy- and $A_4REE_6(SiO_4)_6O_2$ oxy-silicate apatites with A = Mn, Ca, Sr and Pb, the results of which are summarized in Figure 9. An underlying assumption of these formulations is that the smaller A(1) sites will be filled almost entirely by the divalent cation, or at least, the A(1)/A(2) partitioning remains constant across REE compositional series. While this is certainly true for larger REEs such as La, Ce and Nd (Schroeder and Matthew 1978; Fahey et al. 1985; Skakle et al. 2000) it is likely that smaller REEs will partition more strongly to the A(1) site. Consequently, while for the most part the apatite lattices expanded linearly as a function of ionic radii, it is evident that for the $Ca_4REE_6(SiO_4)_6(OH)_2$ and $Mn_4REE_6(SiO_4)_6O_2$ series two distinct linear segments are present, with the discontinuity appearing for REE < Dy, possibly arising because smaller REEs are similar in size to Ca and Mn, leading to mixing over the A(1) and A(2) sites, and therefore a change in the cell constant.

An alternative method to systematize the lattice constants of hexagonal apatites is to examine the cell volume versus the c/a ratio when the A cation is fixed and only (non-silicate) BO_4 and X components are varied (Fig. 10). While there is a considerable spread of data for the calcium apatites, clear trends appear for the strontium, lead and barium apatites. In these cases, gradual incorporation of larger metalloids and halides leads first to an increase in c/a while at larger cell volumes this ratio decreases.

Classification by metaprism twist angle (φ)

The derivation of apatites from a prototype, and in particular the relationship between metaprism twist angle (ϕ) and composition, provides the basis for examining crystal chemical systematics in a more general sense. It has been shown previously that for a fixed A cation, ϕ varies inversely with the average effective ionic radius of the unit cell (White and Dong 2003) because filling of the microporous channels with larger atoms is accommodated by a reduction of twist angle to increase its volume (Table 2, Fig. 11). The rate of change of ϕ is greatest for the smallest A cation (Cd^{2+}) and slowest for the largest (Ba^{2+}) as the channel diameter is already enlarged in latter instance. Twist angle outliers are evident for the Pb- and Ba-apatites, and this data may indicate that these compounds deviate from the reported composition.

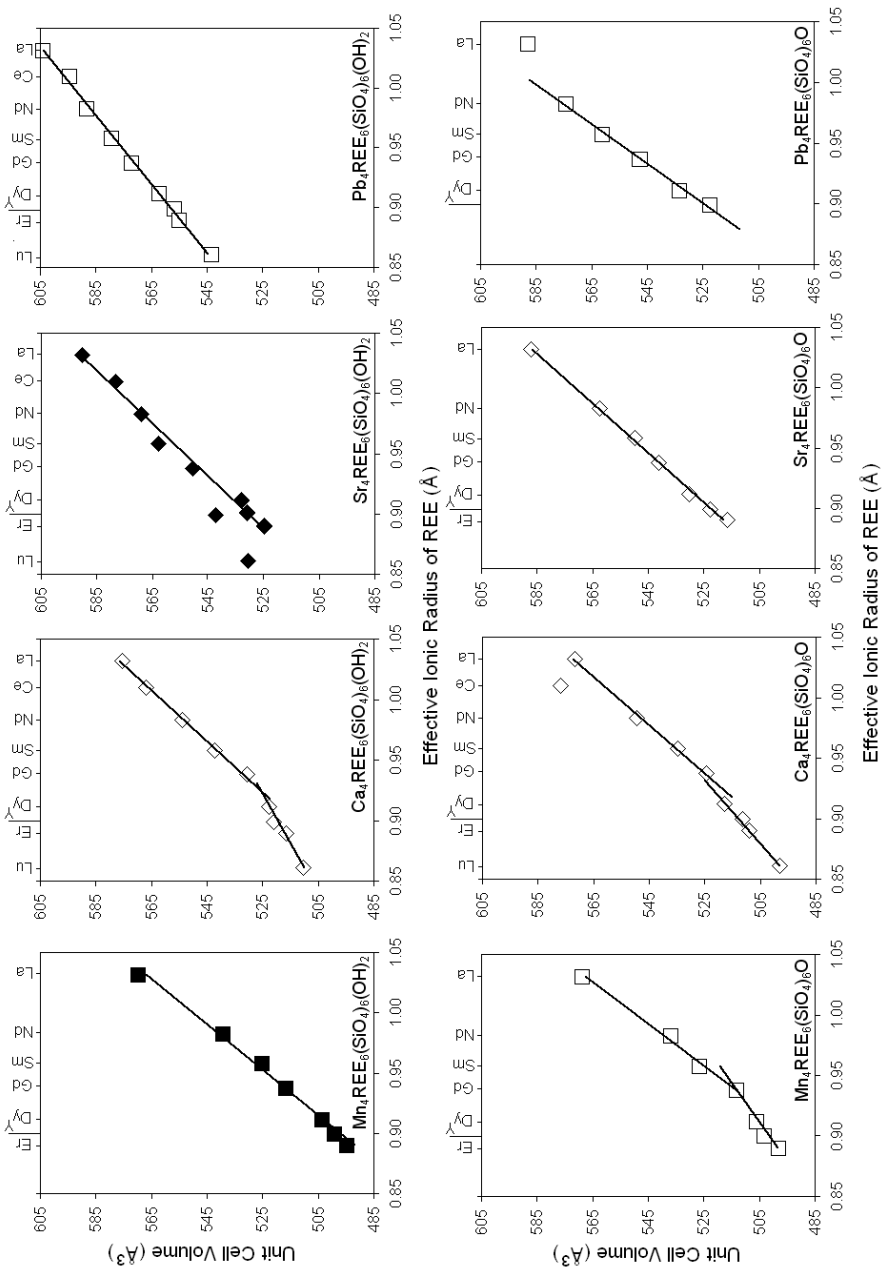

Figure 9. Trends in unit cell volume for $A_4REE_6(SiO_4)_6(OH)_2$ and$A_4REE_6(SiO_4)_6O_2$ apatites with A = Mn, Ca, Sr, Pb [unit cell data from Ito (1968)].

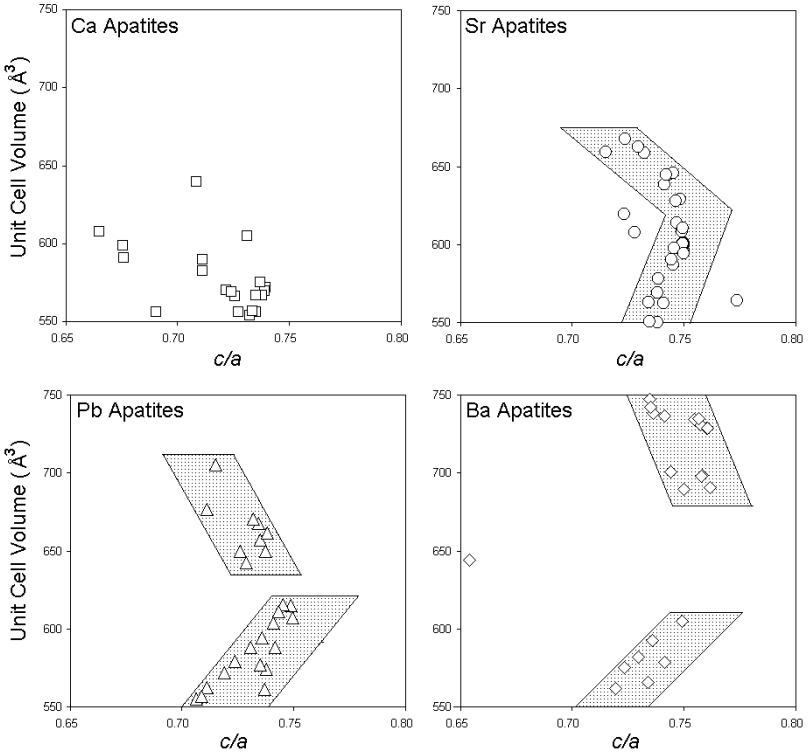

Figure 10. Trends in unit cell volume for $Ca_{10}(BO_4)_6X_2$, $Sr_{10}(BO_4)_6X_2$, $Pb_{10}(BO_4)_6X_2$, and $Ba_{10}(BO_4)_6X_2$ apatites using data for $P6_3/m$ phases extracted from Appendix A.

In apatite solid solution series, trends in twist angle can be used to establish the reliability of crystallographic data, which may be compromised due to disequilibrium effects, or in the case of powder diffraction data, refinement to false minima. For example, the compounds $Ca_{10-x}Pb_x(PO_4)_6Br_2$ were prepared by solid state reaction of the calcium and lead members by heating for 15 h at 850°C (Kim 2001), and the products characterized by Rietveld co-refinement of X-ray and neutron data (Table 3). It would be expected that in passing from the calcium to lead end member ϕ should decrease, with larger Pb^{2+} occupying the A(2) tunnels sites partially accommodated through a reduction in metaprism twist angle. However, while there is a slight downward trend in ϕ from $x = 0$ to 9.53, the values are quite variable, with ϕ for $x = 10$ increasing dramatically to 20.6°. These data are explicable in terms of disequilibrium and compositional changes. Assuming that the single crystal determinations for $Ca_{10}(PO_4)_6Br_2$ (Elliott et al. 1981), $Pb_{10}(PO_4)_6(OH)_2$ (Barinova et al. 1998), and $Ca_{10}(PO_4)_6(OH)_2$ (Kay et al. 1964) are reliable, trend lines can be drawn as shown in Figure 12 that relate ϕ to composition (Table 4). The data of Kim (2001) may be superimposed on this and interpreted in three segments.

For $x < 3$, ϕ lies above the $Ca_{10}(PO_4)_6Br_2$ - $Pb_{10}(PO_4)_6Br_2$ trend line consistent with an enrichment of Pb in the A(1) position and the loss of bromine and its replacement by oxygen.

For $3 < x < 9$, ϕ's lie between the $Ca_{10}(PO_4)_6Br_2$ - $Pb_{10}(PO_4)_6Br_2$ and $Ca_{10}(PO_4)_6Br_2$ - $Pb_{10}(PO_4)_6(OH)_2$ trends consistent with partial oxidation of the bromo-apatites, and as shown by the lead partitioning coefficient, incomplete equilibration of Ca/Pb separation over the A(1) and A(2) sites.

Table 2. Correlation of metaprism twist angle and average effective ionic radius.

Apatite	*Average Radius* (Å)	*Twist Angle* (°)
$Ca_{10}(PO_4)_2F_2$	1.143	23.3
$Ca_{10}(PO_4)_6(OH)_2$	1.146	23.2
$Ca_{10}(PO_4)_6Cl_2$	1.166	19.1
$Ca_{10}(CrO_4)_6(OH)_2$	1.171	17.8
$Ca_{10}(PO_4)_6Br_2$	1.173	16.3
$Ca_{10}(AsO_4)_6Cl_2$	1.189	13.0
$Ca_4Pb_6(AsO_4)_6Cl_2$	1.214	5.2
$Cd_{10}(PO_4)_6(OH)_2$	1.139	25.8
$Cd_{10}(PO_4)_6Cl_2$	1.158	19.5
$Cd_{10}(PO_4)_6Br_2$	1.165	16.0
$Cd_{10}(AsO_4)_6Br_2$	1.189	11.6
$Cd_{10}(VO_4)_6Br_2$	1.192	8.8
$Cd_{10}(VO_4)_6I_2$	1.203	8.4
$Sr_{10}(PO_4)_6F_2$	1.180	24.3
$Sr_{10}(PO_4)_6(OH)_2$	1.183	23.0
$Sr_{10}(PO_4)_6Cl_2$	1.203	21.1
$Sr_{10}(PO_4)_6Br_2$	1.210	19.6
$Pb_6(PO_4)_2$	1.122	27.3
$Pb_{10}(PO_4)_6(OH)_2$	1.189	26.7
$Pb_{10}(GeO_4)_2(CrO_4)$	1.151	25.8
$Pb_{10}(PO_4)_6F_2$	1.185	23.5
$Pb_{10}(PO_4)_6Cl_2$	1.208	17.6
$Pb_{10}(VO_4)_6Cl_2$	1.235	17.5
$Pb_{10}(VO_4)_6I_2$	1.253	16.7
$Pb_{10}(AsO_4)_6Cl_2$	1.232	5.2
$Ba_{10}(PO_4)_6F_2$	1.219	22.5
$Ba_{10}(MnO_4)_6Cl_2$	1.254	22.3
$Ba_{10}(PO_4)_6(OH)_2$	1.222	22.2
$Ba_{10}(PO_4)_6Cl_2$	1.242	21.0
$Ba_{10}(AsO_4)_4(SO_4)_2S$	1.259	16.2

For $x = 10$, ϕ is unexpectedly high probably as a result of substantial Br loss, and consequently its twist angle is close to that determined for $Pb_{10}(PO_4)_6(OH)_2$. Furthermore, the difference in ϕ for $Pb_{10}(PO_4)_6(OH)_2$ in the determinations of Barinova et al. (1998) and Brückner et al. (1995) may arise from the partial loss of oxygen in the latter material, and its approach to $Pb_9(PO_4)_6$ stoichiometry. Inspection of Brückner et al.'s refined powder X-ray diffraction data reports large isotropic thermal parameters ($B = 1.85$ Å^2) for lead that could also be consistent with vacancies.

In passing from $Ca_{10}(PO_4)_6(OH)_2$ to $Pb_{10}(PO_4)_6(OH)_2$ ϕ decreases from 23.2° to 22.1°, thus it follows that as the reliable determination for ϕ in $Ca_{10}(PO_4)_6Br_2$ is 14.8°, the stoichiometric end member $Pb_{10}(PO_4)_6Br_2$ is predicted to adopt a metaprism twist angle close to 13.7° (Table 4). In this respect, the near end member of Kim (2001) with $x = 9.5$ is of particular interest as it refines to a nearly ideal $k_{Pb} = 0.62$, and has apparently suffered only a small loss of Br, leading to $\phi = 14°$ for this material.

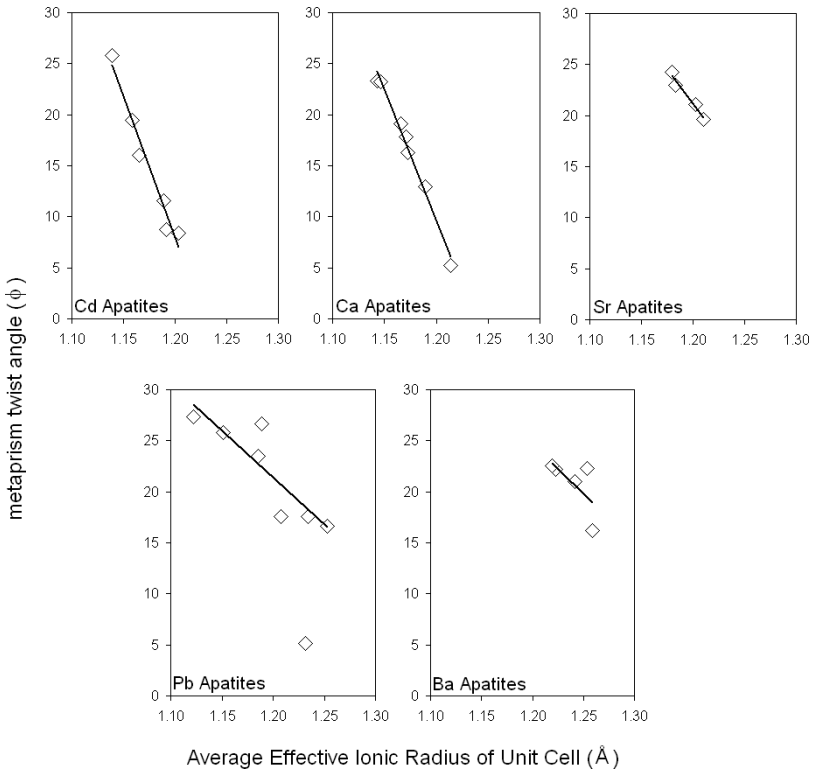

Figure 11. Trends in metaprism twist angle φ for $Cd_{10}(BO_4)_6X_2$, $Ca_{10}(BO_4)_6X_2$, $Sr_{10}(BO_4)_6X_2$, $Pb_{10}(BO_4)_6X_2$ and $Ba_{10}(BO_4)_6X_2$ apatites as a function of average effective ionic radius for the whole unit cell contents using data extracted from Table 2.

Prediction of cell parameters

As apatite topology can be modified by twisting regular triangular nets, and the $A(1)O_6$ and BO_4 polyhedra are corner connected, it is feasible to predict and model the relative changes in unit cell parameters as a function of experimentally derived ϕ's. From a purely geometrical consideration, and using the construction shown in Figure 13, it has been shown by Dong and White (2004b) that the basal unit cell dimension a is related to ϕ and the equilateral triangle edge t such that

$$a = t\sqrt{13 - 28\sin^2\left(\frac{\phi}{4}\right) + 16\sin^4\left(\frac{\phi}{4}\right)}$$

where t is a scaling parameter specific to each apatite system. For example, $t = 2.729 + 0.017x$ and x is the stoichiometry in $(Pb_xCa_{10-x})(VO_4)_6(F_{2-2y}O_y)$. The compositional adjustment factor for t is derived from the increase in ionic radii for Ca^{2+} (IR = 1.18 Å) and Pb^{2+} (IR = 1.35 Å) divided by total A-cation formula content, i.e., (1.35−1.18)/10 = 0.017 Å.

Similarly, the c cell parameter can be related to ϕ as

$$c = 2\sqrt{h^2_{\phi=0} - \frac{4t^2}{3}\sin^2\left(\frac{\phi}{2}\right)}$$

Table 3. Co-refined synchrotron X-ray and neutron data at for $Ca_{10-x}Pb_x(PO_4)_6Br_2$, $0 \le x \le 10$ apatites. [from Kim 2001].

			x = 0	*0.9*	*2.9*	*5.0*	*7.4*	*9.2*	*9.5*	*10*
a (Å)			9.7682(6)	9.7823(5)	9.8452(3)	9.9071(3)	9.9708(2)	10.0116(4)	10.0356(2)	10.0618(3)
c (Å)			6.7388(2)	6.7485(3)	6.8596(4)	7.0086(5)	7.1682(3)	7.2662(3)	7.3203(3)	7.3592(1)
Ca(I), Pb(I)†	z	4*f* (⅓, ⅔, 0)	0.0063(6)	0.0059(4)	0.010(5)	0.0075(3)	0.0066(5)	0.0059(4)	0.0069(2)	0.0067(3)
	B(Å2)		0.3(3)*	0.3(1)*	0.5(3)*	0.5(4)*	0.3(2)*	0.4(5)*	0.3(1)*	0.3(1)*
Ca(II), Pb(II)†	x	6*h* (*x*, *y*, ¼)	0.2600(3)	0.2589(4)	0.2614(2)	0.2634(3)	0.2630(5)	0.2620(3)	0.2615(2)	0.2618(1)
	y		1.0031(4)	0.9832(3)	1.0052(3)	1.0781(4)	1.012(3)	0.8431(4)	0.901(3)	0.0053(2)
	B(Å2)		0.3(3)*	0.3(4)*	0.4(2)*	0.4(4)*	0.2(5)*	0.3(4)*	0.4(4)*	0.3(1)*
P	x	6*h* (x, y,¼)	0.4063(4)	0.4072(4)	0.4001(3)	0.4072(5)	0.3946(4)	0.3802(5)	0.3711(4)	0.3497(3)
	y		0.3724(4)	0.3727(3)	0.3832(4)	0.3995(4)	0.4158(3)	0.4012(4)	0.4345(3)	0.4877(3)
	B(Å2)		0.4(2)*	0.4(2)*	0.4(2)*	0.3(1)*	0.2(4)*	0.6(2)*	0.4(4)*	0.3(3)*
O(1)	x	6*h* (x, y,¼)	0.3490(8)	0.3495(3)	0.3497(4)	0.3558(4)	0.3462(5)	0.3523(4)	0.3648(3)	0.4128(3)
	y		0.4929(6)	0.4946(3)	0.4940(4)	0.4851(2)	0.4872(3)	0.4953(3)	0.4612(2)	0.3795(4)
	B(Å2)		0.4(5)*	0.4(5)*	0.5(2)*	0.4(4)*	0.4(2)*	0.5(3)*	0.7(4)*	0.5(2)*
O(2)	x	6*h* (x, y,¼)	0.5918(6)	0.5924(6)	0.5895(4)	0.5910(4)	0.5986(5)	0.5909(6)	0.5916(5)	0.5904(3)
	y		0.4691(7)	0.4613(5)	0.4689(5)	0.4692(2)	0.4703(4)	0.3622(4)	0.4653(4)	0.4684(3)
	B(Å2)		0.3(7)*	0.4(5)*	0.5(1)*	0.2(1)*	0.4(4)*	0.3(4)*	0.5(3)*	0.4(2)*
O(3)	x	12*i* (x, y, z)	0.3536(5)	0.3584(4)	0.359(4)	0.3610(6)	0.3633(5)	0.3625(3)	0.3694(4)	0.3643(2)
	y		0.2638(4)	0.2685(4)	0.2692(4)	0.2702(5)	0.2739(4)	0.2703(4)	0.2815(3)	0.2747(2)
	z		0.06645(5)	0.06732(3)	0.0677(3)	0.0701(3)	0.0811(3)	0.0726(5)	0.0823(2)	0.0809(3)
	B(Å2)		0.6(2)*	0.6(1)*	0.5(4)*	0.5(1)*	0.5(3)*	0.5(3)*	0.5(4)*	0.5(2)*
Br	*B*(Å2)	4*e* (0, 0, z)	8.3(5)*	1.2(4)*	0.8(3)*	1.1(4)*	0.7(2)*	0.5(2)*	0.4(5)*	0.3(3)*
R_{Bragg}			(5–45)#5.2	6.90	7.04	6.97	7.84	7.46	6.85	6.14
			(45–85)#5.38	7.12	8.95	7.82	7.42	8.11	6.99	7.09
			Neutron3.74	7.99	9.54	6.52	7.27	6.54	7.71	2.81

† End members have only Ca or Pb sites present.
* Equivalent value derived from anisotropic values $B\text{iso} = 8\pi^2(U_{11} + U_{22} + U_{33})/3$ (Å^2).
# The values refer to data from the two IPs used.

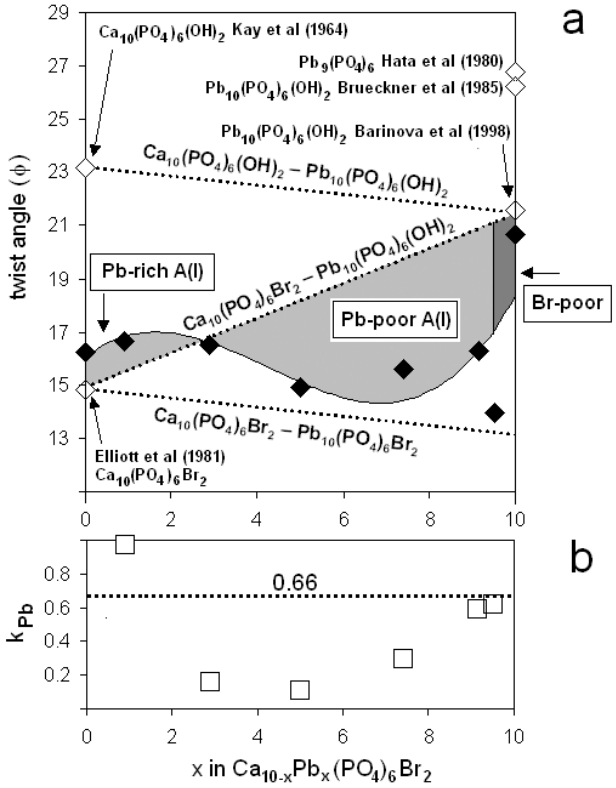

Figure 12. (a) Trends in metaprism twist angle, φ, for the joins $Ca_{10}(PO_4)_6(OH)_2 – Pb_{10}(PO_4)_6(OH)_2$, $Ca_{10}(PO_4)_6Br_2 – Pb_{10}(PO_4)_6(OH)_2$ and $Ca_{10}(PO_4)_6Br_2 – Pb_{10}(PO_4)Br_2$. Open diamonds are derived from single crystal X-ray diffraction determinations. Closed diamonds are derived from the powder neutron diffraction data of Kim (2001) (see also Table 3) for $Ca_{10-x}Pb_x(PO_4)_6Br_2$ solid solution members. Consideration of φ allows the spread of this latter data to be explained in terms of disequilibrium and loss of bromine. (b) Partitioning coefficients for lead k_{Pb}(A1)/(A2) sites is variable due to crystallization times being too short to achieve equilibrium. As the A(2) sites are larger than A(1) preferential entry of lead into A(2) would be expected, except near the lead end member, where $k_{Pb} = 0.66$ for equal partitioning over the A-sites is approached.

where the prism height $h_{\phi=0}$ is the metaprism height in the aristotype. Using again the example of $(Pb_xCa_{10-x})(VO_4)_6(F_{2-2y}O_y)$ $h_{\phi=0} = 3.555 + 0.017x$ at $\phi = 0°$.

While this model contains obvious assumptions and limitations, in particular the projected edges of the metaprisms and tetrahedra are not equal as supposed, it is nonetheless useful for recognizing unexpected departures in Vegard's Law when studying solid solution series.

Symmetry and flexibility

As noted earlier, apatites adopt any of the maximal isomorphic subgroup symmetries of $P6_3/mcm$ (Fig. 3). Broadly, there are two drivers that will impose lower symmetry than the commonly observed $P6_3/m$ on a given apatite—*complex chemistries*, where multiple cation-acceptor sites are required, and *bond strain* induced by "poorly" fitting atoms. As summarized in Table 5, passing from $P6_3/m$ *to* $P2_1/m$ increases the number of unique Wyckoff positions from 7 to 18 resulting in a concomitant enhancement of crystal chemical flexibility. Polyhedral drawings of representative $A_{10}(BO_4)_6X_2$ apatites in all subgroups are shown in Figure 14 (color

Table 4. Comparison of metaprism twist angle ϕ in $Ca_{10-x}Pb_x(PO_4)_6(OH,Br)_2$ as a function of composition.

Composition	*Method*	ϕ (°)	k_{Pb}	*Reference*
Refined Composition				
$Ca_{10}(PO_4)_6Br_2$	X-ray & neutron powder	16.2		Kim (2001)
$Ca_{9.1}Pb_{0.9}(PO_4)_6Br_2$		16.6	0.97	
$Ca_{7.1}Pb_{2.9}(PO_4)_6Br_2$		16.5	0.16	
$Ca_{5.0}Pb_{5.0}(PO_4)_6Br_2$		14.9	0.11	
$Ca_{2.6}Pb_{7.4}(PO_4)_6Br_2$		15.6	0.30	
$Ca_{0.8}Pb_{9.2}(PO_4)_6Br_2$		16.3	0.59	
$Ca_{9.1}Pb_{0.9}(PO_4)_6Br_2$		14.0	0.62	
$Pb_{10}(PO_4)_6(OH)_2$		20.6		
Nominal Composition				
$Ca_{10}(PO_4)_6Br_2$	X-ray single crystal	14.8		Elliott et al. (1981)
$Ca_{10}(PO_4)_6(OH)_2$	Neutron single crystal	22.1		Kay et al. (1964)
$Pb_{10}(PO_4)_6Br_2$	—	13.7		predicted
$Pb_{10}(PO_4)_6(OH)_2$	X-ray single crystal	22.1		Barinova et al. (1998)
"$Pb_{10}(PO_4)_6(OH)_2$"	X-ray powder	26.7		Brückner et al. (1995)
$Pb_9(PO_4)_6$	X-ray single crystal	27.3		Hata et al. (1980)

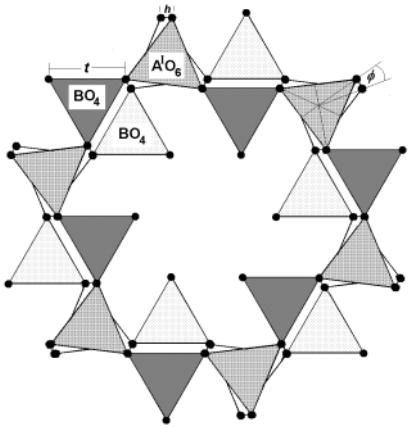

Figure 13. Construction used for the derivation of equations for the calculation of cell parameters from overlapping, at different heights, triangular anion nets. The triangle edge length (*t*), metaprism height (*h*) and twist angle (φ) are shown. This idealized representation should be compared with the real structures in Figure 14. [Used with permission of the International Union of Crystallography (http://journals.iucr.org/), from Dong and White (2004a), *Acta Crystallographica*, Vol. B60, Fig. 7, p. 152.]

figure on page 312). The compilation in Appendix A contains approximately 500 distinct compounds with apatites lower in the hierarchical tree less common, or at least, not yet reported as extensively.

P6₃/m. In this space group the metaprisms and tetrahedral cations are confined to lattice positions with 4*f* and 6*h* symmetry respectively. The prototype mineral $Ca_{10}(PO_4)_6(OH,F)_2$ adopts this space group, as do many binary representatives including vanadates, arsenates, silicates, chromates and germanates. More intricate chemistries such as $Nd_2Ca_6Na_2(PO_4)_6F_2$ have been reported (Mayer et al. 1975), but rarely. For this space group all metaprisms exhibit the same twist angle ϕ.

***P6₃* and *P*$\bar{3}$.** These space groups allow ordering of metaprism sites (2*b* × 2 and 2*d* × 2) and in addition free the tetrahedrally bonded tunnel oxygen to twist. Therefore, they are observed

Table 5. Atom acceptor sites in apatites adopting different space groups.

Site Types	*Space Group*									
	P*6$_3$/*m **176**		***P*6$_3$** **173**		***P*$\bar{3}$** **147**		***P*$\bar{6}$** **174**		***P*2$_1$/*m*** **11**	
	Wyckoff Number	No. Site Types	Wyckoff Number	No. Site Types	Wyckoff Number	No. Site Types	Wyckoff Number	No. Site Types	Wyckoff Number	No. Site Types
Large A Cations	6*h*	1	6*c*	1	6*g*	1	3*k*, 3*j*	2	2*a*, 2*e* × 2	3
Small A Cation	4*f*	1	2*b* × 2	2	2*d* × 2	2	2*i*, 2*h*	2	4*f*	1
B Cations	6*h*	1	6*c*	1	6*g*	1	3*k*, *3j*	2	2*e* × 3	3
Total No. of Cation Acceptor Sites		**3**		**4**		**4**		**6**		**7**
Oxygen anions	6*h* × 2, 12*i*	3	6*c* × 4	4	6g × 4	4	3*k* × 2, *3j* × 2, 6*l* × 2	6	2*e* × 6, 4*f* × 3	9
X anions	2*a* or 2*b* or 4*e*	1	2*a*	1	1*a*, 1*b*	2	1*a*, 1*b* or 2*g*	1/2	2*a* or 2*e*	2
Total No. of Anion Acceptor Sites		**4**		**5**		**6**		**7/8**		**11**
Examples of Cation Occupancy	$[Ca_6][Ca_4][P_6]$		$[K_6][K_2Sn_2][S_6]$		$[Ba_4Nd_1Na_1][Nd_2Na_2][P_6]$		$[Ba_5La_1][La_1Na_{1.3}Ba_{1.7}][P_6]$		$[Ca_6][Ca_4][Si_3S_3]$	
$[A_6][A_4][B_6][O_{24}][X_2]$	$Ca_{10}(PO_4)_6F_2$		$K_6Sn_4(SO_4)_6Cl_2$		$Ba_4Nd_3Na_3(PO_4)_6F_2$		$Ba_{6.7}La_2Na_{1.3}PO_4)_6F_2$		$Ca_{10}(SiO_4)_3(SO_4)_3(F_{0.16}Cl_{0.48}(OH)_{1.36})$	

where tetrahedral distortion is needed, for example in chromate apatites such as $Sr_{10}(CrO_4)_6Cl_2$, or where two components are incorporated in the tetrahedra, as in $Ca_{10}(P,BO_4)_6(O,B)_{2\delta}$. Where the dual symmetry of the metaprism sites is exploited as in $Sr_{7.3}Ca_{2.7}(PO_4)_6F_2$, the metaprisms have the same twist angle with chemical differences accommodated by oxygen displacements along *z*.

***P*$\bar{6}$.** For this symmetry, two unique tetrahedral sites are available (3*k* and 3*j*), in addition to two independent metaprism positions (2*i* and 2*h*). As a result, the metaprisms exhibit two twist angles as observed in $(La_2Na_2Ba_6)(PO_4)_6F_2$.

***P*2$_1$/*m*.** This space group allows flexibility in the tetrahedral positions (2*e* × 3), but permits only a single metaprism site (4*f*). This symmetry is particularly useful where fluorine is the X anion, as the tunnel has difficulty in collapsing sufficiently purely by metaprism twisting. It has recently been confirmed that $Ca_{10}(VO_4)_6F_2$ adopts this arrangement (Dong and White 2004b), and $Cd_{10}(PO_4)_6F_2$ and $Ca_{10}(AsO_4)_6F_2$ may be isostructural (Kreidler and Hummel 1970).

***P*2$_1$.** In their lowest symmetry, apatites have 3 independent tetrahedral sites and 2 independent metaprisms. This structure was first confirmed for ellestadite, ideally $Ca_{10}(SiO_4)_2(SO_4)_2(PO_4)_2(OH,F,Cl)_2$ (Organova et al. 1994). In both monoclinic space groups, the metaprisms can no longer be described uniquely by a single twist angle.

MICROPOROSITY IN NATURAL APATITES

Apatites are not conventionally regarded as microporous. However, as described above, these minerals do possess crystallographic features—an adaptable framework and "channels"—that while not making them zeolitic may predispose them to exhibiting some of the characteristics of zeolites. Indeed, in certain geological settings apatites and zeolites co-exist. Natural phosphate apatite generally forms as well-shaped hexagonal crystals, which may be elongated or stubby; less commonly in tabular plates or columnar forms; as globular masses, acicular, grainy; and earthy aggregates; but most frequently in enormous beds of massive material, from which industrial phosphate is mined (phosphorites).

Besides apatite *sensu stricto* other end members are well known including vanadinite $Pb_{10}(VO_4)_6Cl_2$, pyromorphite $Pb_{10}(PO_4)_6Cl_2$ and mimetite $Pb_{10}(AsO_4)_6Cl_2$. Vanadinite ranges in color from brown through yellow to orange to red, often forming highly aesthetic crystals generally as short hexagonal prisms terminated by a pinacoid, or flat basal face. The high luster and deep red color of vanadinite appeals to mineral collectors. Named for its vanadium content, vanadinite occurs in association with lead deposits and was in the past an important ore of vanadium but the metal is now usually obtained as a by-product in the production of other metals. A secondary mineral also found in the oxidized zones of lead ore deposits is pyromorphite. It is typically found as green to yellow barrel-shaped hexagonal prisms, in clusters or as druses on matrix. This lead chloride phosphate forms a complete series with mimetite, and many specimens are intermediates. The end-member mimetite is generally found in association with vanadinite and pyromorphite and/or in other settings where lead and arsenic occur together. Usually found as small hexagonal prisms, its color is quite variable, ranging from pale yellow to yellowish-brown to orange-yellow to orange-red, white and colorless. A complete list of natural apatite types is given in Table 6, and while some are rarely occurring, they provide valuable insights for the synthesis of new apatites with specific technological features.

Occurrence

As the most abundant natural phosphate, apatite plays a critical role in the global geobiochemical cycle of phosphorous starting with its mobilization at the Earth's surface, its

Table 6. Mineral apatites and related structures

Name	*Formula*	*Reference*
alforsite	$Ba_{10}(PO_4)_6Cl_2$	Hata et al. (1979)
belovite-(Ce)	$Sr_6Na_2(Ce, La)_2(PO_4)_6(F,OH)_2$	Klevtsova and Borisov (1964)
belovite-(La)	$Sr_6Na_2(La, Ce)_2(PO_4)_6(F,OH)_2$	Kabalov et al. (1997)
carbonate-fluorapatite	$Ca_{10}(PO_4, CO_3)_6F_2$	Leventouri et al. (2000)
carbonate-hydroxylapatite	$Ca_{10}(PO_4, CO_3)_6(OH)_2$	El Feki et al. (1999)
chlorapatite	$Ca_{10}(PO_4)_6Cl_2$	Kim et al. (2000)
clinomimetite	$Pb_{10}(AsO_4)_6Cl_2$	Dai et al. (1991)
fermorite	$(Ca, Sr)_{10}[(As, P)O_4]_6(OH)_2$	Hughes and Drexler (1991)
fluorapatite	$Ca_{10}(PO_4)_6F_2$	Kim et al. (2000)
hedyphane	$Pb_6Ca_4(AsO_4)_6Cl_2$	Rouse et al. (1984)
hydroxylapatite	$Ca_{10}(PO_4)_6(OH)_2$	Kim et al. (2000)
Kuannersuite-(Ce)	$Na_4Ba_4(Ce,Nd,La)_2(PO_4)_6(F,Cl)_2$	Friis et al. (2004)
johnbaumite	$Ca_{10}(AsO_4)_6(OH)_2$	Dunn et al. (1980)
mimetite	$Pb_{10}(AsO_4)_6Cl_2$	Dai et al. (1991)
morelandite	$(Ba, Ca, Pb)_{10}[(As, P)O_4)]_6Cl_2$	Dunne and Rouse (1978)
pyromorphite	$Pb_{10}(PO_4)_6Cl_2$	Dai and Huges (1989)
strontium-apatite	$(Sr, Ca)_{10}(PO_4)_6(OH,F)_2$	Sudarsanan and Young (1980)
svabite	$Ca_{10}(AsO_4)_6F_2$	Kreidler and Hummel (1970)
turneaureite	$Ca_{10}[(As, P)O_4]_6Cl_2$	Wardojo and Hwu (1996)
vanadinite	$Pb_{10}(VO_4)_6Cl_2$	Dai and Huges (1989)
britholite-(Ce)	$(Ce, Ca)_{10}[(Si, P)O_4)]_6(OH,F)_2$	Genkina et al. (1991)
britholite-(Y)	$(Y, Ca)_{10}[(Si, P)O_4)]_6(OH,F)_2$	Noe et al. (1993)
fluorbritholite-(Ce)	$(Ce, La, Na)_{10}[(Si, P)O_4]_6F_2$	Hughes et al (1992)
chlorellestadite	$Ca_{10}[(Si, S)O_4)]_6(Cl,F)_2$	Organova et al. (1994)
fluorellestadite	$Ca_{10}[(Si, P, S)O_4]_6(F,OH,Cl)_2$	Hughes and Drexler (1991)
hydroxylellestadite	$Ca_{10}[(Si, S)O_4]_6(OH,Cl,F)_2$	Sudarsanan (1980)
mattheddleite	$Pb_{20}[SiO_4)_7(SO_4)]_4Cl_4$	Steele et al. (2000)
cesanite	$Na_6Ca_4(SO_4)_6(OH)_2$	Piotrowski et al. (2002b)

transport through the living environment, and ultimately, re-deposition through the formation of new geological apatites by sedimentary processes and/or tectonic recycling.

Igneous. Members of the apatite group are often accessory minerals in almost all igneous rocks from basic to acidic, sometimes amounting for as much as 5% by volume, although 0.1–1% is usual. In igneous rocks, the appearance of apatite is due not only to its low solubility in melts and aqueous solutions, but also because the common rock-forming minerals do not accept phosphorous. Fluorapatite is generally dominant, often with appreciable incorporation of chlorine and hydroxyl. Bromine and iodine can also be present but their concentrations are much lower. Apatite appears in both plutonic and effusive acidic and basic rocks, granitic pegmatites, as well as in hydrothermal veins-cavities (Piccoli and Candela 2002). Carbonatites generally contain appreciable apatite and there are several apatite-rich areas in the Khibina tundra, Kola Peninsula where apatite-nepheline rocks (Pletchov and Sinogeikin 1996) accommodate both crystals and botryoidal apatite (i.e., aggregates resembling bunches of grapes). Apatite forms about 3% of the Palabora shonkinite in the Transvaal and in this locality both apatite-diopside and apatite rocks contain up to 96% phosphate (Birkett and Simandl 1999). Carbonate-apatite also occurs in the calcitic carbonatites of the Alnö alkaline complex (Wilke 1997).

Metamorphic. Apatite appears in both thermally and regionally metamorphosed rocks as well as precipitates from hydrothermal solutions (Spear and Pyle 2002). The compositions of metamorphic apatite typically fall along the F-OH join although apatite with small amounts of chlorine has been reported. Fluorapatite is frequent in metasomatized calc-silicate rocks

and impure limestones, whereas chloroapatite is associated with scapolite in rocks that have undergone chlorine metasomatism (Boudreau 1995). As accessory minerals, apatites have become important for research in metamorphic petrology since the partitioning of trace elements in zoned crystals contains detailed information concerning the reaction history of the host metamorphic rock. The characteristic of apatite to accumulate trace and rare elements in its structure is also important for *in situ* dating techniques based on quantification of such elements and their isotope ratios.

Sedimentary. The presence of apatite, but more generally of phosphates, in sedimentary environments is strictly controlled through interaction of the bio- and geospheres (Knudsen and Gunter 2002). Apatites that crystallize in such environments are often carbonate-fluorapatites where the PO_4^{3-} group is partially substituted by CO_3^{2-}. Exploitable phosphorites occur as sediments of marine origin formed by the upwelling of phosphate-rich waters that are characteristic of large delta systems such as the Volga river outflow to the Caspian Sea (Bushinskiy 1964). Other enormous deposits are the Neocene-Holocene phosphorites of Australia, the Miocene phosphorites of Cuba, the deposits in the upper Oligocene of the San Gregorio Formation at San Juan de la Costa, Baja California, the deposits on the Namibian continental shelf, sediments on the South African continental margin, the Moroccan offshore deposits, the Neocene phosphorites of the Sea of Japan, and the submerged phosphate deposit of Mataiva Atoll, French Polynesia (Burnett and Riggs 1990).

Finally, the role of apatites as the primary minerals in bones, teeth, and in general, for all hard tissues of the human body is well known. Their low perishability and persistence make bones and teeth an important resource in palaeontology and archaeology, particularly for the study of palaeoambients (Kohn and Cerling 2002).

Spinodal decomposition

For a great many mineral families unit cell scale inhomogeneities, or phase separation, are well documented for accommodating nonstoichiometry, especially where the approach to equilibrium is slow. It is then perhaps surprising that the apatites, especially those of some chemical complexity, have stood apart as true "solid solutions" having statistical distributions of cations, notwithstanding that long range ordering of the X anions is known. One reason for this may be that the recognition of spontaneous phase separation at fine scales is usually detected by high-resolution and analytical transmission electron microscopy (HRTEM-AEM). However, many apatites are electron beam sensitive making data collection difficult and its interpretation suspect. Nonetheless, recent atomic scale studies of both natural and synthetic apatites are beginning to reveal unexpected nanometric complexity that arises as the tunnel framework adapts to allow intergrowth of channels of different diameters that separate thermodynamically incompatible chemical compositions.

The co-existence of polyphase apatite assemblages need not be obvious. For example, centimeter-sized blue gem-grade crystals from Ipirá, Brazil (*BAp*) (Ferraris et al. 2004) with an average bulk composition of $(Ca_{3.946}Na_{0.052}Y_{0.001})_{\Sigma=4}(Ca_{5.984}Sr_{0.003}Pb_{0.001}REE^{3+}_{0.008}Th_{0.004})_{\Sigma=6}(P_{5.692}Si_{0.182}S_{0.132})_{\Sigma=6}O_{24}(F_{1.541}Cl_{0.122}OH_{0.337})_{\Sigma=2}$ were shown to possess a complex nanostructure (Table 7). Despite the faceted nature of the crystals, Rietveld analysis of powder X-ray data readily refined into a two-phase apatite model with a wt% ratio of approximately 1:3, and domain sizes of 400 and 250 nm (Fig. 15a,b). These domains could be observed directly by bright-field TEM, and in combination with broad beam AEM analyses, it was established that the two domains are F- and Cl-rich apatites. At finer scale, both domain types were punctuated by bright areas approximately 5-10 nm in diameter that were most clearly evident within the darker chlorapatite areas and which exhibited poorly defined hexagonal facets (Fig. 15c, d). Microchemical analysis revealed partitioning of Si and S into these ellestadite-apatite nanodomains and is consistent with the substitutions $2P^{5+} \leftrightarrow Si^{4+} + S^{6+}$ and $Ca^{2+} + P^{5+} \leftrightarrow$

$Na^{+} + S^{6+}$, however these smaller domains were not detected by powder X-ray diffraction. Thus, an apparent single crystal is actually a composite of three apatite phases with distinct chemical compositions.

In detail, Rietveld refinement of the larger apatite domains revealed anisotropic broadening of the diffraction lines where the reflections *hk*0 are broader than the reflections 00*l* (evidence by the separation of the K_α doublet) and, in addition, non-indexed lines at high-angles. These effects can be explained by the presence of two apatite phases with similar cell parameter *c* but with two different parameters *a*. High-resolution images of (001) domain boundaries showed coherent interfaces, however darker contrast can be attributed to strain arising from lattice mismatch to preserve the coherency of the surrounding domains.

Table 7. Ipirá apatite chemical analyses for the major elements. The atoms per formula unit (apfu) are calculated based on 26 (O, OH, F, Cl). The estimated standard deviations (esd) are indicated only for oxides analyzed by EMPA on the basis of 30 point analyses.

Oxide	*Weight %*	*esd*	*cation*	*apfu*
Na_2O	0.16	0.02	Na	0.052
MgO	< D.L. (0.25)	—	Mg	0.000
Al_2O_3	< D.L. (0.20)	—	Al	0.000
SiO_2	1.12	0.13	Si	0.188
P_2O_5	39.88	0.60	P	5.686
SO_3	1.05	0.09	S	0.132
K_2O	< D.L. (0.10)	—	K	0.000
CaO	55.04	0.99	Ca	9.938
TiO_2	< D.L. (0.03)	—	Ti	0.000
SrO	0.03	—	Sr	0.003
Y_2O_3	0.01	—	Y	0.001
La_2O_3	0.03	—	La	0.002
Ce_2O_3	0.06	—	Ce	0.004
Nd_2O_3	0.02	—	Nd	0.002
ThO_2	0.10	—	Th	0.004
PbO	0.01	—	Pb	0.001
MnO	< D.L. (0.03)	—	Mn	0.000
Fe_2O_3	< D.L. (0.10)	—	Fe	0.000
F	2.89	—	F	1.517
Cl	0.43	—	Cl	0.120
H_2O	0.35	—	OH	0.363
	101.18			
O ≡ F, Cl	1.27			
Total	99.91			

It is postulated that the nanostructure of these single crystals arises from consecutive, or nested, spinodal decompositions as shown schematically in Figure 16. In these simplified representations, the amplitudes of the compositional modulations are assumed constant, with long wavelength separation of F rich-Ap and Cl rich-Ap arising from the bulk composition. Before, during or after this long wave event decomposition with high frequency leads to the formation of ellestadite. This combination of periodicities may indicate that apatite experienced two significant geothermometric events. The long period modulation would have developed close to the coherent spinodal decomposition temperature (T_s) resulting in the separation of X anions primarily and the formation of fluorine-rich and chlorine rich apatites. The short period modulation occurred at higher temperature (perhaps contact metamorphism), and was diffusion-dependant, leading to smaller ellestadite domains. If decomposition into the long and short period modulations occurred separately, it would be expected that compositionally distinct ellestadites would separate from the F rich-Ap and Cl rich-Ap regions. This was not observed, suggesting that simultaneous phase separation occurred. However, it has not been possible to resolve such subtle compositional variations and the question of whether spinoidal decomposition is the most appropriate description of these observations remains unproven.

Historically, apatite was so named (apatos = deception) because of its frequent misidentification as more precious types of gemstones. This reputation would appear to remain intact today as it is not immediately obvious that large, gem grade apatites should be worthy of detailed microscopic examination, or possess such intricate phase structures.

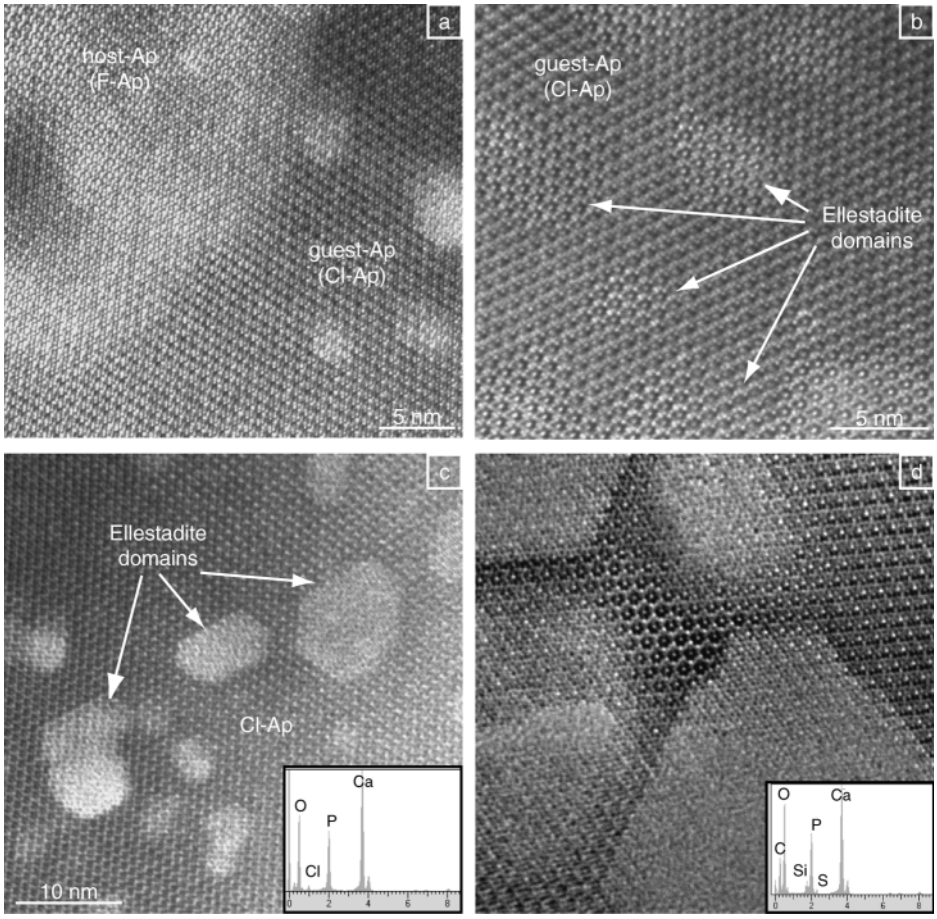

Figure 15. (a) [001] HRTEM image of the interface between *Cl-Ap* (bright contrast) and *F-Ap* (dark contrast) crystals. Within the *Cl-Ap* (b), smaller ellestadite single crystal domains with bright contrast are present. (c) [001] TEM image and (d) [001] HRTEM image showing the development of faceting in ellestadite domains as a result of electron irradiation. Inserts of AEM analyses clearly show enrichment of Si + S in the ellestadite (inset in d) compared to the surrounding *Cl-Ap* (inset in c).

MICROPOROSITY IN SYNTHETIC APATITES

The first known synthesis of an apatite, probably $Ca_{10}(PO_4)_6(OH)_2$ was reported by Daubrée (1851) who obtained it by passing phosphorus trichloride vapor over red hot lime. Since then, a large array of preparative routes have been employed in the synthesis of both phosphate and non-phosphate apatites as tabulated in Appendix B. Broadly, the techniques reported can be divided into three classes.

1. *Solid-state reaction*. High temperature sintering (> 500°C) of stoichiometric mixtures of the starting materials can be used with the phase-forming temperatures deduced from the respective phase diagrams. Depending on the elements involved and their oxidation states, the sintering atmosphere may be oxidizing, reducing or inert although most are carried out in air. Generally, a series of mixing, grinding, pelletizing and heating steps ensure formation of single-phase apatites. This is the

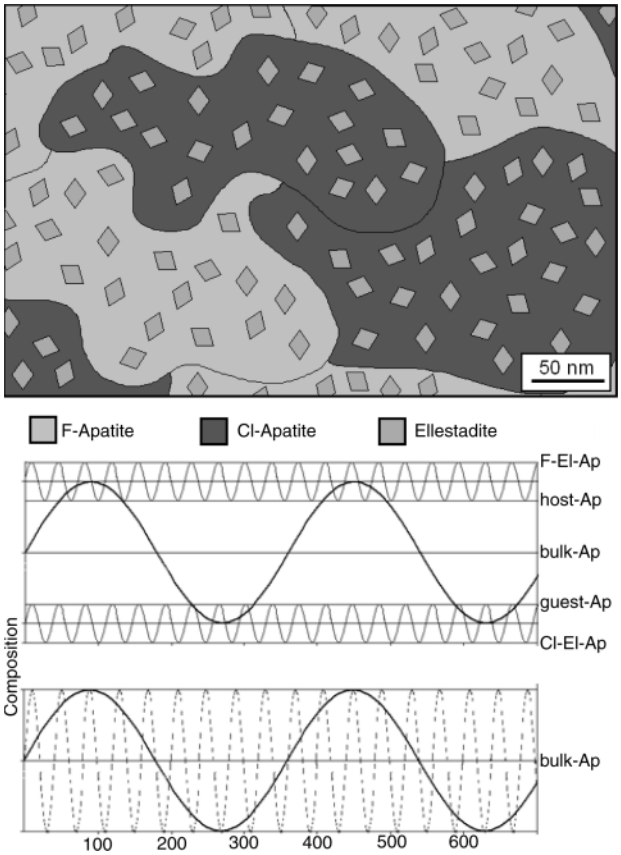

Figure 16. Schematic illustration of the three domain types in Ipirá apatite (upper part) and representation of the spinodal compositional modulations that may have lead to domain formation. The upper schematic illustrates consecutive compositional modulations in which the *ellestadite* domains arise after separation of *F-Ap* and *Cl-Ap*, while the lower portion supposes simultaneous decomposition into *F-Ap*, *Cl-Ap* and ellestadite.

most commonly used method for bulk processing of ceramic apatite powders, and in particular, for the study of phase stability. However, powders prepared in this way usually have irregular external form, large grain sizes, and often exhibit compositional heterogeneity from incomplete reaction owing to the small diffusion coefficients of ions within solids. Non-stoichiometry can also arise due to evaporation of volatile species, particularly the halides and precautions are necessary to prevent such losses.

2. *Hydrothermal reaction*. Under this reaction regime, precursor solutions (especially phosphate apatites) are treated epithermally and hydrothermally. Mass transport is superior to solid-state methods yielding compositionally homogeneous, uniform and easily sinterable powders of good crystallinity. Hydroxyapatites are frequently synthesized by this method (Yoshimura and Suda 1994).

3. *Soft chemical reaction*. This method offers a certain degree of control over the grain size and morphology of apatites. The occurrence of secondary impurity phases is reduced if homogeneous precipitation is achieved. However, powders generated in this way are usually less crystalline as compared to those derived from solid-state reaction.

The largest proportion of apatites have been synthesized by high-temperature solid state reaction. Less frequently used are hydrothermal methods and soft chemical precipitation at relatively low temperatures.

Methods developed to grow large single crystals are used rarely. Gel growth has been applied to calcium phosphate synthesis (McCauley and Roy 1974), while stoichiometric melts were used for the preparation of $Ca_2La_8(SiO_4)_6O_2$ (Ito 1968), $Cd_{10}(PO_4)_6Br_2$ and $Cd_{10}(PO_4)_6Cl_2$ (Sudarsanan et al. 1977), and $Pb_{9.85}(VO_4)_6I_{1.7}$ (Audubert et al. 1999). Melt grown materials are sometimes severely strained as they experience large temperature gradients during crystallization. To overcome this limitation, the flux growth method (Prener 1967), using CaF_2, $CaCl_2$, and $Ca(OH)_2$ mixed with the starting apatite powders, reduce the liquidus temperature and yield crystals with less strain (Yoshimura and Suda 1994). Finally, the sol-gel and polymerization methods (Brendel et al. 1992) have also been developed for processing apatites.

Until comparatively recently, relatively little attention was given to the presence of carbon dioxide in starting materials, particularly the alkali solutions used to control *pH*, and in distilled water. As a consequence many preparations of "pure" apatites, in particular hydroxyapatites, contain significant carbonate. In fact, it can be difficult to obtain apatites that do not contain carbon dioxide, unless very deliberate methods for exclusion are used (McConnell 1973; Wilson et al. 2003).

Cell constant discontinuities and miscibility gaps

While it may not always be feasible to determine directly the absolute stoichiometry of apatites or the partitioning coefficients of elements over the available cation-acceptor sites, it is in principle possible to follow these effects indirectly by monitoring unit cell constants. However, this may not always be straightforward. Figure 17 shows the distribution of *a* and *c* cell constants in hydroxyapatite for 25 data sets gathered by single crystal and powder methods (Table 8). For more than half the materials the ideal Ca/P ratio of 1.667 is assigned, while the remainder are slightly non stoichiometric. It is immediately apparent that while there is a substantial spread of data, well in excess of experimental error, no clear trend is evident suggesting that disequilibrium or compositional effects may be responsible. For the cluster of data near the centre of the graphic, there is obvious variation in *a* with near constant *c*, as

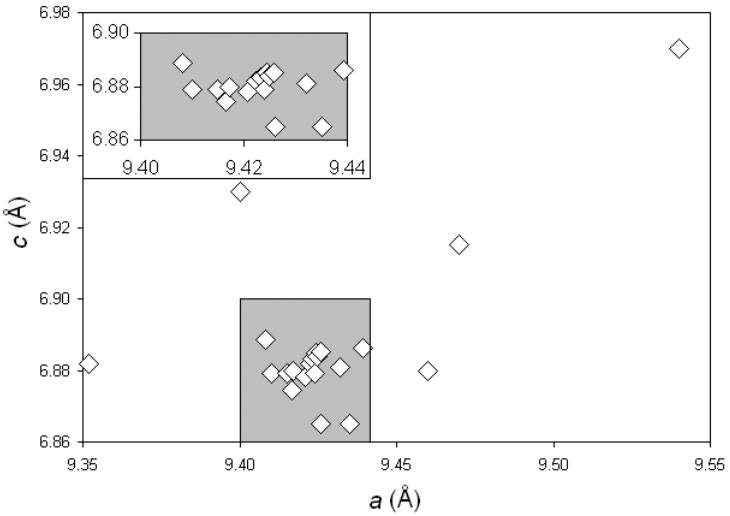

Figure 17. Distribution of lattice constants reported for hydroxyapatite (see also Table 8). The insert shows greater detail surrounding the closest grouped values. The reasons for this distribution may be related to cation order-disorder or compositional variation, especially the uptake of carbonate.

Table 8. Reported parameters for hydroxyapatite.

Reported Composition	*Ca*/*P*	*a* (Å)	*c* (Å)	*c*/*a*	*Vol* (Å^3)	*Refs.*
$Ca_{10}P_6O_{26}H_2$	1.667	9.3520	6.8820	0.736	521.26	(1)
$Ca_{10}P_6O_{26}H_2$	1.667	9.410	6.879	0.731	527.52	(2)
$Ca_{10}P_6O_{26}H_2$	1.667	9.4166	6.8745	0.730	527.91	(3)
$Ca_{10.042}P_{5.952}O_{26.1}H_{2.292}$	1.687	9.4081	6.8887	0.732	528.05	(4)
$Ca_{9.74}P_6O_{26.08}H_{2.08}$	1.623	9.415	6.879	0.731	528.08	(5)
$Ca_9P_6O_{25.68}H_{1.68}$	1.500	9.426	6.865	0.728	528.23	(5)
$Ca_{10.132}P_{5.958}O_{27.09}H_{3.258}$	1.701	9.4172	6.8799	0.731	528.39	(4)
$Ca_{10}P_6O_{26}H_2$	1.667	9.4207	6.878	0.730	528.64	(6)
$Ca_{10}P_6O_{26}H_2$	1.667	9.424	6.879	0.730	529.09	(7)
$Ca_{10}P_6O_{26}H_2$	1.667	9.4223	6.8818	0.730	529.11	(2)
$Ca_{8.8}P_6O_{25.92}H_{1.92}$	1.467	9.435	6.865	0.728	529.24	(5)
$Ca_{10.084}P_{5.94}O_{27.15}H_{3.39}$	1.698	9.4232	6.8833	0.730	529.33	(4)
$Ca_{10}P_6O_{26}H_2$	1.667	9.4249	6.8838	0.730	529.56	(2)
$Ca_{10}P_6O_{26}H_2$	1.667	9.4244	6.885	0.731	529.59	(2)
$Ca_{10}P_6O_{26}H_2$	1.667	9.4257	6.8853	0.730	529.76	(2)
$Ca_{10}P_6O_{26}H_2$	1.667	9.432	6.881	0.730	530.14	(8)
$Ca_{10}P_6O_{26}H_2$	1.667	9.432	6.881	0.730	530.14	(9)
$Ca_{10}P_6O_{26}H_2$	1.667	9.40	6.93	0.737	530.30	(10)
$Ca_{9.868}P_{5.586}O_{26.35}H_{4.006}$	1.767	9.4394	6.8861	0.730	531.36	(4)
$Ca_{8.86}P_6O_{26}H_4$	1.477	9.46	6.88	0.727	533.21	(11)
$Ca_{10}P_6O_{26}H_2$	1.667	9.470	6.915	0.730	537.06	(2)
$Ca_{10}P_6O_{26}H_2$	1.667	9.54	6.970	0.731	549.36	(2)

References: (1) Tomita et al. 1996 (2) Saenger and Kuhs 1992 (3) Hughes et al. 1989 (4) Wilson et al. 1999 (5) JeanJean et al. 1996a (6) Pritzkow and Rentsch 1985 (7) Sudarsanan and Young 1969 (8) Posner and Diorio 1958 (9) Kay et al. 1964 (10) Hendricks et al. 1932 (11) JeanJean et al. 1994

would be expected if the twist angle (ϕ) was modified (smaller *a* corresponding to larger ϕ) due to replacement of phosphate by carbonate and/or nonstoichiometry of the Ca(2) site.

Correlations can be easier to recognize in solid solution series such as $Ca_{10-x}Pb_x(PO_4)_6(OH)_2$. While early studies (e.g., Narasaraju et al. 1972) appeared to show linear trends in lattice parameters between the lead and calcium end members, subsequent work by Engel et al. (1975a), Verbeeck et al. (1981) and Bigi et al. (1989, 1991) revealed more complex behavior (Fig. 18) due to cation ordering. Not only were discontinuities in lattice parameters as a function of composition observed but also distinct and large changes in lattice parameter were recorded depending on firing temperature. Moreover, both Verbeeck et al. (1981) and Bigi et al. (1989, 1991) found miscibility gaps, *albeit* at slightly different compositions.

Nanodomain intergrowths at disequibrium

While a great range of apatites have been synthesized, the very flexibility which gives rise to such an array of compounds, translates to a need for particular rigor during crystal chemical data collection and interpretation. The recent synthesis of the fluoro-vanadinites $(Pb_xCa_{10-x})(VO_4)_6F_{2\delta}$, $0 < x < 9$, which compared and contrasted the crystal structure and local atomic order in equilibrated and non-equilibrated material, is a case in point (Dong and White,

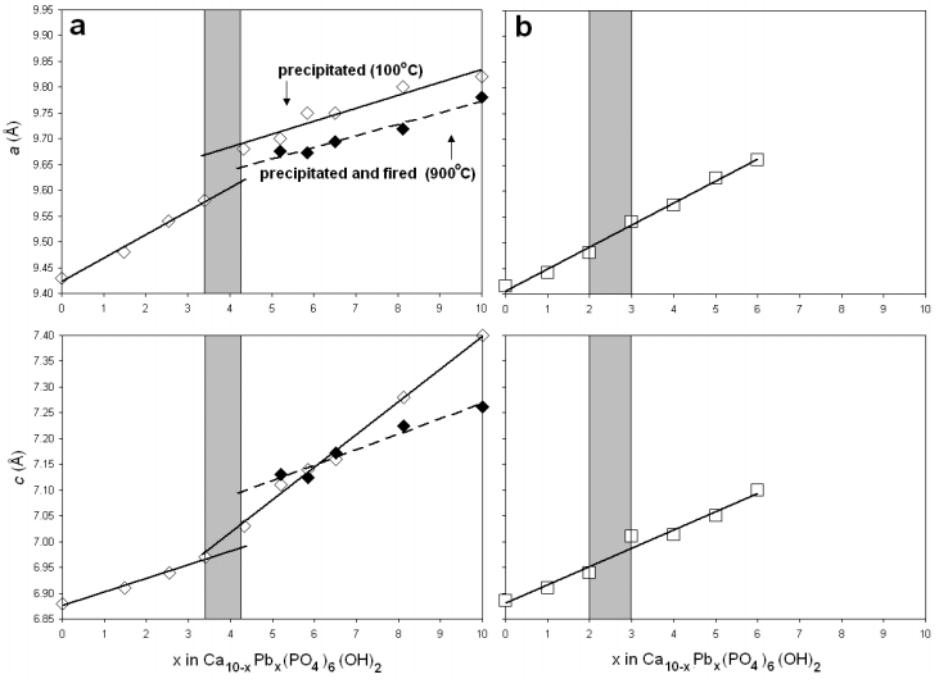

Figure 18. Unit cell parameters as a function of composition in $Ca_{10-x}Pb_x(PO_4)_6(OH)_2$ apatites as determined by (a) Bigi et al. (1991) and (b) Verbeeck et al. (1981). Differences in the trend lines can be attributed to disequilibrium. Both authors reported a miscibility gap (shaded in the drawing) at approximately $2 < x < 4$.

2004a,b). In these experiments, stoichiometric mixtures were annealed 10 h, 1 week, 2 weeks and 7 weeks at 800°C with intermediate grinding. At each stage, the material was assessed by XRD and TEM, and in all cases, single-phase apatite was produced. It was observed that as x increased the unit cell constants dilated as lead (effective ionic radii = 1.29 Å for VIII coordination) replaced calcium (1.12 Å). However, trends in cell constants for 10 h and 4 weeks materials as a function of composition were quite distinct (Fig. 19). Neither equilibrated nor non-equilibrated apatites obeyed Vegard's Law across the entire compositional range from $0 < x < 10$. Rather, the cell constants were best described as two linear segments. This can be understood by considering that vanadinite contains four A(1) sites (the preferred location of Ca) and six A(2) sites (favored by Pb). The change in the slope reflects the changes in the lead partitioning coefficient k_{Pb}.*

The approach to equilibrium is surprisingly slow. For "$Pb_5Ca_5(VO_4)_6F_2$" the c/a lattice constant ratio decreases exponentially as annealing continues such that equilibrium is approached only after 30 days annealing (Fig. 20). Concomitant with this adjustment is the enrichment of lead in the A(2) position and a decrease in the $A(2)O_6$ metaprism twist angle (ϕ) (Table 9, Fig. 21). Fully equilibrated vanadinite that was heat treated for 7 weeks had a substantially smaller k_{Pb}[A(1)/A(2)] of 0.17 as compared to 0.52 for 10 h material, and ϕ was reduced to 14.4° from 22.0°.

* k_{Pb}[A(1)/A(2)] = [2−2N(Ca1)]/[3-3N(Ca2)] where N(Ca) is the fractional occupancy of the site. For equal partitioning of Pb over A^I and A^{II} k_{Pb} would be 0.66 for all compositions.

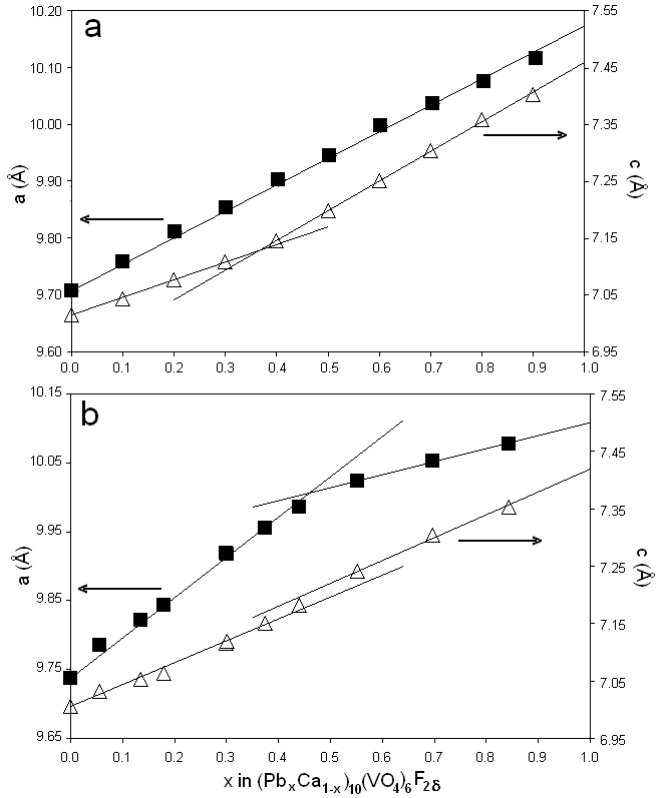

Figure 19. Variation in cell constants for vanadinites of composition $(Pb_xCa_{1-x})_{10}(VO_4)_6F_{2\delta}$ when in disequilibrium after 10 h annealing (a) and in equilibrium after 4 weeks annealing (b).

At the unit cell scale, the structure of the nonequilibrated apatite is complex as shown Figure 22. Nanodomains can be ascribed to local changes in composition, and in particular, to variation in the Ca/Pb ratio. This interpretation is supported by the fact that similar images collected from equilibrated vanadinite failed to display the same complex nanostructure. Within each nanodomain it would be expected that the twist angle will be unique, and the ϕ derived from Rietveld analysis reflects an average of sorts of these angles. Nonetheless, a combination of powder X-ray diffraction and high resolution transmission electron microscopy have demonstrated that long annealing times of several weeks are necessary to completely equilibrate calcium-lead partitioning in $(Pb_xCa_{10-x})(VO_4)_6F_{2\delta}$ with $0 < x < 9$ vanadinite apatite.

Influence of pressure

As apatites behave as flexible one-dimensional tunnel structures, it follows that the application of pressure will lead to their compression through an increase in ϕ. This has been observed by Comodi et al. (2001) who used single crystal X-ray diffraction to determine the structure of synthetic $Ca_{10}(PO_4)_6F_2$ up to pressures of 6.89 GPa. Their data, which includes a large set of unit cell constants and complete structure analyses at atmospheric pressure, 3.04 GPa and 4.72 GPa, showed that the least compressible units were the PO_4 tetrahedra and CaO_6 metaprisms, while the larger CaO_6F polyhedra (the tunnel contents) were most compressible, with bulk moduli of 270, 100 and 84 Gpa, respectively (Fig. 23). During compression to 4.72 GPa the twist angle increased 4.2% from 20.8° to 21.7°, while *a* and *c* decreased 1.6% and

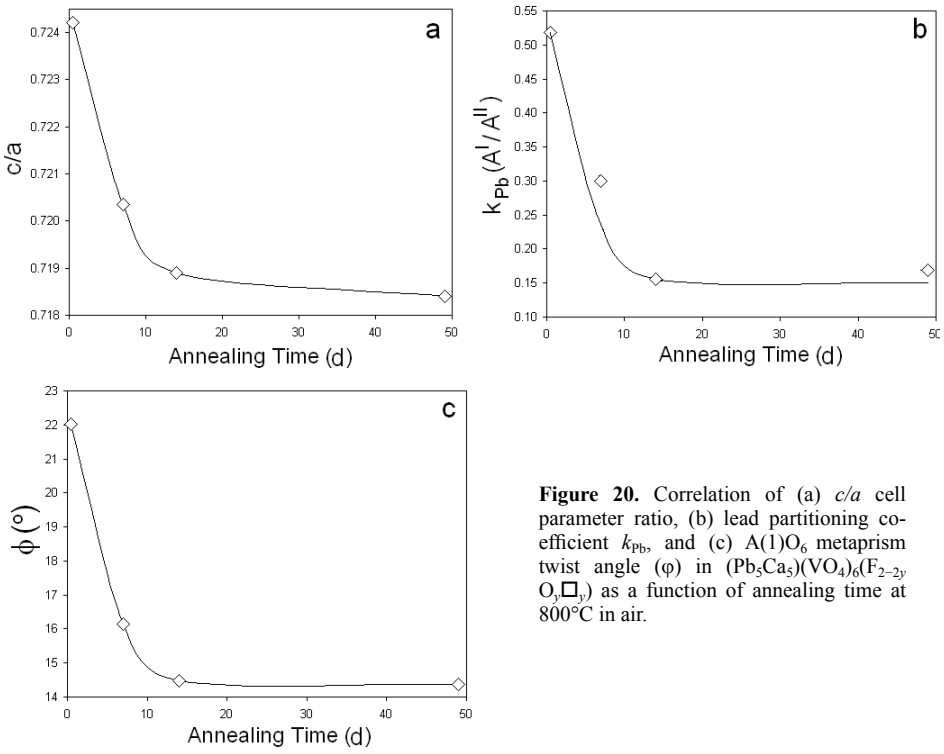

Figure 20. Correlation of (a) *c/a* cell parameter ratio, (b) lead partitioning coefficient k_{Pb}, and (c) A(1)O_6 metaprism twist angle (φ) in $(Pb_5Ca_5)(VO_4)_6(F_{2-2y}O_y\square_y)$ as a function of annealing time at 800°C in air.

1.2%, respectively (Fig. 23). Unlike zeolites, which amorphize under pressure, fluorapatite is stable possibly because structural flexibility is essentially restricted to two-dimensions. It might also be expected that apatites in which the tunnels are more fully extended and therefore have smaller twist angles would be most readily compressed. Brunet et al. (1999) found this trend for hydroxyapatite (ϕ = 23.2°), fluorapatite (23.3°) and chlorapatite (19.1°) with bulk moduli of 98(2), 98(2) and 93(4) GPa respectively. If this phenomena is generally correct it would be predicted that $Ca_{10}(CrO_4)_6(OH)_2$ (17.8°) and $Ca_{10}(AsO_4)_6Cl_2$ (13.0°) should become progressively softer.

ION EXCHANGE PROPERTIES

There are several possible mechanisms for apatite replacement including dissolution-reprecipitation processes, leaching and ion exchange, and a substantial literature has accumulated especially in relation to the treatment of heavy metal wastes (e.g., Reichert and Binner 1996; Sugiyama et al. 2003; Lower et al. 1998; Manecki et al. 2000). However, this discussion is restricted for the most part to pure lattice exchange reactions.

Cadmium. Extensive investigation of cadmium uptake by hydroxyapatites (Jeanjean et al. 1994, 1996a,b; Mandjiny et al. 1998; Fedoroff et al. 1999; McGrellis et al. 2001) has shown unequivocally that cadmium is incorporated in the structure by diffusion and substitution for calcium ions. However, to accelerate the reaction sodium-doped (~ 1 atomic %) apatites were used as the starting materials with probable replacements

$$Ca^{2+} + OH^- \rightarrow Na^+ + H_2O \text{ or } Ca^{2+} + (PO_4)^{3-} \rightarrow Na^+ + (HPO_4)^{2-}.$$

Table 9. Refined crystal and atomic parameters for vanadinites annealed at 800°C for intervals from 10 hours to 7 weeks.

Time/Parameter	*10 hours*	*1 week*	*2 weeks*	*7 weeks*
Composition	$(Pb_{4.62}Ca_{5.38})(VO_4)_6F_2$	$(Pb_{4.90}Ca_{5.10})(VO_4)_6(F_{0.6}O_{0.7})$	$(Pb_{4.78}Ca_{5.22})(VO_4)_6(F_{0.6}O_{0.7})$	$(Pb_{4.76}Ca_{5.64})(VO_4)_6(F_{0.6}O_{0.7})$
Crystal Formula	$[Pb_{1.56}Ca_{2.44}][Pb_{2.06}Ca_{2.94}](VO_4)_6F_2$	$[Pb_{1.12}Ca_{2.88}][Pb_{3.78}Ca_{2.22}](VO_4)_6(F_{0.3}O_{0.7})$	$[Pb_{0.64}Ca_{3.36}][Pb_{4.14}Ca_{1.96}](VO_4)_6(F_{0.25}O_{0.75})$	$[Pb_{0.68}Ca_{3.32}][Pb_{4.08}Ca_{1.92}](VO_4)_6(F_{0.3}O_{0.7})$
a (Å)	9.9462(1)	10.0011(1)	10.0025(2)	10.0124(2)
c (Å)	7.1983(1)	7.1993(1)	7.1858(1)	7.1880(1)
Volume (Å^3)	616.7	623.6	622.6	624.0
c/a	0.7237	0.7199	0.7184	0.7179
N(Ca1)	0.61	0.72	0.84	0.83
N(Ca2)	0.49	0.37	0.31	0.32
$k_{Pb}(A^I/A^{II})^*$	0.52	0.30	0.16	0.17
φ (°)	22.0	16.1	14.5	14.4
z(A1)	0.0095(8)	0.0083(8)	0.0062(11)	0.0059(12)
B(A1)	0.6	1.2	0.4	1.4
x(A2)	0.2427(3)	0.2442(2)	0.2418(2)	0.2426(2)
y(A2)	0.0023(4)	0.0028(3)	0.0026(3)	0.0036(3)
B(A2)	0.6	1.1	1.3	1.7
x(V)	0.4020(7)	0.4066(5)	0.4090(6)	0.4093(6)
y(V)	0.3758(6)	0.3770(5)	0.3813(6)	0.3805(6)
B(V)	0.3	0.2	0.2	0.6
x(O1)	0.3195(18)	0.3363(16)	0.3407(17)	0.3393(18)
y(O1)	0.4915(18)	0.5014(16)	0.5073(16)	0.5057(17)
x(O2)	0.6012(20)	0.6046(19)	0.6056(20)	0.6074(20)
y(O2)	0.4755(18)	0.4782(16)	0.4787(17)	0.4807(17)
x(O3)	0.3353(13)	0.3436(10)	0.3545(10)	0.3499(11)
y(O3)	0.2546(13)	0.2594(11)	0.2635(11)	0.2639(12)
z(O3)	0.0628(13)	0.0602(13)	0.0605(13)	0.0583(14)
N(*F*)	1.0	0.6	0.5	0.6
R_b (%)	4.2	4.4	5.0	4.9

*k_{Pb}[A(1)/A(2)] = (2-2N(Ca1))/[3−3N(Ca2)]. For equal partitioning of Pb over A(1) and A(2) k_{Pb} = 0.66

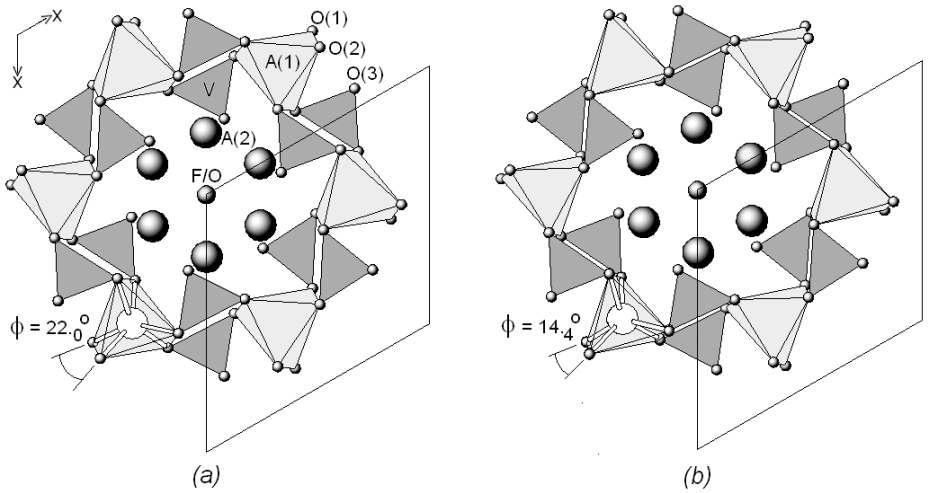

Figure 21. Structures of the fluoro-vanadinites (a) $[Pb_{1.56}Ca_{2.44}][Pb_{2.06}Ca_{2.94}](VO_4)_6F_2$ with refined x = 4.62 and (b) $[Pb_{0.68}Ca_{3.32}][Pb_{4.08}Ca_{1.92}](VO_4)_6(F_{0.3}O_{0.7})$ with x = 4.76 synthesized from stock powders but annealed respectively for 10 h and 7 weeks at 800°C (see Table 9). The $A(1)O_6$ metaprisms and VO_4 tetrahedra are emphasized in [001] projection. As A(2) becomes progressively lead-rich the channel opens through A-O bond dilation and a reduction of metaprism twist angle (φ). [Reproduced with permission of the International Union of Crystallography (http://journals.iucr.org/) from Dong and White (2004a) *Acta Crystallographica*, Vol. B60, Fig. 4, p. 140.]

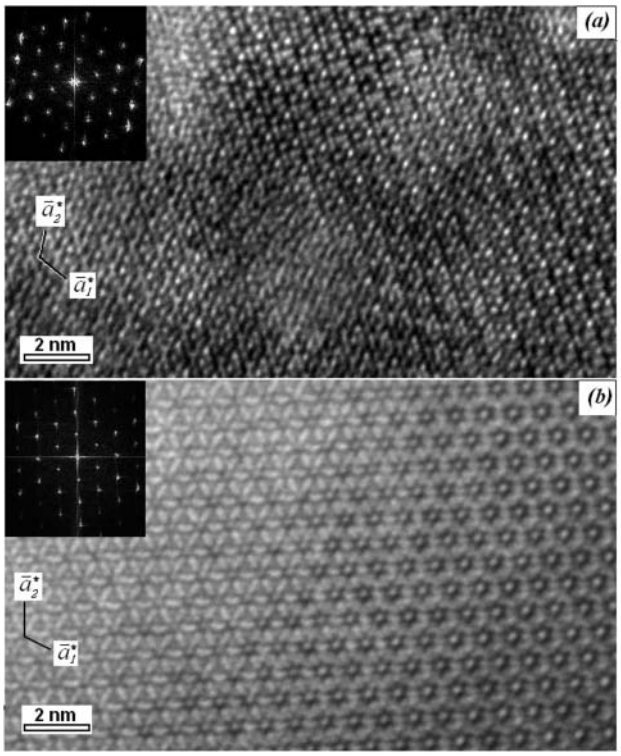

Figure 22. [001] high resolution electron micrographs collected from $(Pb_5Ca_5)(VO_4)_6(F_{1-2y}O_y)_2$ thin crystal wedges annealed for (a) 10 h and (b) 7 weeks. Inserts of the power transforms confirm the orientation. The upper image shows poorly equilibrated microdomains 2 nm in diameter arising from local variation in Ca/Pb content. Conversely, the equilibrated sample shows regular contrast changes in passing from the thin edge (left) to thicker crystal (right). [Used with permission of the International Union of Crystallography (http://journals.iucr.org/), from Dong and White (2004a), *Acta Crystallographica*, Vol. B60, Fig. 6, p. 142.]

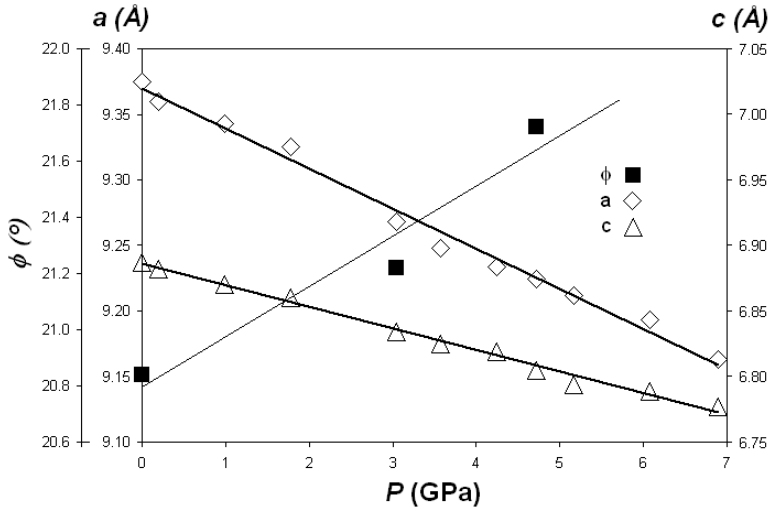

Figure 23. Changes in lattice parameters in fluorapatite as a function of applied pressure. During compression, the tunnel collapses slightly through an increase in metaprism twist angle φ. (Data taken from Comodi et al. 2001).

Crystal structure refinement before exchange were consistent with near full occupancy of the A(1) sites and partial occupancy of the A(2) sites. Ion exchange was monitored over the temperature range 28–75°C using a solution with [Cd] = 3.96×10^{-3} mol/L (2 mol of Cd per mole of apatite) and contact times of 1 min to 12 h. For these conditions, the quantity of calcium released varied directly with the quantity of cadmium fixation, however the release of sodium was negligible. At lower concentrations, cadmium partitioned entirely to the A(2) tunnel sites, while for larger quantities (~ 3.9 atomic %) both the A(1) and A(2) sites were occupied. As the external morphology of the apatite crystals was maintained it is reasonable to suspect lattice diffusion occurs, but the precise mechanism by which cadmium enters the metaprisms is not yet understood. As exchange is only partially reversible with ~20% recovery of cadmium it seems possible that it is quite difficult to remove exchanged ions from the A(1) positions.

Selenium. The interaction of selenite $(SeO_3)^{2-}$ and biselenite $(HSeO_3)^-$ with sodium-bearing hydroxyapatite was studied by Monteil-Rivera et al. (1999). Using solutions with initial selenium concentrations from 10^{-3}–10^{-6} mol/L and ambient reaction temperature, it was shown that the total mole release of phosphorous equaled the uptake of selenium. As neither diffraction nor microscopy indicated the presence of second phase, it was argued that the dominant mechanism for sorption was exchange. Because no oxidation of Se(IV) took place in the exchange solutions possible mechanisms for exchange include

$$2(PO_4)^{3-} + Ca^{2+} \rightarrow 2(SeO_3)^{2-} + \square \quad \text{or} \quad (PO_4)^{3-} + Ca^{2+} \rightarrow (HSeO_3)^- + \square$$

Although the incorporation of BO_3 radicals is less usual in apatites, it is not unknown. The mineral finnemanite, $Pb_{10}(AsO_3)_6Cl_2$, shows complete substitution of $(As^{V}O_4)^{3-}$ by $(As^{III}O_3)^{3-}$ and mimetite, $Pb_{10}(AsO_4)_6Cl_2$, can be produced from arsenite form by direct oxidation as shown in Figure 24 (Effenberger and Pertlik 1977). Therefore, introduction of SeO_3 into the tetrahedral phosphate positions may be possible. Structural studies to confirm this point would be invaluable.

Lead. Pyromorphite, $Pb_{10}(PO_4)_6(OH,Cl)_2$, is frequently cited as a useful phase for the fixation of lead as it is sparingly soluble over a wide pH range. Crystallization occurs either

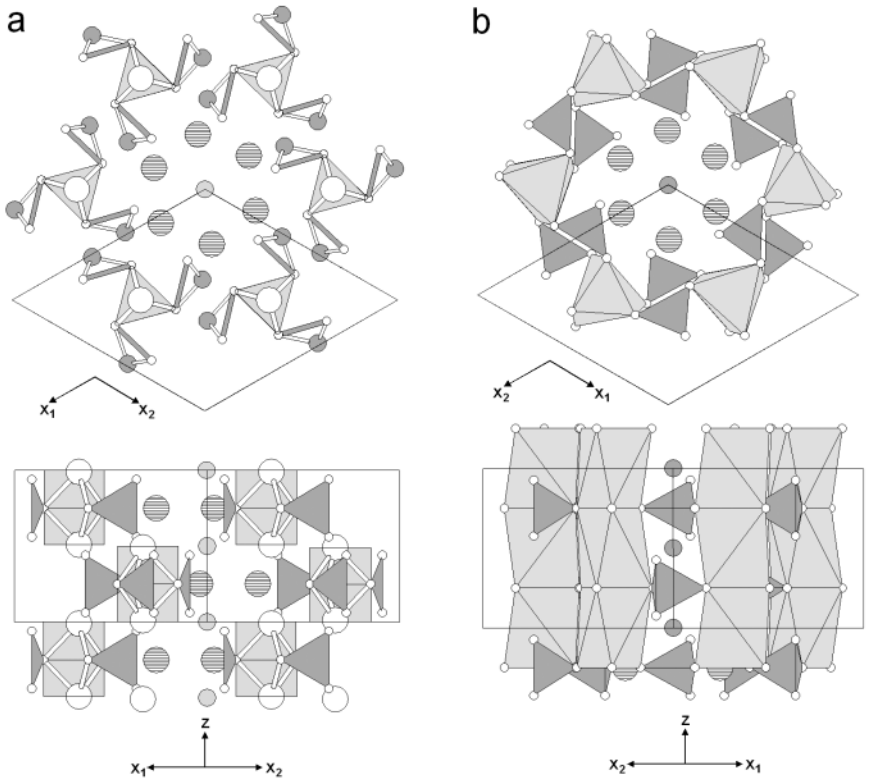

Figure 24. Structure drawings of (a) finnemanite $Pb_{10}(As_{III}O_3)_6Cl_2$ composed of PbO_3 half prisms and $As_{III}O_3$ triangular co-ordination, and its oxidized form (b) mimetite $Pb_{10}(As_VO_4)_6Cl_2$ constructed from the more usual PbO_6 and As_VO_4 polyhedra. The stability of the $As_{III}O_3$ unit suggests that reports of ion exchange of $Se_{IV}O_3$ for PO_4 may be crystallographically feasible.

by replacement of hydroxyapatite or through amendment with various phosphates (Xu and Schwartz 1994). But, there appears to be little evidence for cation exchange (Arnich et al. 2003). Miyake et al. (1986) reportedly conducted Rietveld analysis of lead-exchanged hydroxy-, fluor- and chlorapatites. However, their data do not show preferential entry of lead into the A(2) site suggestive of disequilibrated material, as might be produced by rapid reprecipitation, and the cell parameters are consistent with near pure lead endmembers $Pb_{10}(PO_4)_6(F,OH,Cl)_2$.

While ion exchange in phosphate apatites appears to be established for cadmium and selenium, it is clearly a competitive process with precipitation and in those cases where insoluble metal phosphates form, then lattice exchange will be overwhelmed. It is also apparent that exchange reactions are kinetically slow and as noted by Fedoroff et al. (1999) may take several weeks or longer to equilibrate.

APATITE TECHNOLOGIES

Chemical fertilizers were introduced after a method for production was devised by Lawes in 1843, and by the 1850s, more than a dozen superphosphate works were operating in Britain and Germany (Brock 1993). In 1900, world production was over 4.5 million metric tons per

year (Mtpy) with large quantities of sulfuric acid being used in processing. Today three main types of phosphate fertilizers are used—normal super phosphate (20% of the total), ammonium phosphate (65%), and triple super phosphate (10%)—with total consumption amounting to 130 Mtpy (International Fertilizer Industry Association). This traditional use of phosphate rock, including apatite *sensu stricto*, as a raw material for phosphoric acid extraction remains the largest application in terms of volume and investment. However, over the past two decades a number of advanced ceramic technologies based upon apatites have emerged.

Remediation of radioactive wastes

Ceramic options for the disposal of nuclear wastes have been under development in various forms for more than 50 years (Lutze and Ewing 1988) with the first experiments detailing the possible role of apatite presented by Roy and his coworkers (1982). Apatites are appropriate immobilization matrices for three reasons. First, they can accommodate a wide range of fission products, actinides and processing contaminants, often to high concentration. Second, the radiation resistance of apatites in nature is well known (Utsunomiya et al. 2003), and extensive laboratory investigations suggest that durability will not be compromised even under high radiation fluxes as might be experienced shortly after disposal (Ewing et al. 2000; Ewing and Wang 2002). Finally, the synthesis of apatites is relatively straightforward in shielded environments. For certain fission products such as ^{129}I, apatite is one of a limited number of less soluble structures that can condition such waste for storage (Audubert et al. 1997). Most recently, silicate apatites have been studied for the incorporation of plutonium and uranium (Vance et al. 2003).

The intrinsic potential of the apatite structure type for radioactive waste disposal arises directly from crystal chemical adaptation of its framework structure (Dong et al. 2002; Kim et al. 2004), its capacity to be nonstoichiometric, and the ability to increase the number of cation acceptor sites through reduction in symmetry. These properties allow apatites to respond to variations in waste stream composition without intervention to adjust the constitution of stabilization additives.

Catalysis

Several apatites are under investigation as heterogeneous catalysts (Matsumura et al. 1997). For example, hydroxyapatite showed high catalytic activity and selectivity in a Michael addition reaction (Zahouily et al. 2003) involving thiophenol and various chalcones. Interestingly, it is believed that in this instance the catalytic activity of hydroxyapatite does not originate from inside the tunnels, as is the case for some zeolites, but rather at the surface whose acidic character enhanced thiol nucleophilicity. If such catalytic reactions proved viable, they would be environmentally benign compared to basic homogeneous catalysts.

Hydroxyapatite also shows potential in photocatalysis, both as a catalyst in its own right, and as a carrier material for semiconductors such as titania (Nishikawa and Omamiuda 2002). In this case, the highly sorptive capacity of apatite is coupled with its catalytic activity to simultaneously destroy pollutants and capture them for later disposal.

Fuel cell electrolytes

Alumino-silicate (Kahlenberg and Kruger 2004) and germano-silicate (Sansom and Slater 2004) apatites may play a role as electrolytes in solid oxide fuel cells (SOFCs) that will be important components of future clean energy systems. The aim is to achieve high ionic conductivity (σ) at the lowest temperatures possible. Thus, for example, while yttria stablised zirconia (YSZ) is presently the *de facto* standard oxide with $\sigma = 1 \times 10^{-3}$ S cm^{-1} at 500°C, $La_{10}(SiO_4)_6O_3$ is more than four times as conductive with $\sigma = 4.3 \times 10^{-3}$ S cm^{-1} at the same temperature (Nakayama et al. 1995). Reducing SOFC operating temperatures (currently between 950 and 1050°C) could increase their service life by reducing damaging reactions at

interfaces and make them much less expensive due to replacement of ceramic interconnectors by less expensive metals.

A recent neutron diffraction investigation by León-Reina et al. (2004) of $La_{10-x}(SiO_4)_6O_{3-1.5x}$ ($9.33 \leq 10-x \leq 9.73$) conducted at room temperature, 500°C and 900°C showed the presence of interstitial oxygen [the "O(5) site"] in the tunnels located in positions almost directly above or below the La(2) cations (Fig. 25a). Using computer modeling techniques Tolchard et al. (2003) demonstrated that local relaxation of the SiO_4 tetrahedra permit O(5)-vacancy conduction through the apatite tunnels by a sinusoidal pathway. It is perhaps relevant that $A_{10}(BO_5)_6X_2$ apatites such as $Sr_{10}(ReO_5)_6Cl_2$ are fully stoichiometric in terms of O(5) resulting in the expansion of the BO_4 tetrahedra to BO_5 square pyramids (Fig. 25b). The synthesis of mixed silico-rhenate apatites could therefore be a useful method for controlling O(5)-vacancy combinations and to optimize ionic conductivity.

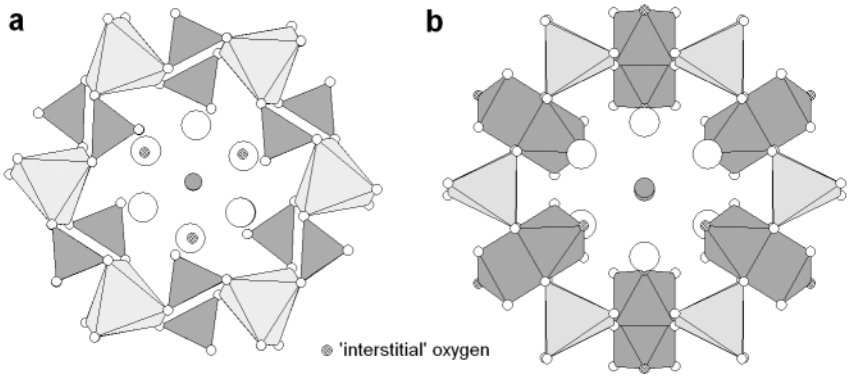

Figure 25. Location of "interstitial" oxygen in (a) $La_{9.55}(SiO_4)_6O_{2.32}$ and (b) $Sr_{10}(ReO_5)_6Cl_2$.

Permeable reaction barriers

The concept of a permeable reaction barrier (PRB) involves the installation of trenches around contaminated sites that will be filled with material of specific chemical reactivity and high permeability to water, to effectively prevent the migration of pollutants to the wider environment. Several designs have been implemented including zeolites, zero valent iron and apatites. In the latter case, a technology known as Apatite II® is best developed and is being trialed at various sites (Wright et al. 2004). This phosphate apatite has been optimized chemically and microstructurally to adsorb and fix a wide range of toxic and radioactive species and has the nominal composition $Ca_{10-x}Na_x(PO_4)_{6-x}(CO_3)_x(OH)_2$. The principle features of this material that make it especially suitable for remediation include low fluorine content, higher substitutions of carbonate and sodium, high purity with few trace elements, X-ray amorphosity and high porosity.

For metal fixation, dissolution-precipitation reactions are the dominant immobilization mechanism rather than lattice ion exchange. In the case of lead (and also uranium, cerium and plutonium) the reaction sequence is

$$Ca_{10-x}Na_x(PO_4)_{6-y}(CO_3)_y(OH)_2 + 14H^+ \rightarrow (10-x)Ca^{2+} + xNa^+ + (6-y)[H_2(PO_4)]^- + yH_2CO_3 + 2H_2O$$

$$10Pb^{2+} + 6[H_2(PO_4)]^- + 2OH^- \rightarrow Pb_{10}(PO_4)_6(OH)_2 + 12H^+$$

However, for zinc, cadmium and other transition metals non-apatite phases are precipitated.

CONCLUSION

The crystal chemistry of apatites continues to be a highly active field of study more than 70 years after Hausen (1929) recognized eight apatite types including fluorapatite, alkali-apatite, chlorapatite, carbonate apatite, sulfate apatite, hydroxyapatite, manganese apatite and rare earth bearing apatites. The ongoing pursuit for understanding these materials is driven both by a fundamental interest in exploring the range of natural and synthetic compositions, and technology-focused initiatives to develop new materials with specific properties. This article has attempted to draw together several lines of contemporary thought concerning the underlying principles that lead to the crystallization of such a diverse structural family. However, the topic is vast, and inevitably, important areas have been excluded or dealt with in a cursory fashion. Aside from the voluminous literature concerning biological apatites (Weiner and Wagner 1998; Elliott 2002), other interesting apatite variants are known. For instance, Carrillo-Cabrera and von Schnering (1999) were the first to insert metal-oxygen strings along the apatite channels when they synthesized $Sr_{10}(VO_4)_6(Cu_{0.896}O_{0.95})_2$. More recent work has lead to a number of phosphate analogues including $Ca_{10}(PO_4)_6(Cu_{0.27}O_{0.86}H_y)_2$, $Sr_{10}(PO_4)_6(Cu_{0.33}O_{0.66})_2$ and $Ba_{10}(PO_4)_6(Cu_{0.30}O_{0.86}H_y)_2$ that display brilliant blue colors and may find application as paint pigment (Karpov et al. 2003; Kazin et al. 2003).

Polysomatism is another structural modification that has to date received little attention. While $[A(1)_4][A(2)_6](BO_4)_6X_2$ apatites regularly fill every other BO_4 tetrahedral interstice occurring as corner-connected strings along [001] alternate filling schemes are possible. Accordingly, nasonite with the ideal formula $Pb_6Ca_4(Si_2O_7)_3Cl_2$ contains alternating pairs of filled and empty tetrahedra (Engel 1972; Giuseppetti et al. 1971). It is then possible to construct an apatite-nasonite polysomatic series in which ganomalite is an intermediate member (White and Dong 2003) having the ideal formula $Pb_6Ca_{3.33}Mn_{0.67}(SiO_4)_2(Si_2O_7)_2$ in which Si_2O_7 units alternate with SiO_4 tetrahedra (Carlson et al. 1997). In addition to these minerals, the synthetic analogue of ganomalite $Pb_{10}(GeO_4)_2(Ge_2O_7)_2$ has been studied extensively due to its ferroelectric properties (Newnham et al. 1973; Iwata 1977) and Stemmermann (1992) synthesized the longer period $Pb_{40}(Si_2O_7)_6(Si_4O_{13})_3$. All the members so far reported for the apatite-nasonite family are lead-rich with the role of lone-pair stabilization yet to be fully investigated.

As there are numerous possibilities for structural adaptation and their utility in contemporary technologies is growing, it is anticipated that apatites will continue to surprise in terms of their chemical and physical complexity for some time to come.

ACKNOWLEDGMENTS

The authors are most appreciative of the efforts of Professor Donald B. McIntyre for recovering copies of the plates reproduced in Figure 1, and for providing the historical context of his work with C.A. Beevers and the influence of V.M. Goldschmidt. Reproduction of the color plates was generously funded by the Carnegie Trust for the Universities of Scotland. This work was supported through Singapore Agency for Science, Technology and Research (A*STAR) Grants 012 105 0123, 033 141 01 and M47030104. The authors are grateful to Dr. Dong ZhiLi for access to unpublished data and for the calculation of the twist angles reported throughout the text.

REFERENCES

Akao M, Aoki H, Innami Y, Minamikata S, Yamada T (1989) Flux growth and crystal structure of pyromorphite. Iyo Kiazai Kenkyusho Hokoku, Tokyo Ika Shika Daigu 23:25-29

Akhavan-Niaki AN (1961) Contribution a l'étude des substitutions dans les apatites. Ann Chim (Paris) 6: 51-79

Alberius-Henning P, Landa-Cánovas, Larsson A-K, Lidin S (1999a) Elucidation of the crystal of oxyapatite by high-resolution electron microscopy. Acta Crystallogr B55:170-176

Alberius-Henning P, Lidin S, Petrícek V (1999b) Iodo-oxyapatite, the first example from a new class of modulated apatites. Acta Crystallogr B55:165-169

Alberius-Henning PA, Moustiakimov M, Lidin S (2000) Incommensurately modulated cadmium apatites. J Solid State Chem 150:154-158

Andersson S (1978) An alternative description of the structures of Rh_7Mg_{44} and Mg_6Pd. Acta Crystallogr A34: 833-835

Andres-Verges M, Highes-Rolando FJ, Valenzuela-Calahorro C, Gonzalez-Diaz PF (1983) On the structure of calcium-lead phosphate apatites. Spectrochim Acta A39:1077-1082

Arnich N, Lanhers MC, Laurensot F, Podor R, Montiel A, Burnel D (2003) In vitro and in vivo studies of lead immobilization by synthetic hydroxyapatite. Env Poll 124:139-149

Audubert F, Carpena J, Lacout JL, Tetard F (1997) Elaboration of an iodine-bearing apatite – iodine diffusion into a $Pb_3(VO_4)_2$ matrix. Solid State Ionics 95:113-119

Audubert F, Savariault JM, Lacout JL (1999) Pentaleadtris (vanadate) iodide, a defect vanadinite-type compound. Acta Crystallogr C55:271-273

Badraoui B, Bigi A, Debbabi M, Gazzano M, Roveri N, Thouvenot R (2002a) X-ray powder diffraction and solid-state NMR investigations in cadmium-lead hydroxyapatites. Eur J Inorg Chem 6:1261-1267

Badraoui B, Bigi A, Debbabi M, Gazzano M, Roveri N, Thouvenot R (2002b) Physicochemical properties and structural refinement of strontium-lead hydroxyapatites. Eur J Inorg Chem 7:1864-1870

Badrour L, Sadel A, Zahir M, Kimakh L, El Hajbi (1998) Synthesis and physical and chemical characterization of $Ca_{10-x}Ag_x(PO_4)_6(OH)_{2-x}\square_x$ apatites. Ann Chim Sci Mat 23:61-64

Banks E, Jaunarajs KL (1965) Chromium analogs of apatite and spodiosite. Inorg Chem 4:78-83

Barinova AV, Bonin M, Pushcharovskii DYu, Rastsvetaeva RK, Schenk K, Dimitrova OV (1998) Crystal structure of synthetic hydroxylpyromorphyte $Pb_5(PO_4)_3(OH)$. Crystallogr Rep 43:189

Baud G, Besse JP, Capestan M, Sueur G, Chevalier R (1980) Etude comparative d'apatites contenant l'ion $(ReO_5)^{3-}$. Structure des fluoro et des carbonatoapatites. Ann Chim Sci Mat 5:575-583

Baud G, Besse JP, Sueur G, Chevalier R (1979) Structure de nouvelles apatites au rhenium contenant des anions volumineux: $Ba_{10}(ReO_5)_6X_2$ (X = Br, I). Mater Res Bull 14:675-682

Bauer M, Klee WE (1993) Induced ferrielectricity in chlorapatite. Z Kristallogr 206:15-24

Beevers CA, McIntyre DB (1946) The atomic structure of fluor-apatite and its relation to that of tooth and bone material. Mineral Mag 27:254-257

Belokoneva EL, Troneva EA, Dem'yanets LN, Duderov NG, Belov NV (1982) Crystal structure of synthetic fluoropyromorphite $Pb_5(PO_4)_3F$. Sov Phys Crystallogr 27:476-477

Benmoussa H, Mikou M, Bensaoud A, Bouhaouss A, Morineaux R (2000) Electrical properties of lanthanum containing vanadocalcic oxyapatite. Mater Res Bull 35:369-375

Berastegui P, Hull S, Garcia Garcia FJ, Grins J (2002) A structural investigation of $La_2(GeO_4)O$ and alkaline-earth-doped $La_{9.33}(GeO_4)_6O_2$. J Solid State Chem 168:294-305

Bertoni E, Bigi A, Cojazzi G, Gandolfi M, Panzavolta S, Roveri N (1998) Nanocrystals of magnesium and fluoride substituted hydroxyapatite. J Inorg Biochem 72:29-35

Besse JP, Baud G, Chevalier R, Zarembowitch J (1980) Mise en évidence de l'ion O^{2-} dans l'apatite au rhenium $Ba_5(ReO_5)_3O_2$. Mater Res Bull 15:1255-1261

Besse JP, Baud G, Levasseur G, Chevalier R (1979) Structure crystalline de $Ba_5(ReO_5)_3Cl$: une nouvelle apatite contenant l'ion $(ReO_5)^{3-}$. Acta Crystallogr B35:1756-1759

Bigi A, Falini G, Foresti E, Gazzano M, Ripamonti A, Roveri N (1996) Rietveld structure refinements of calcium hydroxylapatite containing magnesium. Acta Crystallogr B52:87-92

Bigi A, Gandolfi M, Gazzano M, Ripamonti A, Roveri N, Thomas S (1991) Structural modifications of hydroxyapatite induced by lead substitution for calcium. J Chem Soc Dalton Trans 2883-2886

Bigi A, Ripamonti A, Brückner S, Gazzano M, Roveri N, Thomas SA (1989) Structure refinements of lead-substituted calcium hydroxyapatite by X-ray powder fitting. Acta Crystallogr B45:247-251

Birkett TC, Simandl GJ (1999) Carbonatite-associated deposits: magmatic, replacement and residual. *In*: Selected British Columbia Mineral Deposit Profiles. Vol 3. Simandl GJ, Hora ZD, Lefebure DV (eds) British Columbia Ministry of Energy and Mines

Boechat CB, Eon J-C, Rossi AM, de Castro Perez CA, da Silva San Gil RA (2000) Structure of vanadate in calcium phosphate and vanadate apatite solid solutions. Phys Chem Chem Phys 2:4225-4230

Bondareva OS, Malinovskii YuA (1986) Crystal structure of synthetic Ba hydroxylapatite. Sov Phys Crystallogr 31:136-138

Borodin LS, Kazakova ME (1954) Belovite-(Ce): a new mineral from an alkaline pegmatite. Dokl Akad Nauk SSSR 96:613-616 (in Russian)

Boudreau AE (1995) Formation of chlor- and fluor-apatite in layered intrusions: a comment. Mineral Mag 59: 757-760
Boyer L, Carpena J, Lacout JL (1997) Synthesis of phosphate-silicate apatites at atmospheric pressure. Solid State Ionics 95:121-129
Boyer L, Savariault JM, Carpena J, Lacout JL (1998) A neodymium-substituted britholite compound. Acta Crystallogr C54:1057-1059
Brégiroux D, Audubert F, Champion E, Bernache-Assollant D (2003) Mechanical and thermal properties of hot pressed neodymium-substituted britholite $Ca_9Nd(PO_4)_5(SiO_4)F_2$. Mater Lett 57:3526-3531
Brendel T, Engel A, Russel C (1992) Hydroxyapatite coating by polymeric route. J Mater Sci Mater Med 3: 175-179
Brock WH (1993) The Norton history of chemistry. WW Norton & Company, New York (p 285)
Brown PW, Constantz B (1994) Hydroxyapatite and related materials. CRC Press, Boca Raton
Brückner S, Lusvardi G, Menabue L, Saladini M (1995) Crystal structure of lead hydroxyapatite from powder X-ray diffraction data. Inorg Chim Acta 236:209-212
Brunet F, Allan DR, Redfern SA, Angel RJ, Miletich R, Reichmann HJ, Sergent J, Hanfland M (1999) Compressibility and thermal expansivity of synthetic apatites $Ca_5(PO_4)_3X$ with X = OH, F and Cl. Eur J Mineral 11:1023-1035
Burnett WC, Riggs SR (1990) Phosphate deposits of the world, Neogene to modern phosphorites. Vol 3 Burnett, WC Riggs SR (eds). Cabridge University Press, New York
Bushinskiy GI (1964) On shallow water origin of phosphorite sediments, deltaic and shallow marine deposits. Develop Sediment 1:62-70
Buvaneswari G, Varadaraju UV (2000) Synthesis and characterization of new apatite-related phosphates. J Solid State Chem 149:133-136
Calos NJ, Kennard CHL (1990) Crystal structure of mimetite, $Pb_5(AsO_4)_3Cl$. Z Kristallogr 191:125-129
Calvo C, Faggiani R, Krishnamachari N (1975) Crystal structure of $Sr_{9.402}Na_{0.209}(PO_4)_6B_{0.996}O_2$ - a deviant apatite. Acta Crystallogr B31:188-192
Carlson S, Norrestam R, Holstam D, Spengler R (1997) The crystal structure of ganomalite, $Pb_9Ca_{5.44}Mn_{0.56}Si_9O_{33}$. Z Kristallogr 212:208-212
Carrillo-Cabrera W, Von Schnering HG (1999) Pentastrontium tris[tetraoxovanadate(V)] *catena*-monoxocuprate(I), $Sr_5(VO_4)_3(CuO)$ - an apatite derivative with inserted linear $[CuO]^{1-}$ chains. Z Anorg Allg Chem 625:183-185
Cockbain AG, Smith GV (1967) Alkaline-earth-rare-earth silicate and germanate apatites. Mineral Mag 36: 411-421
Collin RL (1959) Strontium-calcium hydroxyapatite solid solutions: preparation and lattice constant measurements. J Am Chem Soc 81:5275-5278
Comodi P, Liu Y, Zanazzi PF, Montagnoli M (2001) Structural and vibrational behaviour of fluorapatite with pressure. Part I: *in situ* single-crystal X-ray diffraction investigation. Phys Chem Mineral 28:219-224
Corker DL, Chai BHT, Nicholls J, Loutts GB (1995) Neodymium-doped $Sr_5(PO_4)_3F$ and $Sr_5(VO_4)_3F$. Acta Crystallogr C51:549-551
Dai YS, Hughes JM (1989) Crystal structure refinements of vanadinite and pyromorphite. Can Mineral 27: 189-192
Dai YS, Hughes JM, Moore PB (1991) The crystal structures of mimetite and clinomimetite, $Pb_5(AsO_4)_3Cl$. Can Mineral 29:369-376
Dardenne K, Vivien D, Huguenin D (1999) Color of Mn(V)-substituted apatites $A_{10}[(B,Mn)O_4]_6F_2$, A = Ba, Sr, Ca; *B* = P, V. J Solid State Chem 146:464-472
Daubrée A (1851) Expériences sur la production artificielle de l'apatite, de la topaze, et de quelques autres métaux fluoriféres. Compt Rend Acad Sci Paris 32:625
De Boer BG, Sakthivel A, Cagle JR, Young RA (1991) Determination of the antimony substitution site in calcium fluorapatite from powder x-ray diffraction data. Acta Crystallogr B47:683-692
Donaldson JD, Grimes SM (1984) Novel tin(II) sites in X-ray crystal structures of the tin(II) halide sulphates $K_3Sn_2(SO_4)_3X$ (X = Br or Cl). J Chem Soc Dalton Trans 1301-1305
Dong ZL, Kim J, White TJ (2005a) Crystal chemical systematics in $[Ca]_{10}[(P_{10-x}V_x)O_4]_6[F]_2$ and $[Ca]_{10}[(P_{10-x}V_x)O_4]_6[Cl]_2$ apatites. In preparation
Dong ZL, Sun K, Wang LM, White TJ, Ewing RC (2005b) Electron irradiation induced transformation of $(Pb_5Ca_5)(VO_4)_6F_2$ apatite to $CaVO_3$ perovskite. J Am Ceram Soc 88:184-190
Dong ZL, White TJ (2004a) Calcium-lead fluoro-vanadinite apatites. I. Disequilibrium structures. Acta Crystallogr B60:138-145
Dong ZL, White TJ (2004b) Calcium-lead fluoro-vanadinite apatites. II. Equilibrium structures. Acta Crystallogr B60:146-154
Dong ZL, White TJ, Wei B, Laursen, K. (2002) Model apatite systems for the stabilization of toxic metals: I. calcium lead vanadate. J Am Ceram Soc 85:2515-2522

Dunn PJ, Peacor DR, Newberry N (1980) Johnbaumite, a new member of the apatite group from Franklin, New Jersey. Am Mineral 65:1143-1145

Dunn PJ, Rouse RC (1978) Morelandite, a new barium arsenate chloride member of the apatite group. Can Mineral 16:601-604

Effenberger H, Pertlik F (1977) Anzeiger der oesterreichischen Akademie der Wissenschaften, mathematisch-naturwissenschaftliche Klasse 114:209-211

El Feki H, Savariault JM, Ben Salah A (1999) Structure refinements by the Rietveld method of partially substituted hydroxyapatite: $Ca_9Na_{0.5}(PO_4)_{4.5}(CO_3)_{1.5}(OH)_2$. J All Comp 287:114-120

El Koumiri M, Oishi S, Sato S, El Ammari L, Elouadi B (2000) The crystal structure of the lacunar apatite $NaPb_4(PO_4)_3$. Mater Res Bull 35:503-513

Elliott JC (1973) Problems of composition and structure of mineral components of hard tissues. Clinic Orthopaedics Related Res 93:313-345

Elliott JC (1994) Structure and chemistry of the apatites and other calcium orthophosphates. Elsevier, Amsterdam

Elliott JC (2002) Calcium phosphate biominerals. Rev Mineral Geochem 48:427-453

Elliott JC, Bonel G, Trombe JC (1980) Space group and lattice constants of $Ca_{10}(PO_4)_6CO_3$. J Appl Crystallogr 13:618-621

Elliott JC, Dykes E, Mackie PE (1981) Structure of bromapatite, $Ca_5(PO_4)_3Br$, and the radius of the bromide ion. Acta Crystallogr B37:435-438

Elliott JC, Mackie PE, Young RA (1973) Monoclinic hydroxyapatite. Science 180:1055-1057

El Ouenzerfi R, Goutaudier C, Panczer G, Moine B, Cohen-Adad MT, Trabelsi-Ayedi M, Kbir-Ariguib N (2003) Investigation of the $CaO–La_2O_3–SiO_2–P_2O_5$ quaternary diagram: synthesis, existence domain, and characterization of apatitic phosphosilicates. Solid State Ionics 156:209–222

Engel G (1965) Untersuchungen zur Kristallchemie von Cadmiumphosphaten,-arsenaten und-vanadaten mit Apatitstruktur. Diplomarbeit Tech Hochsch Karlsruhe

Engel G (1970) Hydrothermalsynthese von Bleihydrooxylapatiten $Pb_5(XO_4)_3OH$ mit X = P, As, V. Naturwissenschaften 57:355

Engel G (1972) Ganomalite an intermediate between the nasonite and apatite types. Naturwissenschaften 59: 121-122

Engel G (1978) Fluoroberyllate mit apatitstruktur und ihre beziehungen zu sulfaten und silicaten. Mater Res Bull 13:43-48

Engel G, Deppisch B (1988) Die Kristallstruktur von $Pb_5(GeO_4)_2SO_4$ und $Pb_5(Ge\ O_4)_2\ CrO_4$, zweier Bleiapatite mit unbesetzten Halogenlagen. Z Anorg Allg Chem 562:131-140

Engel G, Fischer U (1990) Die Kristallstruktur von $Na_3Pb_2(BeF_4)_3F$, einem Fluoroberyllat mit Apatitstruktur. J Less-Common Metals 158:123-130

Engel G, Krieg, Reif G (1975a) Mischkristallbildung und Kationenordnung im System Bleihydroxylapatit-Calciumhydroxylapatit. J Solid State Chem 15:117-126

Engel G, Pretzsch J, Gramlich V, Baur WH (1975b) The crystal structure of hydrothermally grown manganese chlorapatite, $Mn_5(PO_4)_3Cl_{0.9}(OH)_{0.1}$. Acta Crystallogr B31:1854-1860

Engin NO, Tas AC (2000) Preparation of porous $Ca_{10}(PO_4)_6(OH)_2$ and β-$Ca_3(PO_4)_2$ bioceramics. J Am Ceram Soc 83:1581-1584

Ewing RC, Meldrum A, Wang LM, Wang SX (2000) Radiation-induced amorphization. Rev Mineral Geochem 39:319-354

Ewing RC, Wang LM (2002) Phosphates as Nuclear Waste Forms. Rev Mineral Geochem 48:673-699

Fahey JA, Weber WJ, Rotella FJ (1985) An X-ray and neutron powder diffraction study of the $Ca_{2+x}Nd_{8-x}(SiO_4)_6O_{2-0.5x}$ system. J Solid State Chem 60:145-158

Fayos J, Watkin DJ, Pérez-Méndez M (1987) Crystal structure of apatite-like compound $K_3Ca_2(SO_4)_3F$. Am Mineral 72:209-212

Fedoroff M, Jeanjean J, Rouchaud JC, Mazerolles I, Trocellier P, Maireles-Torres P, Jones DJ (1999) Sorption kinetics and diffusion of cadmium in calcium hydroxyapatites. Solid State Sci 1:71-83

Felsche J (1972) Rare earth silicates with the apatite structure. J Solid State Chem 5:266-275

Ferraris C, White TJ, Plévert J, Wegner R (2004) First evidence for nano-scale exsolution in apatite. Submitted

Fleet ME, Liu X (2003) Carbonate apatite type A synthesized at high pressure: new space group (*P*3) and orientation of channel carbonate ion. J Solid State Chem 174:412-417

Friis H, Balić-Žunić T, Pekov IV, Petersen OV (2004) Kuannersuite-(Ce), $Ba_6Na_2REE_2(PO_4)_6FC1$, a new member of the apatite group, from the ilímaussaq alkaline complex, South Greenland: description and crystal chemistry. Can Mineral 42:95-106

Gaude J, L'Haridon P, Hamon C, Marchand R, Laurent Y (1975) Composés à structure apatite. I. Structure de l' oxynitrure $Sm_{10}Si_6N_2O_{24}$. Bull Soc Fr Mineral Crist 98:214-217

Genkina EA, Malinovskii YuA, Khomyakov AP (1991) Crystal structure of Sr-containing britholith. Sov Phys Crystallogr 36:19-21

Giuseppetti G, Rossi G, Tadini C (1971) The crystal structure of nasonite. Am Mineral 56:1174-1179
Grisafe DA, Hummel FA (1970a) Pentavalent ion substitutions in the apatite structure Part A. Crystal chemistry. J Solid State Chem 2:160-166
Grisafe DA, Hummel FA (1970b) Crystal chemistry and color in apatites containing cobalt, nickel and rare-earth ions. Am Mineral 55:1131-1145
Gunawardane RP, Howie RA, Glasser FP (1982) Structure of the oxyapatite $NaY_9(SiO_4)_6O_2$. Acta Crystallogr B38:1564-1566
Habelitz S, Pascual L, Durán A (1999) Nitrogen-containing apatite. J Eur Ceram Soc 19:2685-2694
Hashimoto H, Matsumoto T (1998) Structure refinements of two natural pyromorphites, $Pb_5(PO_4)_3Cl$, and crystal chemistry of chloroapatite group, $M_5(PO_4)_3Cl$. Z Kristallogr 213:585-590
Hata M, Marumo F (1983) Syntheses and superstructures of $(Cd, M)_5(PO_4)_3OH$ (M = Mn, Fe, Co, Ni, Cu, Hg). Mineral J 11:317-330
Hata M, Marumo F, Iwai S (1979) Structure of barium chlorapatite. Acta Crystallogr B35:2382-2384
Hata M, Marumo F, Iwai S, Aoki H (1980) Structure of a lead apatite $Pb_9(PO_4)_6$. Acta Crystallogr B36:2128-2130
Hata M, Okada K, Iwai S (1978) Cadmium hydroxyapatite. Acta Crystallogr B34:3062-3064
Hausen H (1929) Die Apatite, deren chemische Zusammensetzung und ihr Verhältnis zu den physikalischen und morphologischen Eigenschaften. Acta Acad Åbo Math-Phys 5
Hendricks SB, Jefferson ME, Mosley VM (1932) The crystal structures of some natural and synthetic apatite-like substances. Z Kristallogr Kristallogeom Kristallphys Kristallchem 81:352-369
Herdtweck E (1991) Structure of decastrontium hexachromate(V) difluoride. Acta Crystallogr C47:1711-1712
Higuchi M, Katase H, Kodaira K, Nakayama S (2000) Float zone growth and characterization of $Pr_{9.33}(SiO_4)_6O_2$ and $Sm_{9.33}(SiO_4)_6O_2$ single crystals with an apatite structure. J Crystal Growth 218:282-286
Hitmi N, LaCabanne C, Bonel G, Roux P, Young RA (1986) Dipole co-operative motions in an A-type carbonated apatite, $Sr_{10}(AsO_4)_6CO_3$. J Phys Chem Solids 47:507-515
Howie RA, Moser W, Starks RG, Woodhams FWD, Parker W (1973) Potassium tin(II) sulphate and related tin apatites: Mossbauer and X-ray studies. J Chem Soc Dalton Trans 14:1478-1484
Huang J, Sleight AW (1993) The apatite structure without an inversion center in a new bismuth calcium vanadium oxide $BiCa_4V_3O_{13}$. J Solid State Chem 104:52-58
Hughes JM, Cameron M, Crowley KD (1989) Structural variations in natural F, OH, and Cl apatites. Am Mineral 74:870-876
Hughes JM, Cameron M, Crowley KD (1991) Ordering of divalent cations in the apatite structure: Crystal structure refinements of natural Mn- and Sr-bearing apatite. Am Mineral 76:1857-1862
Hughes JM, Drexler JW (1991) Cation substitution in the apatite tetrahedral site: crystal structures of type hydrxylellstadite and type fermorite. N Jahrb Mineral Monatsh 1991:327-336
Hughes JM, Mariano AN, Drexler W (1992) Crystal structures of synthetic Na-REE-Si oxyapatites, synthetic monoclinic britholite. N Jahrb Mineral Monatsh 1992:311-319
Hughes JM, Rakovan J (2002) The crystal structure of apatite $Ca_5(PO_4)_3(F, OH, Cl)$. Rev Mineral Geochem 48:1-12
Huminicki DMC, Hawthorne FC (2002) The crystal chemistry of the phosphate minerals. Rev Mineral Geochem 48: 123-254
Ikoma T, Yamazaki A, Nakamura S, Akao M (1999) Preparation and structure refinement of monoclinic hydroxyapatite. J Solid State Chem 144:272-276
Ito J (1968) Silicate apatites and oxyapatites. Am Mineral 53:890-907
Ivanov SA (1990) Refinement of the crystal structure of $Pb_5(GeO_4)(VO_4)_2$ relative to the powder diffraction patterns profile. J Struct Chem 31:80-84
Ivanov SA, Zavodnik VE (1989) Crystal structure of $Pb_5GeV_2O_{12}$. Sov Phys Crystallogr 34:493-496
Ivanova TI, Frank-Kamenetskaya OV, Kol'tsov AB, Ugolkov VL (2001) Crystal structure of calcium-deficient carbonated hydroxyapatite - thermal decomposition. J Solid State Chem 160:340-349
Iwata Y (1977) Neutron diffraction study of the structure of paraelectric of $Pb_5Ge_3O_{11}$. J Phys Soc Japan 43: 961-967
Jeanjean J, McGrellis S, Rouchaud JC, Fedoroff M, Rondeau A, Perocheau A, Dubis A (1996a) A crystallographic study of the sorption of cadmium on calcium hydroxyapatites: incidence of cationic vacancies. J Solid State Chem 126:195-201
Jeanjean J, Vincent U, Fedorof M (1994) Structural modification of calcium hydroxyapatite induced by sorption of cadmium ions. J Solid State Chem 108:68-72
Jeanjean J, Vincent U, Fedorov M (1996b) Structural modification of calcium hydroxyapatite induced by sorption of cadmium ions. J Solid State Chem 108:68-72
Kabalov YK, Sokolova EV, Pekov IV (1997) Crystal structure of belovite-(La) Dokl Akad Nauk 355:182-185

Kahlenberg V, Krüger H (2004) $LaAlSiO_5$ and apatite-like $La_{9.71}(Si_{0.81}Al_{0.19}O_4)_6O_2$ – the crystal structures of two synthetic lanthanum aluminosilicates. Solid State Sci 6:553-560

Kalsbeek N, Larsen S, Ronsbo JG (1990) Crystal structures of rare elements rich apatite analogues. Z Kristallogr 191:249-263

Karpov AS, Nuss J, Jensen M (2003) Synthesis, crystal structure and properties of calcium and barium hydroxyapatites containing copper ions in hexagonal channels. Solid State Sci 5:1277-1283

Kauffman GB (1997) Victor Moritz Goldschmidt (188-1947): A tribute to the founder of modern geochemistry on the fiftieth anniversary of his death. Chem Educator 2:S1430-4171.

Kay MI, Young RA, Posner AS (1964) Crystal structure of hydroxyapatite. Nature 204:1050-1052

Kazin PE, Karpov AS, Jansen M, Nuss J, Tretyakov YD (2003) Crystal structure and properties of strontium phosphate apatite with oxocuprate ions in hexagonal channels. Z Anorg Allg Chem 629:344-352

Khomyakov AP, Kulikova IM, Rastsvetaeva RK (1997) Fluorcaphite, $Ca(Sr,Na,Ca)(Ca,Sr,Ce)_3(PO_4)_3F$ - a new mineral with the apatite structural motif. Zap Vser Mineral Obshch 126:87-97 (in Russian)

Khomyakov AP, Lisitsin DV, Kulikova IM, Rastsvetsaeva RK (1996) Deloneite-(Ce) $NaCa_2SrCe(PO_4)_3F$ - a new mineral with a belovite-like structure. Zap Vser Mineral Obshch 125:83-94 (in Russian)

Kikuchi M, Yamazaki A, Otsuka R, Akao M, Aoki H (1994) Crystal structure of Sr-substituted hydroxyapatite synthesized by hydrothermal method. J Solid State Chem 113:373-378

Kim JY (2001) Structural studies of lead containing apatites. PhD dissertation, School of Chemistry – The University of Sydney

Kim JY, Dong ZL, White, TJ (2005) Model apatite systems for the stabilization of toxic metals: II netalloid substitutions. J Am Ceram Soc, in press

Kim JY, Fenton RR, Hunter BA, Kennedy BJ (2000) Powder diffraction studies of calcium and lead apatites. Aust J Chem 53:679-686

Klement R, Dihn P (1941) Isomorphe apatitarten. Naturwissenschaften 29:301

Klement R, Harth R (1961) Das verhalten von tertiären erdalkaliphosphaten,-arsenaten und-vanadaten in geschmolzenen halogeniden. Chem Ber 94:1452-1456

Klement R, Haselbeck H (1965) Apatite and wagnerite zweiwertige metalle. Z Anorg Allgem Chem 336: 113-128

Klevtsova RF (1964) About the crystal structure of strontiumapatite. Zh Strukt Khim 5:318-320 (in Russian)

Klevtsova RF, Borisov SV (1964) The crystal structure of belovite. Zh Strukt Khim 5:151-153 (in Russian)

Kluver E, Mueller-Buschbaum (1995) Uber einen lanthanoid-mangan-apatit: $Nd_4Mn(SiO_4)_3O$. Z Naturforsch Teil B50:61-65

Knudsen AC, Gunter ME (2002) Sedimentary phosporites – An example: phosphoria formation, southeastern Idaho, U.S.A. Rev Mineral Geochem 48:363-390

Kohn MJ, Cerling TE (2002) Stable isotope compositions of biological apatite. Rev Mineral Geochem 48: 455-488

Kohn MJ, Rakovan J, Hughes JM (eds) (2002) Phosphates – geochemical, geobiological, and materials importance. Mineralogical Society of America and Geochemical Society, Washington DC

Kottaisamy M, Jagannathan R, Jeyagopal P, Rao RP, Narayanan (1994) Eu^{2+} luminescence in $M_5(PO_4)_3X$ apatites, where M is Ca^{2+}, Sr^{2+} and Ba^{2+}, and X is F^-, Cl^-, Br^- and OH^-. J Phys D: Appl Phys 27:2210-2215

Kreidler ER, Hummel FA (1970) The crystal chemistry of apatite: structure fields of fluor- and chlorapatite. Am Mineral 55:170-184

Kutoglu A Von (1974) Structure refinement of the apatite $Ca_5(VO_4)_3(OH)$. N Jahrb Mineral Monatsh 1974: 210-218

Kutoglu A Von, Schulien S (1972) Synthese und Kristallstruktur eines Calcium-vanadates. Naturwiss 59:36

Kuzmin EA, Belov NV (1965) Crystalline structure of simple silicates, lanthanum and samarium. Dokl Akad Nauk SSSR 165:88-90

León-Reina L, Losilla ER, Martínez-Lara M, Bruque S, Aranda MAG (2004) Interstitial oxygen conduction in lanthanum oxy-apatite electrolytes. J Mat Chem 14:1142-1149

Leventouri Th, Chakoumakos BC, Moghaddam HY, Perikatsis V (2000) Powder neutron diffraction studies of a carbonate fluorapatite. J Mater Res 15:511-517

Liu DM, Quanzu Yang Q, Troczynski T, Tseng WJ (2002) Structural evolution of sol-gel-derived hydroxyapatite. Biomaterials 23:1679-1687

Liou S-C, Chen S-Y, Lee H-Y, Bow J-S (2004) Structural characterization of nano-sized calcium deficient apatite powders. Biomaterials 25:189-196

Lower SK, Maurice PA, Traina SJ, Carlson EH (1998) Aqueous Pb sorption by hydroxylapatite: application of atomic force microscopy to dissolution, nucleation, and growth studies. Am Mineral 83:147-158

Lutze W, Ewing RC (1988) Radioactive waste forms for the future. North-Holland, Amsterdam

Mackie PE, Elliott JC, Young RA (1972) Monoclinic structure of synthetic $Ca_5(PO_4)_3Cl$ chlorapatite. Acta Crystallogr B28:1840-1848

Malinovskii YuA, Genkina EA, Dimitrova OV (1990) TR-ordering in crystal structure of $La_3Nd_{11}(SiO_4)_9O_3$. Sov Phys Crystallogr 35:184-186

Malinovskii YuA, Pobedimskaya EA, Belov NV (1975) Synthesis and crystal structure of the germanate-carbonate apatite, $Ba_5(Ge,C)(O,OH)_4)_3(OH)$. Sov Phys Crystallogr 20:395-396

Mandjiny S, Matis KA, Zouboulis I, Fedoroff M, Jeanjean J, Rouchaud JC, Toulhoat N, Potocek V, Loos-Neskovic C, Maireles-Torres P, Jones D (1998) Calcium hydroxyapatites: evaluation of sorption properties for cadmium ions in aqueous solution. J Mater Sci 33:5433-5439

Manecki M, Maurice PA, Traina SJ (2000) Uptake of aqueous Pb by Cl^-, F^-, and OH^- apatites: mineralogic evidence for nucleation mechanism. Am Mineral 85:932-942

Manjubala I, Sivakumar M, Najma Nikkath S (2001) Synthesis and characterisation of hydroxyl/fluoroapatite solid solution. J Mater Sci 36:5481-5486

Mathew M, Brown WE, Austin M, Negas T (1980) Lead alkali apatites without hexad anion: the crystal structure of $Pb_8K_2(PO_4)_6$. J Solid State Chem 35:69-76

Mathew M, Mayer I, Dickens B, Schroeder LW (1979) Substitution in barium-fluoride apatite: the crystal structures of $Ba_{10}(PO_4)_6F_2$, $Ba_6La_2Na_2(PO_4)_6F_2$ and $Ba_4La_3Na_3(PO_4)_6F_2$. J Solid State Chem 28:79-95

Matsumura Y, Kanai H, Moffat JB (1997) Catalytic oxidation of carbon monoxide over stoichiometric and non-stoichiometric hydroxyapatites. J Chem Soc, Faraday Trans 93:4383-4387

Mattausch Von HJ, Mueller-Buschbaum HK (1973) The crystal structure of $Ba_5(CrO_4)_3OH$. Z Anorg Allg Chem 400:1-9

Maunaye M, Hamon C, L'Haridob P, Laurent Y (1976) Composés à structure apatite. IV. Étude structurale de l' oxynitrure $Sm_8Cr_2Si_6N_2O_{24}$. Bull Soc Mineral Crist Fr 99:203-205

Mayer I, Cohen S (1983) The crystal structure of $Ca_6Eu_2Na_2(PO_4)_6F_2$. J Solid State Chem 48:17-20

Mayer I, Fischbein E, Cohen S (1975) Apatites of divalent europium. J Solid State Chem 14:307-312

Mayer I, Roth RS, Brown WE (1974) Rare earth substituted fluoride-phosphate apatites. J Solid State Chem 11:33-37

Mayer I, Semadja A (1983) Bismuth substituted calcium, strontium, and lead apatites. J Solid State Chem 46: 363-366

Mazelsky R, Ohlmann RC, Steinnbruegge KB (1968) Crystal growth of a new laser material, fluorapatite. J Electrochem Soc 115:68-70

Mazza D, Tribaudino M, Delmastro A, Lebech B (2000) Synthesis and neutron structure of $La_5Si_2BO_{13}$, an analogue of the apatite mineral. J Solid State Chem 155:389-393

McCarthy G, White WB, Roy R (1967) Preparation of $Sm_4(SiO_4)_3$. J Inorg Nucl Chem 29:253-254

McCauley JW, Roy R (1974) Controlled nucleation and crystal growth of various $CaCO_3$ phases by the silica gel technique. Am Miner 59:947-963

McConnell D (1973) Apatite. Its Crystal Chemistry, Mineralogy, Utilization and Geologic and Biologic Occurrences. Springer, New York

McCusker LB, Liebau F, Engelhardt G (2001) Nomenclature of structural and compositional characteristics of ordered microporous and mesporous materials with inorganic hosts. Pure Appl Chem 73:381-394

McGrellis S, Serafini JN, Jeanjean J, Pastol JL, Fedorof M (2001) Influence of the sorption protocol on the uptake of cadmium ions in calcium hydroxyapatite. Sep Pur Tech 24:129-138

McIntyre DB (2004) Personal Communication: "*...it was Goldschmidt - a great crystallographer recognized today as "father of geochemistry" - who persuaded Beevers to refine the structure of apatite. Goldschmidt led the field in the determination of ionic radii, and I was privileged to hear him on how appropriate ions are captured by crystal structures acting as 3-dimensional fishing nets.*

After his escape from the Nazis, Goldschmidt found refuge at the Macaulay Institute of Soil Research. He had already studied apatite deposits in Scandinavia and he knew well the importance of apatite as the source of P in soil. I believe he was confident that F entered apatite because it fitted so well into the Ca-P-O structure, and that this was why in 1944-45 Beevers took time out from structures like strychnine and sucrose to refine the structure of apatite."

Merker L, Wondratschek H (1959) Bleiverbindungen mit apatitstruktur, insbesondere blei-jod-und blei-brom-apatite. Z Anorg Allg Chem 300:41-50

Miyake M, Ishigaki K, Suzuki T (1986) Structure refinements of Pb^{2+} ion-exchanged apatites by X-ray powder patter-fitting. J Solid State Chem 61:230-235

Mohseni-Koutchesfehani S (1961) Contribution a l'étude des apatites barytiques. Ann Chim 463-479

Monteil-Rivera F, Masset S, Dumonceau J (1999) Sorption of selenite ions on hydroxyapatite. J Mat Sci Lett 18:1143-1145

Moore PB, Araki T (1977) Samuelsonite: its crystal structure and relation to apatite and octacalcium phosphate. Am Mineral 62:229-245

Morgan MG, Wang M, Mar A (2002) Samarium orthosilicate oxyapatite, $Sm_5(SiO_4)_3O$. Acta Crystallogr E58: i70-i71

Müller-Buschbaum HK, Sander K (1978) Zur Kristallstruktur von $Sr_5(CrO_4)_3Cl$. Z Naturforsch 33b:708-710

Nadal M, Le Geros RZ, Bonel G, Montel G (1971) Mise en evidence d'un phénomène d'order-désordre dans le réseau des carbonate-apatites strontique. Compt Rend Acad Sci 272:45-48
Naddari T, Feki HE, Savariault JM, Salles P, Salah AB (2003) Structure and ionic conductivity of the lacunary apatite $Pb_6Ca_2Na_2(PO_4)_6$. Solid State Ionics 158:157-166
Naddari T, Savariault JM, El Feki H, Salles P, Ben Salah A (2002) Conductivity and structural investigations in lacunary $Pb_6Ca_2Li_2(PO_4)_6$ apatite. J Solid State Chem 166:237-244
Nadezhina TN, Pushcharovskii DY, Khomyakov AP (1987) The refinement of crystal structure of belovite. Mineral Zh 9:45-48 (in Russian)
Nakayama S, Kagayama T, Aono H, Sadoaka Y (1995) Ionic conductivity of lanthanoid silicates, $Ln_{10}(SiO_4)_6O_3$ (Ln = La, Nd, Sm, Gd, Dy, Y, Ho, Er and Yb). J Mat Chem 5:1801-1806
Narasaraju TSB, Singh RP, Rao VLN (1972) A new method of preparation of solid solutions of calcium and lead hydroxlapatites. J Inorg Nucl Chem 34:2072-2074
Negas T, Roth RS (1968) High temperature dehydroxylation of apatitic phosphates. J Res Natn Bur Stand A 72A:783-787
Newkirk AE, Hughes VB (1969) Identification of the "lead(II) hydroxide" of Robin and Theólier. Inorg Chem 9:401-404
Newnham RE, Wolfe RW, Darlington CNW (1973) Prototype structure of $Pb_5Ge_3O_{11}$. J Solid State Chem 6: 378-383
Nishikawa H, Omamiuda K (2002) Photocatalytic activity of hydroxyapatite for methyl mercaptane. J Mol Catalysis 179:193-200
Noe DC, Hughes JM, Mariano AN, Drexler JW, Kato A (1993) The crystal structure of monoclinic britholite-(Ce) and britholite-(Y). Z Kristallogr 206:233-246
Nötzold D, Wulff H (1998) Determining the crystal structure of $Sr_5(PO_4)_3Br$, a new compound in the apatite series, by powder diffraction modeling. Powder Diffr 13:70-73
Nötzold D, Wulff H, Herzog G (1994) Differenzthermoanalyse der Bildung des Pentastrontiumchloridphospha ts und röntgenographische Untersuchung seiner Struktur. J Alloys Compd 215:281-288
Nötzold D, Wulff H (1996) Structural and optical properties of the system $(Sr, Ba, Eu)_5(PO_4)_3Cl$. Phys Stat Sol (a) 158:303-311
Nounah A, Lacout JL (1993) Thermal behaviour of cadmium-containing apatites. J Solid State Chem 107: 444-451
Nriagu JO, Moore PB (1984) Phosphate Minerals. Springer-Verlag, New York
Nyman H, Andersson S (1979) On the structure of Mn_5Si_3, Th_6Mn_{23} and γ-brass. Acta Crystallogr A35:580-583
O'Keeffe M, Hyde BG (1985) An alternative approach to crystal structures with emphasis on the arrangements of cations. Struct Bonding 61:79-144
Organova NI, Rastsvetaeva RK, Kuz'mina OV, Arapova GA, Litsarev MA, Fin'ko VI (1994) The crystal structure of low-symmetry ellestadite in comparison with other apatitelike structures. Crystallogr Rep 39:234-238
Owada H, Yamashita K, Umegaki T, Kanazawa T (1989) Humidity-sensitivity of yittrium substituted apatite ceramics. Solid State Ionics 35:401-404
Pan Y, Fleet ME (2002) Compositions of the apatite-group minerals: substitution mechanism and controlling factors. Rev Mineral Geochem 48:13-50
Parmentier J, Liddell K, Thompson DP, Lemercier H, Schneider N, Hampshire S, Bodart PR, Harris RK (2001) Influence of iron on the synthesis and stability of yttrium silicate apatite. Solid State Sci 3:495–502
Perret R, Bouillet AM (1975) The sulfate apatites $Na_3Cd_2(SO_4)_3Cl$ and $Na_3Pb_2(SO_4)_3Cl$. Bull Soc fr Minéral Cristallogr 98:254-255
Pekov IV, Kulikova IM, Kabalov YuK, Eletskaya OV, Chukanov NV, Menshikov YP, Khomyakov AP (1996) Belovite-(La), $Sr_3Na(La,Ce)[PO_4]_3(F,OH)$ - a new rare earth mineral in the apatite group. Zap Vser Mineral Obshch 125(2):101-109 (in Russian)
Piccoli MP, Candela PA (2002) Apatite in igneous systems. Rev Mineral Geochem 48:255-292
Piotrowski A, Kahlenberg V, Fischer RX (2002a) The solid solution series of the sulfate apatite system $Na_{6.45}Ca_{3.55}(SO_4)_6(F_xCl_{1-x})_{1.55}$. J Solid State Chem 163:398-405
Piotrowski A, Kahlenberg V, Fischer RX, Lee Y, Parise JB (2002b) The crystal structures of cesanite and its synthetic analogue - a comparison. Am Mineral 87:715-720
Piriou B, Fahmi D, Dexpert-Ghys J, Taïtaï A, Lacout JL (1987) Unusual fluorescent properties of Eu^{3+} in oxyapatites. J Lumines 39:97-103
Pletchov PY, Sinogeikin SV (1996) The origin of apatite-nepheline ores of the Khibina massive. Vestnik MGU (Herald of the Moscow State Univ.) (Russian) Ser. 4, Geology 1:77-80
Posner AS, Diorio AF (1958) Refinement of the hydroxylapatite structure. Acta Crystallogr 11:308-209
Povarennykh AS (1972) Crystal chemical classification of minerals. Plenum Press, New York/London

Prener JS (1967) The growth and crystallographic properties of calcium fluor- and chlorapatite crystals. J Electrochem Soc 114:77-83
Prener JS (1971) Nonstoichiometry in calcium chlorapatite. J Solid State Chem 3:49-55
Pritzkow W, Rentsch H (1985) Structure refinement with X-ray powder diffraction data for synthetic calcium hydroxyapatite by Rietveld method. Crystal Res Tech 20:957-960
Pushcharovskii DY, Dorokhova GI, Pobedimskaya EA, Belov NV (1978) Potassium-neodymium silicate $KNd_9[SiO_4]_6O_2$ with apatite structure. Sov Phys Dokl 23:694-696
Pushcharovskii DY, Nadezhina TN, Khomyakov AP (1987) Crystal structure of strontium apatite from Khibiny. Sov Phys Crystallogr 32:524-526
Rakovan JF, Hughes JM (2000) Strontium in the apatite structure: strontium fluorapatite and belovite-(Ce). Can Mineral 38:839-845
Redhammer GR, Roth G (2003) Lithium and sodium yttrium orthosilicate oxyapatite, $LiY_9(SiO_4)_6O_2$ and $NaY_9(SiO_4)_6O_2$ at both 100 K and near room temperature. Acta Crystallogr C59:i120-i124
Reichert J, Binner JGP (1996) An evaluation of hydroxyapatite-based filters for removal of heavy metal ions from aqueous solutions. J Mat Sci 31:1231-1241
Reinen D, Lachwa H, Allmann R (1986) EPR- und ligandenfeldspektroskopische Untersuchungen an Mn^{V}–haltigen Apatiten sowie die Struktur von $Ba_5(MnO_4)_3Cl$. Z Anorg Allg Chem 542:71-88
Robin J, Theólier A (1956) Preparation and properties of lead hydroxide. Bull Soc Chim France 680:9921
Rouse RC, Dunn PJ, Peacor DR (1984) Hedyphane from Franklin, New Jersey and L Ångban, Sweden: canon ordering in an arsenate apatite. Am Mineral 69:920-927
Roux P, Bonel G (1977) Sur la preparation de l'apatite carbonatée de type A, à haute température par evolution, sous pression de gaz carbonique, des arséniates tricalcique et tristrontique. Ann Chim 159-165
Roy R (1982) Radioactive waste disposal. Pergamon Press, New York
Saenger AT, Kuhs WF (1992) Structural disorder in hydoxyapatite. Z Kristallogr 199:123-148
Sansom JEH, Slater PR (2004) Oxide ion conductivity in the mixed Si/Ge apatite-type phases $La_{9.33}Si_{6-x}Ge_xO_{26}$. Solid State Ionics 167:23-27
Sansom JEH, Tolchard JR, Slater PR, Islam MS (2004) Synthesis and structural characterisation of the apatite-type phases $La_{10-x}Si_6O_{26+z}$ doped with Ga. Solid State Ionics 167:17-22
Schiff-Francois A, Savelsberg G, Schaefer H (1979) Preparation and crystal structure of $Ba_5S(AsO_4)_2SO_4$, $Sr_5S(AsO_4)_2SO_4$ und $Sr_5S(PO_4)_2SO_4$. Z Naturforsch Teil B34:764-765
Schneider W (1967) Caracolit, das $Na_3Pb_2(SO_4)_3Cl$ mit Apatitstruktur. N Jahrb Mineral Monatsh 1967:284-289
Schriewer MS, Jeitschko W (1993) Preparation and crystal structure of the isotypic orthorhombic strontium perrhenate halides $Sr_5(ReO_5)_3X$ (X = Cl, Br, I) and structure refinement of the related hexagonall apatite-like compound $Ba_5(ReO_5)_3Cl$. J Solid State Chem 107:1-11
Schroeder LW, Mathew M (1978) Cation ordering in $Ca_2La_8(SiO_4)_6O_2$. J Solid State Chem 26:383-387
Schwarz H (1967a) Apatite des Typs $Pb_6K_4(X^{V}O_4)_4(X^{VI}O_4)_2$ (X^{V} = P, As; X^{VI} = S, Se). Z Anorg Allgem Chem 356:29-35
Schwarz H (1967b) Apatite des Typs $M^{II}{}_{10}(X^{VI}O_4)_3(X^{IV}O_4)_3F_2$ (M^{II} = Sr, Pb; X^{VI} = S, Cr; X^{IV} = Si, Ge). Z Anorg Allgem Chem 356:36-45
Schwarz H (1967c) Vergindungen mit Aptitstruktur. I. Ungewohnliche Silicatapatite. Inorg Nucl Chem Lett 3:231-236
Schwarz H (1968) Strontiumapatite des Typs $Sr_{10}(PO_4)_4(X^{IV}O_4)_2$ (X^{IV}= Si, Ge). Z Anorg Allgem Chem 357: 43-53
Skakle JMS, Dickson CL, Glasser FP (2000) The crystal structures of $CeSiO_4$ and $Ca_2Ce_8(SiO_4)_6O_2$. Powder Diff 15:234-238
Sirotinkin SP, Oboznenko, Oboznenko Yu V, Nevskii NN (1989) Alkali metal lead double vanadates. Russ J Inorg Chem 34:1716-1718
Spear FS, Pyle JM (2002) Apatite, monazite, and xenotime in metamorphic rocks. Rev Mineral Geochem 48: 293-336
Steele IM, Pluth JJ, Livingstone A (2000) Crystal structure of mattheddleite: a Pb, S, Si phase with the apatite structure. Mineral Mag 64:915-921
Stemmermann P (1992) Silikatapatite: Struktur, Chemismus und Anwendung als Speichermineral zur Konditionierung von Rauchgasreinigungsrückständen. PhD Dissertation, Naturwissenschaftlichen Fakultaten, Freidrich-Alexander-Universität, Erlangen-Nurnberg, Germany
Sudarsanan K (1980) Structure of hydroxyellestadite. Acta Crystallogr B36:1636-1639
Sudarsanan K, Mackie PE, Young RA (1972) Comparison of synthetic and mineral fluorapatite, $Ca_5(PO_4)_3F$, in crystallographic detail. Mater Res Bull 7:1331-1338
Sudarsanan K, Young RA (1969) Significant precision in crystal structural details: holly springs hydroxyapatite. Acta Crystallogr 25:1534-1543

Sudarsanan K, Young RA (1972) Structure of strontium hydroxide phosphate, $Sr_5(PO_4)_3OH$. Acta Crystallogr B28:3668-3670

Sudarsanan K, Young RA (1974) Structure refinement and random error analysis for strontium 'chlorapatite', $Sr_5(PO_4)_3Cl$. Acta Crystallogr B30:1381-1386

Sudarsanan K, Young RA (1980) Structure of partially substituted chlorapatite $(Ca, Sr)_5(PO_4)_3Cl$. Acta Crystallogr B36:1525-1530

Sudarsanan K, Young RA, Wilson AJC (1977) The structures of some cadmium "apatites" $Cd_5(MO_4)_3X$. I. Determination of the structures of $Cd_5(VO_4)_3I$, $Cd_5(PO_4)_3Br$, $Cd_5(AsO_4)_3Br$ and $Cd_5(VO_4)_3Br$. Acta Crystallogr B33:3136-3142

Suetsugu Y, Takahashi Y, Okamura FP, Tanaka J (2000) Structure analysis of A-type carbonate apatite by a single-crystal X-ray diffraction method. J Solid State Chem 155:292-297

Sugiyama S, Ichii T, Fujisawa M, Kawashiro K, Tomida T, Shigemoto N, Hayashi H (2003) Heavy metal immobilization in aqueous solution using calcium phosphate and calcium hydrogen phosphates. J Colloid Interface Sci 259:408-410

Suitch PR, Taïtaï A, Lacout JL, Young RA (1986) Structural consequences of the coupled substitution of Eu, S, in calcium sulfoapatite. J Solid State Chem 63:267-277

Suwa Y, Naka S, Noda T (1968) Preparation and properties of yttrium magnesium silicate with apatite structure. Mat Res Bull 3:139-148

Tachihante M, Zambon D, Arbus A, Zahir M, Sadel A, Cousseins JC (1993) Optical properties of trivalent terbium doped calcium fluorapatite. Mat Res Bull 28:605-613

Takahashi M, Uematsu K, Ye ZG, Sato M (1998) Single-crystal growth and structure determination of a new oxide apatite, $NaLa_9(GeO_4)_6O_2$. J Solid State Chem 139:304-309

Takeda H, Ohgaki M, Kizuki T, Hashimoto K, Toda Y, Udagawa S, Yamashita K (2000) Formation mechanism and synthesis of apatite-type structure $Ba_{2+x}La_{8-x}(SiO_4)_6O_{2-\delta}$. J Am Cer Soc 83:2884-2886

Tao S, Irvine JTS (2001) Preparation and characterisation of apatite-type lanthanum silicates by a sol-gel process. Mat Res Bull 36:1245–1258

Tolchard JR, Saiful Islam M, Slater PR (2003) Defect chemistry and oxygen ion migration in the apatite-type materials $La_{9.33}Si_6O_{26}$ and $La_8Sr_2Si_6O_{26}$. J Mater Chem 13:1956-1961

Tomita K, Kawano M, Shiraki K, Otsuka H, (1996) Sulfatian apatite from the Katanoyama formation in Nishina-omote City, Kagoshima prefecture. J Mineral Petrol Econ Geol 91:11-20

Toumi M, Smiri-Dogguy L, Bulou A (2000) Crystal structure and polarized Raman spectra of $Ca_6Sm_2Na_2(PO_4)_6F_2$. J Solid State Chem 149:308-313

Trombe J-C, Montel G (1975) Sur les conditions de preparation d'une nouvelle apatite contenant des ions sulfure. Compt Rend Acad Sci 280:567-570

Trombe J-C, Montel G (1978) Some features of the incorporation of oxygen in different oxidation states in the apatite lattice-II. On the synthesis and properties of calcium and strontium peroxiapatites. J Inorg Nuclear Chem 40:23-26

Utsunomiya S, Yudintsev S, Wang LM, Ewing RC (2003) Ion-beam and electron-beam irradiation of synthetic britholite. J Nuclear Mater 322:180–188

Vance ER, Ball CJ, Begg BD, Carter ML, Day RA, Thorogood GJ (2003) Pu, U, and Hf incorporation in Gd silicate apatite. J Am Ceram Soc 86:1223-1225

Vegas A, Jansen M (2002) Structural relationships between cations and alloys; an equivalence between oxidation and pressure. Acta Crystallogr B58:38-51

Vegas A, Romero A, Martinez-Ripoll M (1991) A new approach to describing non-molecular crystal structures. Acta Crystallogr B47:17-23

Verbeeck RMH, Lassuyt CJ, Heijligers HJM, Driessens FCM, Vrolijk JWGA (1981) Lattice parameters and cation distribution of solid solutions of calcium and lead hydroxyapatite. Calcif Tissue Int 33:243-247

Wallaeys R (1952) Contribution à l'étude des apatites phosphocalciques. Ann Chim 7:808-848

Wang LM, Weber WJ (1999) Transmission electron microscopy study of ion-beam-induced amorphization of $Ca_2La_8(SiO_4)_6O_2$. Phil Mag A79:237-253

Wardojo TA, Hwu S-J (1996) Chlorapatite: $Ca_5(AsO_4)_3Cl$. Acta Crystallogr C52:2959-2960

Weiner S, Wagner HD (1998) The material bone: structure-mechanical function relations. Annu Rev Mat Sci 28:271-298

White TJ, Zhili D (2003) Structural derivation and crystal chemistry of apatites. Acta Crystallogr B59:1-16

Wilhemi KA, Jonsson O (1965) X-Ray studies on some alkali and alkaline-earth chromates. Acta Chem Scand 19:177-184

Wilke HJ (1997) Die mineralien und fundstellen von Schweden. Christian Weise Verlag, München

Wilson AJC, Sudarsanan K, Young RA (1977) The structures of some cadmium "apatites" $Cd_5(MO_4)_3X$. II. The distributions of the halogen atoms in $Cd_5(VO_4)_3I$, $Cd_5(PO_4)_3Br$, $Cd_5(AsO_4)_3Br$, $Cd_5(VO_4)_3Br$ and $Cd_5(PO_4)_3Cl$. Acta Crystallogr B33:3142-3154

Wilson RM, Elliott JC, Dowker SEP (1999) Rietveld refinement of the crystallographic structure of human dental enamel apatites. Am Mineral 84:1406-1414

Wilson RM, Elliott JC, Dowker SEP (2003) Formate incorporation in the structure of Ca-deficient apatite: Rietveld structure refinement. J Solid State Chem 174:132-140

Wilson RM, Elliott JC, Dowker SEP, Smith RI (2004) Rietveld structure refinement of precipitated carbonate apatite using neutron diffraction data. Biomaterials 25:2205-2213

Wondratschek H (1963) Untersuchungen zur kristallchemie der blei-apatite (pyromorphite). N Jahrb Mineral Abh 99:113-160

Wondratschek H, Merker L, Schubert K (1964) Relations between the apatite structure and the structure of the compounds of the Mn_5Si_3 (D88)-type. Z Kristallogr 120:393-395

Wright J, Hansen B, Conca J (2005) PIMS: an apatite II permeable reactive barrier to remediate groundwater containing Zn, Pb and Cd. Submitted to J Contam Hydrol

Wyckoff RWG (1965) Inorganic compounds $R_x(MX_4)_y$, $R_x(MnX_p)_y$, Hydrates and Ammoniates. *In:* Crystal Structures. Vol 3. John Wiley and Sons, New York, p 228-234

Xu Y, Schwartz FW (1994) Lead immobilization by hydroxyapatite in aqueous solutions. J Contamin Hydr 15:187-206

Yasuda I, Hishinuma M (1995) Electrical conductivity and chemical stability of calcium chromate hydroxyl apatite, $Ca_5(CrO_4)_3OH$, and problems caused by the apatite formation at the electrode/separator interface in solid oxide fuel cells. Solid State Ionics 78:109-114

Yoshimura M, Suda H (1994) Hydrothermal processing of hydroxyapatite: past, present, and future. *In*: Hydroxyapatite and Related Materials. Brown P, Constantze B (eds), CRC Press, Inc., Boca Raton p 45-72

Young RA, Mackie PE, Von Dreele RB (1977) Application of the pattern-fitting structure-refinement method of X-ray powder diffractometer patterns. J Appl Crystallogr 10:262-269

Zahouily M, Abrouki Y, Bahlaouan B, Rayadh A, Sebti S (2003) Hydroxyapatite: new efficient catalyst for the Michael addition. Catalysis Com 4:521-52

APPENDIX A – APATITE LATTICE PARAMETERS

Table A1. Cell Parameters for apatites reported with $P6_3/m$ symmetry.

Table A2. Cell parameters for apatites reported with $P6_3$, $P\bar{3}$ or $P\bar{6}$ symmetry.

Table A3. Cell parameters for monoclinic apatites reported with $P2_1/m$, $P2_1/b$ or $P2_1$ symmetry.

Table A4. Cell parameters for apatites reported with $P6_3cm$ and *Pnma* symmetry.

Table A1. Cell Parameters for apatites reported with $P6_3/m$ symmetry.

Composition	*a* (Å)	*c* (Å)	*c/a*	*Volume* (Å^3)	*Reference*
$Ba_{10}(AsO_4)_6F_2$	10.41	7.83	0.752	734.8	Kreidler and Hummel (1970)
$Ba_{10}(AsO_4)_6Cl_2$	10.54	7.73	0.733	743.7	Kreidler and Hummel (1970)
$Ba_{10}(AsO_4)_4(SO_4)_2S_2$	10.526(5)	7.737(1)	0.735	742.4	Schiff- Francois et al. (1979)
$Ba_{10}(CrO_4)_6Cl_2$	10.50	7.73	0.736	738.1	Banks and Jaunarajs (1965)
$Ba_{10}(CrO_4)_6Cl_2$	10.511	7.764	0.739	742.9	Wilhelmi and Jonsson (1965)
$Ba_{10}(CrO_4)_6(OH)_2$	10.428	7.89	0.757	743.0	Mattausch and Mueller-Buschbaum (1973)
$Ba_{10}(MnO_4)_6F_2$	10.3437	7.8639	0.760	728.7	Dardenne et al. (1999)
$Ba_{10}(MnO_4)_6Cl_2$	10.459	7.762	0.742	735.3	Grisafe and Hummel (1970a)
$Ba_{10}(PO_4)_6(Cu_{0.30}O_{0.86}H_y)_2$	10.2073(1)	7.7401(1)	0.758	698.4	Karpov et al. (2003)
$Ba_{10}(PO_4)_6Cl_2$	10.284(2)	7.651(3)	0.744	700.8	Hata et al. (1979)
$Ba_{10}(PO_4)_6CO_3$	10.20(1)	7.65(1)	0.750	689.3	Mohensi-Koutchesfehani (1961)
$Ba_{10}(PO_4)_6F_2$	10.153(2)	7.733(1)	0.762	690.3	Mathew et al. (1979)
$Ba_{10}(PO_4)_6(OH)_2$	10.177	7.731	0.760	693.4	Negas et al. (1968)
$Ba_{9.98}Eu_{0.02}(PO_4)_6Cl_2$	10.2712(1)	7.6500(1)	0.745	698.9	Nötzold and Wulff (1996)
$Ba_{10}(P_{0.20}Mn_{0.80}O_4)_6F_2$	10.300	7.825	0.760	718.9	Dardenne et al. (1999)
$Ba_{10}(P_{0.40}Mn_{0.60}O_4)_6F_2$	10.250	7.802	0.761	709.9	Dardenne et al. (1999)
$Ba_{10}(P_{0.50}Mn_{0.50}O_4)_6F_2$	10.247	7.784	0.760	707.8	Dardenne et al. (1999)
$Ba_{10}(P_{0.70}Mn_{0.30}O_4)_6F_2$	10.211	7.740	0.758	698.9	Dardenne et al. (1999)
$Ba_{10}(P_{0.80}Mn_{0.20}O_4)_6F_2$	10.194	7.738	0.759	696.4	Dardenne et al. (1999)
$Ba_{10}(P_{0.9}Mn_{0.1}O_4)_6F_2$	10.176	7.726	0.759	692.9	Dardenne et al. (1999)
$Ba_{10}(P_{0.95}Mn_{0.05}O_4)_6F_2$	10.163	7.720	0.760	690.5	Dardenne et al. (1999)
$Ba_{10}(P_{0.967}Mn_{0.033}O_4)_6F_2$	10.172	7.733	0.760	692.9	Dardenne et al. (1999)
$Ba_{10}(P_{0.98}Mn_{0.02}O_4)_6F_2$	10.150	7.712	0.760	688.1	Dardenne et al. (1999)
$Ba_{10}(P_{0.99}Mn_{0.01}O_4)_6F_2$	10.152	7.712	0.760	688.3	Dardenne et al. (1999)
$Ba_{10}(P_{0.999}Mn_{0.001}O_4)_6F_2$	10.155	7.720	0.760	689.5	Dardenne et al. (1999)
$Ba_2La_8(SiO_4)_6O_2$	9.77	7.32	0.749	605.1	Ito (1968)
$Ba_2Nd_8(SiO_4)_6O_2$	9.66	7.16	0.741	578.6	Ito (1968)
$Ba_2Sm_8(SiO_4)_6O_2$	9.62	7.06	0.734	565.8	Ito (1968)
$Ba_4Dy_6(SiO_4)_6(OH)_2$	9.66	6.95	0.719	561.7	Ito (1968)
$Ba_4Gd_6(SiO_4)_6(OH)_2$	9.72	7.03	0.723	575.2	Ito (1968)
$Ba_4Nd_6(SiO_4)_6(OH)_2$	9.76	7.18	0.736	592.3	Ito (1968)
$Ba_4Sm_6(SiO_4)_6(OH)_2$	9.73	7.10	0.730	582.1	Ito (1968)
$Ba_{10}(VO_4)_6Cl_2$	10.55	7.75	0.735	747.0	Kreidler and Hummel (1970)
$Ba_{10}(VO_4)_6F_2$	10.420	7.854	0.754	738.5	Grisafe and Hummel (1970a)

Table A1 continued.

Composition	*a* (Å)	*c* (Å)	*c/a*	*Volume* (Å^3)	*Reference*
$Ba_{10}(VO_4)_6F_2$	10.44	7.86	0.654	644.3	Kreidler and Hummel (1970)
$Ba_{10}(V_{0.60}Mn_{0.40}O_4)_6F_2$	10.368	7.851	0.757	730.9	Dardenne et al. (1999)
$Ba_{10}(V_{0.80}Mn_{0.20}O_4)_6F_2$	10.396	7.844	0.755	734.2	Dardenne et al. (1999)
$Ba_{10}(V_{0.98}Mn_{0.02}O_4)_6F_2$	10.39	7.86	0.756	734.8	Dardenne et al. (1999)
$Bi_2Ca_8(PO_4)_6O_2$	9.461(8)	6.95(1)	0.735	538.7	Buvaneswari and Varadaraju (2000)
$Bi_2Ca_6Sr_2(PO_4)_6O_2$	9.534(7)	7.032(7)	0.738	553.5	Buvaneswari and Varadaraju (2000)
$Bi_2Ca_4Sr_4(PO_4)_6O_2$	9.605(7)	7.121(8)	0.741	568.9	Buvaneswari and Varadaraju (2000)
$Bi_2Ca_2Sr_6(PO_4)_6O_2$	9.669(7)	7.209(8)	0.746	583.7	Buvaneswari and Varadaraju (2000)
$Bi_2Sr_8(PO_4)_6O_2$	9.725(8)	7.30(1)	0.751	597.9	Buvaneswari and Varadaraju (2000)
$Ca_{10}(AsO_4)_6Cl_2$	10.076(1)	6.807(1)	0.676	598.5	Wardojo and Hwu (1996)
$Ca_{10}(AsO_4)_6F_2$	9.63	6.99	0.726	561.4	Kreidler and Hummel (1970)
$Ca_{10}(AsO_4)_6CO_3$	9.858	7.010	0.711	590.0	Roux and Bonel (1977)
$Ca_4Pb_6(AsO_4)_6Cl_2$	10.140(3)	7.185(4)	0.709	639.8	Rouse et al. (1984)
$Ca_{10}(CrO_4)_6Cl_2$	10.03	6.78	0.676	590.7	Banks and Jaunarajs (1965)
$Ca_{10}(CrO_4)_6(OH)_2$	9.66	7.01	0.726	566.5	Banks and Jaunarajs (1965)
$Ca_{10}(CrO_4)_6(OH)_2$	9.683	7.01	0.724	569.2	Wilhelmi and Jonsson (1965)
$Ca_4La_6(GeO_4)_6(OH)_2$	9.850	7.200	0.731	605.0	Cockbain and Smith (1967)
$Ca_{10}(PO_4)_6Br_2$	9.761(1)	6.739(1)	0.690	556.1	Elliot et al. (1981)
$Ca_{10}(PO_4)_6Br_2$	9.7682(6)	6.7388(2)	0.690	643.0	Kim et al. (2000)
$Ca_9Na_{0.5}(PO_4)_{4.5}(CO_3)_{1.5}(OH)_2$	9.3892(4)	6.9019(3)	0.735	526.9	El Feki et al. (1999)
$Ca_{10}(PO_4)_6F_2$	9.3475(3)	6.8646(1)	0.743	519.4	Kim et al. (2000)
$Ca_{10}(PO_4)_6F_2$	9.367(1)	6.884(1)	0.735	523.1	Sudarsanan et al. (1972)
$Ca_{10}(PO_4)_6F_2$	9.374(3)	6.889(3)	0.735	524.2	Schwarz (1967b)
$Ca_{10}(PO_4)_6F_2$	9.374(2)	6.882(2)	0.734	523.7	Mayer and Semadja (1983)
$Ca_{10}(PO_4)_6F_2$	9.3842	6.8878	0.734	527.7	Boyer et al. (1997)
$Ca_{9.2}(PO_4)_{5.55}F_2$	9.3653(3)	6.8816(2)	0.735	522.7	Young et al. (1977)
$Ca_{8.80}(PO_4)_{5.34}F_2$	9.3661(4)	6.8826(3)	0.735	522.9	Young et al. (1977)
$Ca_{10}(PO_4)_6Cl_2$	9.5902(6)	6.7666(2)	0.720	539.0	Kim et al. (2000)
$Ca_{10}(PO_4)_6Cl_2$	9.52(3)	6.85(3)	0.720	537.6	Hendricks et al. (1932)
$Ca_{15}(PO_4)_9IO$ (superstructure)	9.567(1)	20.754(2)	2.170	1645.1	Alberius-Henning et al. (1999a)
$Ca_{10}(PO_4)_6(NCN)\square$	9.424	6.852	0.727	527.0	Habelitz et al. (1999)
$Ca_{10}(PO_4)_6O\square$	9.416	6.8747	0.730	527.7	Boyer et al. (1997)
$Ca_{10}(PO_4)_6(OH)_2$	9.4302(5)	6.8911(2)	0.731	530.7	Kim et al. (2000)
$Ca_{10}(PO_4)_6(OH)_2$	9.432	6.881	0.730	530.1	Posner and Diorio (1958)

Table A1 continued.

Composition	*a* (Å)	*c* (Å)	*c/a*	*Volume* (Å^3)	*Reference*
$Ca_{10}(PO_4)_6(OH)_2$	9.4166	6.8745	0.730	527.9	Hughes et al. (1989)
$Ca_{10}(PO_4)_6(OH)_2$	9.424(4)	6.879(4)	0.730	529.1	Sudarsanan and Young (1969)
$Ca_{10}(PO_4)_6(OH)_2$	9.422(3)	6.885(3)	0.730	529.3	Schwarz (1967b)
$Ca_{10}(PO_4)_6[O,(OH)_2]$	9.402	6.888	0.733	527.3	Engel et al. (1975a)
$Ca_{10}(PO_4)_6OH_{1.9}F_{0.1}$	9.418(2)	6.876(2)	0.730	528.2	Bertoni et al. (1998)
$Ca_{10}(PO_4)_6OH_{1.9}F_{0.1}$	9.404(5)	6.907(6)	0.734	529.0	Manjubala et al. (2001)
$Ca_{10}(PO_4)_6OH_{1.94}F_{0.06}$	9.412(3)	6.907(6)	0.734	529.9	Manjubala et al. (2001)
$Ca_{10}(PO_4)_6OH_{1.98}F_{0.02}$	9.423(2)	6.880(2)	0.730	529.1	Bertoni et al. (1998)
$Ca_{10}(PO_4)_6OH_{1.98}F_{0.02}$	9.427(5)	6.909(8)	0.733	531.7	Manjubala et al. (2001)
$Ca_{10}(PO_4)_6O_{0.75}(OH)_{0.5}\square_{0.75}$	9.402	6.888	0.733	527.3	Trombe and Montel (1978)
$Ca_{10}(PO_4)_6(Cu_{0.27}O_{0.86}H_y)_2$	9.4303(1)	6.9069(1)	0.732	531.9	Karpov et al. (2003)
$Ca_{10}(P_{0.98}Mn_{0.02}O_4)_6F_2$	9.377	6.885	0.734	524.3	Dardenne et al. (1999)
$Ca_{10}(P_{0.999}Mn_{0.001}O_4)_6F_2$	9.376	6.885	0.734	524.2	Dardenne et al. (1999)
$Ca_{10}(P_{0.99}Mn_{0.01}O_4)_6F_2$	9.384	6.887	0.734	525.2	Dardenne et al. (1999)
$Ca_{9.45}Ag_{0.55}(PO_4)_6(OH)_{1.45}\square_{0.55}$	9.443	6.917	0.733	534.2	Badrour et al. (1998)
$Ca_{9.55}Ag_{0.45}(PO_4)_6(OH)_{1.55}\square_{0.45}$	9.439	6.911	0.732	533.2	Badrour et al. (1998)
$Ca_{9.6}Ag_{0.4}(PO_4)_6(OH)_{1.6}\square_{0.4}$	9.441	6.901	0.731	532.7	Badrour et al. (1998)
$Ca_{9.7}Ag_{0.3}(PO_4)_6(OH)_{1.7}\square_{0.3}$	9.436	6.897	0.731	531.8	Badrour et al. (1998)
$Ca_{9.8}Ag_{0.2}(PO_4)_6(OH)_{1.8}\square_{0.2}$	9.432	6.884	0.730	530.4	Badrour et al. (1998)
$Ca_{7.30}Co_{2.70}(PO_4)_6F_2$	9.347	6.833	0.731	517.0	Grisafe and Hummel (1970b)
$Ca_{8.20}Co_{1.80}(PO_4)_6F_2$	9.347	6.839	0.732	517.4	Grisafe and Hummel (1970b)
$Ca_{9.10}Co_{0.90}(PO_4)_6F_2$	9.358	6.849	0.732	519.4	Grisafe and Hummel (1970b)
$Ca_{9.55}Co_{0.45}(PO_4)_6F_2$	9.365	6.862	0.733	521.2	Grisafe and Hummel (1970b)
$Ca_{5.50}Co_{4.50}(PO_4)_6Cl_2$	9.644	6.749	0.700	543.6	Grisafe and Hummel (1970b)
$Ca_{6.40}Co_{3.60}(PO_4)_6Cl_2$	9.643	6.748	0.700	543.4	Grisafe and Hummel (1970b)
$Ca_{7.30}Co_{2.70}(PO_4)_6Cl_2$	9.643	6.748	0.700	543.4	Grisafe and Hummel (1970b)
$Ca_{8.20}Co_{1.80}(PO_4)_6Cl_2$	9.643	6.751	0.700	543.7	Grisafe and Hummel (1970b)
$Ca_{9.10}Co_{0.90}(PO_4)_6Cl_2$	9.644	6.754	0.700	544.0	Grisafe and Hummel (1970b)
$Ca_{9.55}Co_{0.45}(PO_4)_6Cl_2$	9.643	6.755	0.701	544.0	Grisafe and Hummel (1970b)
$Ca_8Eu_2(PO_4)_6O_2$	9.385	6.875	0.733	524.4	Piriou et al. (1987)
$Ca_{9.95}Eu_{0.05}(PO_4)_6O_{1.03}\square_{0.98}$	9.401	6.880	0.732	526.6	Piriou et al. (1987)
$Ca_6Eu_2Na_2(PO_4)_6F_2$	9.385(2)	6.893(3)	0.734	525.8	Mayer and Cohen (1983)
$Ca_9Mg(PO_4)_6F_2$	9.355	6.867	0.734	520.5	Kreidler and Hummel (1970)
$Ca_{8.11}Mg_{0.05}Na_{1.17}(PO_4)_{4.09}(CO_3)_{1.91}(H_2O)_{1.05}(OH)_{1.38}$	9.3446(3)	6.9199(4)	0.741	523.3	Wilson et al. (2004)

Table A1 continued.

Composition	*a* (Å)	*c* (Å)	*c/a*	*Volume* (Å^3)	*Reference*
$Ca_{9.1}Na_{0.5}(PO_4)_{4.7}(HPO_4)_{1.3}.2.9H_2O$	9.436	6.880	0.729	530.5	Mandjiny et al. (1998)
$Ca_{9.1}Na_{0.5}(PO_4)_6(OH)_{0.7}.4.2H_2O$	9.436	6.880	0.729	530.5	Mandjiny et al. (1998)
$Ca_{9.8}Na_{0.06}(PO_4)_{5.6}(HPO_4)_{0.4}.0.84H_2O$	9.415	6.879	0.731	528.1	Mandjiny et al. (1998)
$Ca_{9.8}Na_{0.06}(PO_4)_6(OH)_{1.6}.1.2H_2O$	9.415	6.879	0.731	528.1	Mandjiny et al. (1998)
$Ca_{9.24}Cd_{0.70}Na_{0.06}(PO_4)_6(OH)_{1.6}.1.2H_2O$	9.410(5)	6.875(5)	0.731	527.2	Jeanjean et al (1996a)
$Ca_{9.50}(NH_4)_{0.10}(PO_4)_{5.05}(CO_3)_{0.95}(OH)_2$	9.437(1)	6.888(1)	0.730	531.2	Ivanova et al. (2001)
$(Ca_{9.02}Nd_{0.98})[(PO_4)_{5.1}(SiO_4)_{0.9}]F_{1.53}O_{0.27}$	9.3938(8)	6.9013(5)	0.735	527.4	Boyer et al. (1998)
$Ca_9Ni(PO_4)_6F_2$	9.364	6.870	0.734	521.7	Kreidler and Hummel (1970)
$Ca_{9.8}Sb_{0.2}(PO_4)_6F_2$	9.3750	6.8904	0.735	524.5	DeBoer et al. (1991)
$Ca_{9.7}Sb_{0.3}(PO_4)_6F_2$	9.3715	6.8867	0.735	523.8	DeBoer et al. (1991)
$Ca_8BiNa(PO_4)_6F_2$	9.396(2)	6.914(2)	0.736	528.6	Mayer and Semadja (1983)
$Ca_6Bi_2Na_2(PO_4)_6F_2$	9.449(2)	6.952(2)	0.736	537.5	Mayer and Semadja (1983)
$Ca_4Bi_3Na_3(PO_4)_6F_2$	9.465(2)	6.968(2)	0.736	540.6	Mayer and Semadja (1983)
$Ca_6Sm_2Na_2(PO_4)_6F_2$	9.3895(3)	6.8950(4)	0.734	526.4	Toumi et al. (2000)
$Ca_{5.2}Sr_{4.8}(PO_4)_6F_2$	9.859(1)	7.206(2)	0.731	606.6	Sudarsanan and Young (1980)
$Ca_{8.83}Sr_{1.17}(PO_4)_6F_2$	9.416(1)	6.924(1)	0.735	531.6	Rakovan and Hughes (2000)
$Ca_{9.37}Sr_{0.63}(PO_4)_6F_2$	9.3902(10)	6.9011(7)	0.735	527.0	Hughes et al. (1991)
$Ca_{5.15}Sr_{4.85}(PO_4)_6Cl_2$	9.737(2)	7.022(4)	0.721	576.6	Sudarsanan and Young (1980)
$Ca_{9.27}Sr_{0.73}(PO_4)_6Cl_2$	9.653(3)	6.777(1)	0.702	546.9	Sudarsanan and Young (1980)
$Ca_{9.77}Sr_{0.23}(PO_4)_6Cl_2$	9.643(1)	6.766(1)	0.702	544.9	Sudarsanan and Young (1980)
$Ca_{9.42}Sr_{0.18}H_{0.8}(PO_4)_6(OH)_2$	9.3920(7)	6.890(1)	0.734	526.3	Kikuchi et al. (1994)
$Ca_{10}(PO_4)_4(SO_4)(SiO_4)F_2$	9.45	6.96	0.737	538.0	Schwarz (1967b)
$Ca_{10}(PO_4)_4(SO_4)(SiO_4)(OH)_2$	9.44	6.96	0.737	537.0	Schwarz (1967b)
$Ca_6La_4(SiO_4)_4(PO_4)_2F_2$	9.5911	7.0717	0.737	563.4	Boyer et al. (1997)
$Ca_8La_2(SiO_4)_2(PO_4)_4F_2$	9.5027	6.9806	0.735	545.9	Boyer et al. (1997)
$Ca_6La_4(SiO_4)_4(PO_4)_2O\square$	9.5843	7.0444	0.735	561.9	Boyer et al. (1997)
$Ca_8La_2(SiO_4)_2(PO_4)_4O\square$	9.4802	6.9570	0.734	541.5	Boyer et al. (1997)
$Ca_{10}(PO_4)_{5.7}(VO_4)_{0.3}(OH)_2$	9.4267(5)	6.8944(5)	0.731	530.6	Boechat et al. (2000)
$Ca_{10}(PO_4)_{4.5}(VO_4)_{1.5}(OH)_2$	9.4904(6)	6.9166(5)	0.729	539.5	Boechat et al. (2000)
$Ca_{10}(PO_4)_3(VO_4)_3(OH)_2$	9.5624(10)	6.9400(8)	0.726	549.6	Boechat et al. (2000)
$Ca_{10}(PO_4)_{1.5}(VO_4)_{4.5}(OH)_2$	9.6713(7)	6.9732(7)	0.721	564.9	Boechat et al. (2000)
$Ca_{10}(SiO_4)_3(SO_4)_3F_2$	9.54	6.99	0.733	550.9	Klement and Dihn (1941)
$Ca_{10}(SO_4)_3(SiO_4)_3F_2$	9.447(3)	6.938(3)	0.734	536.2	Schwarz (1967b)
$Ca_2Dy_8(SiO_4)_6O_2$	9.37	6.81	0.727	517.8	Ito (1968)

Table A1 continued.

Composition	*a* (Å)	*c* (Å)	*c/a*	*Volume* (Å^3)	*Reference*
$Ca_4La_6(SiO_4)_6F_2$	9.6503	7.1412	0.740	576.0	Boyer et al (1997)
$Ca_2Er_8(SiO_4)_6O_2$	9.33	6.75	0.723	508.9	Ito (1968)
$Ca_2Gd_8(SiO_4)_6O_2$	9.39	6.87	0.732	524.6	Ito (1968)
$Ca_2La_8(SiO_4)_6O_2$	9.63	7.12	0.739	571.8	Ito (1968)
$Ca_4La_6(SiO_4)_6O\square$	9.6351	7.1341	0.740	573.6	Boyer et al (1997)
$Ca_6La_2Ce_2(SiO_4)_6$	9.52	7.00	0.735	549.4	Cockbain and Smith (1967)
$Ca_4La_3Ce_3(SiO_4)_6(OH)_2$	9.52	7.01	0.736	550.2	Cockbain and Smith (1967)
$Ca_2Lu_8(SiO_4)_6O_2$	9.28	6.68	0.720	498.2	Ito (1968)
$Ca_2Na_2La_6Si_4P_2O_{24}(OH)_2$	9.62	7.11	0.739	569.8	Ito (1968)
$Ca_2Nd_8(SiO_4)_6O_2$	9.52	7.00	0.735	549.4	Ito (1968)
$Ca_6Nd_4(SiO_4)_6$	9.52	7.00	0.735	549.4	Cockbain and Smith (1967)
$Ca_6Nd_4(SiO_4)_6(OH)_2$	9.52	7.02	0.737	550.9	Cockbain and Smith (1967)
$Ca_2Pu_8(SiO_4)_6O_2$	9.561	7.028	0.735	556.4	Ito (1968)
$Ca_2Pu_8(SiO_4)_6O_2$	9.561	7.028	0.735	556.4	Vance et al. (2003)
$Ca_2Sm_8(SiO_4)_6O_2$	9.44	6.93	0.734	534.8	Ito (1968)
$Ca_2Y_8(SiO_4)_6O_2$	9.34	6.77	0.725	511.5	Ito (1968)
$Ca_4Ce_6(SiO_4)_6(OH)_2$	9.61	7.09	0.738	567.1	Ito (1968)
$(Ca_{4.30}Ce_{5.70})(SiO_4)_6[F_{1.0}(OH)_{1.0}]$	9.580(5)	6.980(3)	0.719	554.8	Noe et al. (1993)
$Ca_4Dy_6(SiO_4)_6(OH)_2$	9.40	6.83	0.727	522.6	Ito (1968)
$Ca_4Er_6(SiO_4)_6(OH)_2$	9.38	6.78	0.723	516.6	Ito (1968)
$Ca_4Gd_6(SiO_4)_6(OH)_2$	9.43	6.89	0.731	530.6	Ito (1968)
$Ca_4La_6(SiO_4)_6(OH)_2$	9.66	7.12	0.737	575.4	Ito (1968)
$Ca_4La_6Si_4P_2O_{26}$	9.62	7.07	0.735	566.6	Ito (1968)
$Ca_6La_4Si_2P_4O_{26}$	9.57	7.02	0.734	556.8	Ito (1968)
$Ca_8La_6Ce_6(SiO_4)_{12}(OH)_4$	9.52	7.01	0.736	550.2	Cockbain and smith (1967)
$Ca_4Lu_6(SiO_4)_6(OH)_2$	9.35	6.74	0.721	510.3	Ito (1968)
$Ca_4Na_2La_4Si_2P_4O_{24}(OH)_2$	9.51	7.00	0.736	548.3	Ito (1968)
$Ca_4Nd_6(SiO_4)_6(OH)_2$	9.56	7.00	0.732	554.0	Ito (1968)
$Ca_4Sm_6(SiO_4)_6(OH)_2$	9.50	6.94	0.731	542.4	Ito (1968)
$Ca_4Y_6(SiO_4)_6(OH)_2$	9.40	6.81	0.724	521.1	Ito (1968)
$Ca_4Y_6Si_4P_2O_{26}$	9.35	6.82	0.729	516.3	Ito (1968)
$Ca_6Y_4Si_2P_4O_{26}$	9.36	6.84	0.731	519.0	Ito (1968)
$Ca_6Y_4Si_4P_2O_{24}(OH)_2$	9.39	6.83	0.727	521.5	Ito (1968)
$Ca_8Y_2Si_2P_4O_{24}(OH)_2$	9.41	6.87	0.730	526.8	Ito (1968)

Table A1 continued.

Composition	*a* (Å)	*c* (Å)	*c/a*	*Volume* (Å^3)	*Reference*
$CaY_9Si_5BO_{26}$	9.28	6.78	0.731	505.7	Ito (1968)
$Ca_4Na_6(SO_4)_6F_2$	9.49	6.87	0.724	535.8	Klement and Dihn (1941)
$Ca_{10}(VO_4)_6Cl_2$	10.13	6.55	0.647	582.1	Kreidler and Hummel (1970)
$Ca_{10}(VO_4)_6F_2$	9.68	7.01	0.724	568.9	Kreidler and Hummel (1970)
$Ca_{10}(VO_4)_6(OH)_2$	9.7405(6)	7.0040(8)	0.719	575.5	Boechat et al. (2000)
$Ca_{10}(VO_4)_6(OH)_2$	9.818	6.981	0.711	582.8	Kutoglu (1974)
$Ca_{10}(V_{0.98}Mn_{0.02}O_4)_6F_2$	9.70	7.00	0.722	570.4	Dardenne et al. (1999)
$Cd_{10}(AsO_4)_6Br_2$	10.100(1)	6.519(1)	0.645	575.9	Sudarsanan et al. (1977)
$Cd_{10}(AsO_4)_6Cl_2$	10.04	6.51	0.648	568.3	Engel (1965)
$Cd_{10}(PO_4)_6(OH)_2$	9.335(2)	6.664(3)	0.714	502.9	Hata et al. (1978)
$Cd_{10}(PO_4)_6Br_2$	9.733(1)	6.468(1)	0.665	530.6	Sudarsanan et al. (1977)
$Cd_{9.64}(PO_4)_6Br_{3.04}$	9.733(1)	6.468(1)	0.665	530.6	Sudarsanan et al. (1977)
$Cd_{10}(PO_4)_6F_2$	9.30	6.63	0.713	496.6	Kreidler and Hummel (1970)
$Cd_{10}(PO_4)_6Cl_2$	9.633(4)	6.484(4)	0.673	521.1	Sudarsanan et al. (1977)
$Cd_{9.84}(PO_4)_6Cl_{1.814}$	9.633(4)	6.484(4)	0.673	521.1	Sudarsanan et al. (1977)
$Cd_{0.5}Pb_{9.5}(PO_4)_6(OH)_2$	9.861(1)	7.3604(1)	0.746	619.8	Badraoui et al. (2002a)
$Cd_{1.0}Pb_{9.0}(PO_4)_6(OH)_2$	9.810(1)	7.3315(6)	0.747	611.0	Badraoui et al. (2002a)
$Cd_{2.0}Pb_{8.0}(PO_4)_6(OH)_2$	9.741(1)	7.2522(7)	0.745	595.9	Badraoui et al. (2002a)
$Cd_{3.0}Pb_{7.0}(PO_4)_6(OH)_2$	9.692(1)	7.174(1)	0.740	583.6	Badraoui et al. (2002a)
$Cd_2La_8(SiO_4)_6O_2$	9.64	7.09	0.735	570.6	Ito (1968)
$Cd_{10}(VO_4)_6Br_2$	10.173(2)	6.532(1)	0.642	585.4	Sudarsanan et al. (1977)
$Cd_{9.72}(VO_4)_6Br_{2.82}$	10.173(2)	6.532(1)	0.642	585.4	Sudarsanan et al. (1977)
$Cd_{9.28}(VO_4)_6I_{2.78}$	10.307(1)	6.496(1)	0.630	597.6	Sudarsanan et al. (1977)
$Cd_{10}(VO_4)_6Cl_2$	10.11	6.52	0.645	577.1	Engel (1965)
$Cd_{10}(VO_4)_6I_2$	10.307(1)	6.496(1)	0.630	597.6	Sudarsanan et al. (1977)
$Ce_{9.33}\square_{0.67}(SiO_4)_6O_2$	9.657	7.121	0.737	575.1	Felsche (1972)
$(Ce_{0.4}Ca_{0.35}Sr_{0.25})_4(Ce_{0.86}Ca_{0.14})_6(SiO_4)_6(O_{0.5}F_{0.38})_2$	9.638(1)	7.081(1)	0.735	569.6	Genkina et al. (1991)
$Dy_{9.33}\square_{0.67}(SiO_4)_6O_2$	9.373	6.784	0.724	516.2	Felsche (1972)
$Er_2Sr_6Na_2(PO_4)_6F_2$	9.605	7.112	0.740	568.2	Mayer et al. (1974)
$Er_{9.33}\square_{0.67}(SiO_4)_6O_2$	9.324	6.686	0.717	503.4	Felsche (1972)
$Eu_{10}(AsO_4)_6(OH)_2$	9.995(2)	7.345(2)	0.735	635.5	Mayer et al. (1975)
$Eu_{10}(PO_4)_6Cl_2$	9.866(3)	7.187(2)	0.728	605.8	Mayer et al. (1975)
$Eu_{10}(PO_4)_6F_2$	9.726(3)	7.265(5)	0.747	595.2	Mayer et al. (1975)
$Eu_2Ca_6Na_2(PO_4)_6F_2$	9.374	6.882	0.734	523.7	Mayer et al. (1975)

Table A1 continued.

Composition	*a* (Å)	*c* (Å)	*c/a*	*Volume* (Å^3)	*Reference*
$Eu_3Ca_4Na_3(PO_4)_6F_2$	9.374	6.882	0.734	523.7	Mayer et al. (1975)
$Eu_4Ca_2Na_4(PO_4)_6F_2$	9.374	6.882	0.734	523.7	Mayer et al. (1975)
$Eu_2Sr_6Na_2(PO_4)_6F_2$	9.620	7.142	0.742	572.4	Mayer et al. (1975)
$Eu_3Sr_4Na_3(PO_4)_6F_2$	9.557	7.041	0.737	556.9	Mayer et al. (1975)
$K_8Na_2(VO_4)_6$	10.106(1)	7.451(1)	0.737	659.0	Sirotinkin et al. (1989)
$Eu_{9.33}\square_{0.67}(SiO_4)_6O_2$	9.472	6.905	0.729	536.6	Felsche (1972)
$Gd_{9.33}\square_{0.67}(SiO_4)_6O_2$	9.431	6.873	0.729	529.4	Felsche (1972)
$Ho_{9.33}\square_{0.67}(SiO_4)_6O_2$	9.346	6.744	0.722	510.3	Felsche (1972)
$KNd_9(SiO_4)_6O_2$	9.576(2)	7.009(2)	0.732	556.6	Pushcharovskii et al. (1978)
$La_{9.33}(GeO_4)_6O_2$	9.9117(1)	7.2833(2)	0.735	619.7	Berastegui et al. (2002)
$La_3Ba_4Na_3(PO_4)_6F_2$	9.856	7.369	0.748	619.9	Mayer et al. (1975)
$La_2Sr_6Na_2(PO_4)_6F_2$	9.690	7.219	0.745	587.0	Mayer et al. (1974)
$\square_{0.67}La_{9.33}(SiO_4)_6\square_2$	9.55	7.14	0.748	563.9	Kuzmin and Belov (1965)
$La_{9.33}\square_{0.67}(SiO_4)_6O_2$	9.713	7.194	0.741	587.8	Felsche (1972)
$La_6Ca_{3.5}(SiO_4)_6(H_2O)F$	9.664	7.090	0.734	573.4	Kalsbeek et al. (1990)
$La_3Nd_{11}(SiO_4)_9O_3$	9.638(2)	21.35(8)	2.215	1717.5	Malinovskii et al. (1990)
$La_{9.33}Si_6O_{26}$	9.719	7.183	0.739	587.6	Mazza et al. (2000)
$La_{9.66}Si_5BO_{26}$	9.630	7.196	0.747	577.9	Mazza et al. (2000)
$La_{10}Si_4B_2O_{26}$	9.5587(2)	7.2171(2)	0.755	571.1	Mazza et al. (2000)
$LiY_9(SiO_4)_6O_2$	9.34	6.72	0.719	507.7	Ito (1968)
$LiY_9(SiO_4)_6O_2$ (at 100K)	9.3108(14)	6.7088(10)	0.721	503.7	Redhammer et al. (2003)
$LiY_9(SiO_4)_6O_2$(at 295K)	9.3376(14)	6.7321(10)	0.721	508.3	Redhammer et al. (2003)
$LiLa_9(SiO_4)_6O_2$	9.681	7.160	0.739	581.2	Felsche (1972)
$LiCe_9(SiO_4)_6O_2$	9.623	7.091	0.736	568.7	Felsche (1972)
$LiPr_9(SiO_4)_6O_2$	9.575	7.040	0.735	558.8	Felsche (1972)
$LiNd_9(SiO_4)_6O_2$	9.529	6.994	0.733	550.1	Felsche (1972)
$LiSm_9(SiO_4)_6O_2$	9.464	6.918	0.730	536.6	Felsche (1972)
$LiEu_9(SiO_4)_6O_2$	9.437	6.876	0.728	530.3	Felsche (1972)
$LiGd_9(SiO_4)_6O_2$	9.413	6.852	0.727	525.8	Felsche (1972)
$LiTb_9(SiO_4)_6O_2$	9.381	6.803	0.725	522.0	Felsche (1972)
$LiDy_9(SiO_4)_6O_2$	9.362	6.769	0.723	513.9	Felsche (1972)
$LiHo_9(SiO_4)_6O_2$	9.337	6.763	0.724	508.6	Felsche (1972)
$LiEr_9(SiO_4)_6O_2$	9.316	6.696	0.718	503.3	Felsche (1972)
$LiTm_9(SiO_4)_6O_2$	9.301	6.672	0.717	499.8	Felsche (1972)

Table A1 continued.

Composition	*a* (Å)	*c* (Å)	*c/a*	*Volume* (Å^3)	*Reference*
$LiYb_9(SiO_4)_6O_2$	9.270	6.637	0.715	493.8	Felsche (1972)
$LiLu_9(SiO_4)_6O_2$	9.265	6.615	0.713	490.9	Felsche (1972)
$Lu_{9.33}\square_{0.67}(SiO_4)_6O_2$	9.260	6.621	0.715	491.6	Felsche (1972)
$Mg_{1.0}Ca_{9.0}(PO_4)_6(OH)_2$	9.416(2)	6.858(3)	0.728	526.6	Bigi et al. (1996)
$Mg_{1.5}Ca_{8.5}(PO_4)_6(OH)_2$	9.418(2)	6.833(3)	0.726	524.9	Bigi et al. (1996)
$Mg_{2.5}Ca_{7.5}(PO_4)_6(OH)_2$	9.432(3)	6.806(6)	0.722	524.4	Bigi et al. (1996)
$Mg_{3.0}Ca_{7.0}(PO_4)_6(OH)_2$	9.459(5)	6.800(8)	0.719	526.9	Bigi et al. (1996)
$Mg_2Dy_8(SiO_4)_6O_2$	9.31	6.69	0.719	502.2	Ito (1968)
$Mg_2Er_8(SiO_4)_6O_2$	9.28	6.58	0.709	490.7	Ito (1968)
$Mg_2Gd_8(SiO_4)_6O_2$	9.33	6.75	0.723	508.9	Ito (1968)
$Mg_2La_8(SiO_4)_6O_2$	9.59	7.05	0.735	561.5	Ito (1968)
$Mg_2Nd_8(SiO_4)_6O_2$	9.45	6.86	0.726	530.5	Ito (1968)
$Mg_2Sm_8(SiO_4)_6O_2$	9.38	6.8	0.725	518.1	Ito (1968)
$Mg_2Y_8(SiO_4)_6O_2$	9.31	6.64	0.713	498.4	Ito (1968)
$MgY_9Si_5BO_{26}$	9.18	6.73	0.733	491.2	Ito (1968)
$Mn_{10}(PO_4)_6Cl_2$	9.30	6.20	0.667	464.4	Klement and Haselbeck (1965)
$Mn_{10}(PO_4)_6Cl_{1.8}(OH)_{0.2}$	9.532(1)	6.199(1)	0.650	487.8	Engel et al. (1975b)
$Mn_2Dy_8(SiO_4)_6O_2$	9.33	6.71	0.719	505.8	Ito (1968)
$Mn_2Er_8(SiO_4)_6O_2$	9.30	6.65	0.715	498.1	Ito (1968)
$Mn_2Gd_8(SiO_4)_6O_2$	9.34	6.79	0.727	513.0	Ito (1968)
$Mn_2La_8(SiO_4)_6O_2$	9.63	7.08	0.735	568.6	Ito (1968)
$Mn_2Nd_8(SiO_4)_6O_2$	9.47	6.91	0.730	536.7	Ito (1968)
$Mn_2Sm_8(SiO_4)_6O_2$	9.42	6.85	0.727	526.4	Ito (1968)
$Mn_2Y_8(SiO_4)_6O_2$	9.32	6.69	0.718	503.3	Ito (1968)
$Mn_4Dy_6(SiO_4)_6(OH)_2$	9.33	6.68	0.716	503.6	Ito (1968)
$Mn_4Er_6(SiO_4)_6(OH)_2$	9.28	6.63	0.714	494.5	Ito (1968)
$Mn_4Gd_6(SiO_4)_6(OH)_2$	9.38	6.78	0.723	516.6	Ito (1968)
$Mn_4La_6(SiO_4)_6(OH)_2$	9.66	7.05	0.730	569.7	Ito (1968)
$Mn_4Nd_6(SiO_4)_6(OH)_2$	9.50	6.90	0.726	539.3	Ito (1968)
$Mn_4Sm_6(SiO_4)_6(OH)_2$	9.43	6.82	0.723	525.2	Ito (1968)
$Mn_4Y_6(SiO_4)_6(OH)_2$	9.31	6.65	0.714	499.2	Ito (1968)
$Na_6Ca_4(BeF_4)_6F_2$	9.247	6.809	0.736	504.2	Engel (1978)
$Na_6Pb_4(BeF_4)_6F_2$	9.497	6.997	0.737	546.5	Engel (1978)
$Na_6Pb_4(BeF_4)_6F_2$	9.531(3)	7.028(2)	0.737	552.9	Engel and Fischer (1990)

Table A1 continued.

Composition	*a* (Å)	*c* (Å)	*c/a*	*Volume* (Å^3)	*Reference*
$NaLa_9(GeO_4)_6O_2$	9.883(2)	7.267(3)	0.735	614.7	Takahashi et al. (1998)
$Na_2Ca_6Sm_2(PO_4)_6F_2$	9.3895(3)	6.895(4)	0.734	526.4	Toumi et al. (2000)
$Na_6Cd_4(SO_4)_6Cl_2$	9.574(4)	6.780(3)	0.708	538.2	Perret and Bouillet (1975)
$Na_6Pb_4(SO_4)_6Cl_2$	9.815(4)	7.105(3)	0.724	592.7	Perret and Bouillet (1975)
$Na_6Pb_4(SO_4)_6Cl_2$	9.810(20)	7.140(20)	0.728	595.1	Schneider (1967)
$Na_{6.35}Ca_{3.65}(SO_4)_6F_{1.65}$	9.4364(21)	6.9186(16)	0.733	533.5	Piotrowski et al. (2002a)
$Na_{6.39}Ca_{3.61}(SO_4)_6Cl_{1.61}$	9.5423(1)	6.8429(1)	0.717	539.6	Piotrowski et al. (2002a)
$NaLa_9(SiO_4)_6O_2$	9.69	7.18	0.741	583.9	Ito (1968)
$NaLa_9(SiO_4)_6O_2$	9.687	7.180	0.741	583.5	Felsche (1972)
$NaCe_9(SiO_4)_6O_2$	9.628	7.117	0.739	571.3	Felsche (1972)
$NaPr_9(SiO_4)_6O_2$	9.580	7.080	0.739	562.6	Felsche (1972)
$NaNd_9(SiO_4)_6O_2$	9.535	7.027	0.737	553.4	Felsche (1972)
$NaSm_9(SiO_4)_6O_2$	9.472	6.943	0.733	539.6	Felsche (1972)
$NaEu_9(SiO_4)_6O_2$	9.456	6.912	0.731	535.2	Felsche (1972)
$NaGd_9(SiO_4)_6O_2$	9.419	6.878	0.730	528.4	Felsche (1972)
$NaTb_9(SiO_4)_6O_2$	9.390	6.840	0.728	522.2	Felsche (1972)
$NaDy_9(SiO_4)_6O_2$	9.362	6.800	0.726	516.2	Felsche (1972)
$NaHo_9(SiO_4)_6O_2$	9.337	6.760	0.724	510.4	Felsche (1972)
$NaEr_9(SiO_4)_6O_2$	9.321	6.728	0.721	506.2	Felsche (1972)
$NaTm_9(SiO_4)_6O_2$	9.310	6.688	0.718	502.0	Felsche (1972)
$NaYb_9(SiO_4)_6O_2$	9.300	6.661	0.716	498.8	Felsche (1972)
$NaLu_9(SiO_4)_6O_2$	9.290	6.635	0.714	495.9	Felsche (1972)
$Na_2La_8(SiO_4)_6(OH)_2$	9.74	7.17	0.736	589.1	Ito (1968)
$(Na_{1.46}La_{8.55})(SiO_4)_6(F_{0.9}O_{0.11})$	9.678(1)	7.1363(3)	0.737	578.9	Hughes et al. (1992)
$(Na,Th,La)_{10}(SiO_4)_6O_2$	9.66	7.13	0.738	576.2	Ito (1968)
$NaY_9(SiO_4)_6O_2$	9.334(2)	6.759(1)	0.724	510.0	Gunawardane et al. (1982)
$NaY_9(SiO_4)_6O_2$	9.33	6.75	0.723	508.9	Ito (1968)
$Na_2Y_8(SiO_4)_6(OH)_2$	9.34	6.78	0.726	512.2	Ito (1968)
$NaY_9(SiO_4)_6O_2$ (at 100K)	9.3274(10)	6.7554(7)	0.724	508.9	Redhammer et al. (2003)
$NaY_9(SiO_4)_6O_2$(at 270K)	9.3386(10)	6.7589(8)	0.724	510.5	Redhammer et al. (2003)
$Nd_2Ca_6Na_2(PO_4)_6F_2$	9.406	6.907	0.734	529.2	Mayer et al. (1975)
$Nd_3Ca_4Na_3(PO_4)_6F_2$	9.421	6.923	0.735	532.1	Mayer et al. (1975)
$Nd_4Ca_2Na_4(PO_4)_6F_2$	9.436	6.956	0.737	536.4	Mayer et al. (1975)
$Nd_2Sr_6Na_2(PO_4)_6F_2$	9.640	7.168	0.744	576.9	Mayer et al. (1975)

Table A1 continued.

Composition	*a* (Å)	*c* (Å)	*c/a*	*Volume* (Å^3)	*Reference*
$Nd_3Sr_4Na_3(PO_4)_6F_2$	9.638	7.168	0.744	576.6	Mayer et al. (1975)
$Nd_{9.33}\square_{0.67}(SiO_4)_6O_2$	9.563	7.029	0.735	556.9	Felsche (1972)
$Nd_8Mn_2(SiO_4)_6O_2$	9.4986(9)	6.944(2)	0.731	542.6	Kluver and Muller-Buschbaum (1995)
$Pb_{10}(AsO_4)_6F_2$	10.07	7.42	0.737	651.6	Merker and Wondratschek (1959)
$Pb_{10}(AsO_4)_6Cl_2$	10.250(2)	7.454(1)	0.727	678.2	Calos and Kennard (1990)
$Pb_{10}(AsO_4)_6Cl_2$	10.25	7.46	0.728	678.8	Merker and Wondratschek (1959)
$Pb_{10}(AsO_4)_6(OH)_2$	10.154(2)	7.515(2)	0.740	671.0	Engel (1970)
$Pb_6K_4(AsO_4)_4(SO_4)_2$	10.130	7.459	0.736	662.8	Schwarz (1967a)
$Pb_9K(AsO_4)_5(SiO_4)$	10.06	7.40	0.736	648.6	Wondratschek (1963)
$Pb_{10}(CrO_4)_3(GeO_4)_3F_2$	10.115(3)	7.466(3)	0.738	661.5	Schwarz (1967b)
$Pb_{10}(CrO_4)_3(SiO_4)_3F_2$	9.973(3)	7.401(3)	0.742	637.5	Schwarz (1967b)
$Pb_{10}(GeO_4)_4(CrO_4)_2$	10.105(3)	7.428(2)	0.735	656.9	Engel and Deppisch (1988)
$Pb_{10}(GeO_4)_4(SO_4)_2$	10.058(4)	7.416(1)	0.737	649.7	Engel and Deppisch (1988)
$Pb_{10}(GeO_4)_2(VO_4)_4$	10.099(3)	7.400(2)	0.733	652.9	Ivanov (1990)
$Pb_{10}(PO_4)_6(OH)_2$	9.8612(4)	7.4242(2)	0.753	625.2	Kim et al. (2000)
$Pb_{10}(PO_4)_6(OH)_2$	9.866(3)	7.426(2)	0.753	626.0	Brückner et al. (1995)
$Pb_{10}(PO_4)_6Br_2$	10.0618(3)	7.3592(1)	0.731	645.2	Kim et al. (2000)
$Pb_{10}(PO_4)_6Cl_2$	9.9767(4)	7.3255(1)	0.734	631.5	Kim et al. (2000)
$Pb_{10}(PO_4)_6Cl_2$	9.9764(10)	7.3511(20)	0.737	633.6	Dai and Hughes (1989)
$Pb_{10}(PO_4)_6Cl_2$	9.95(2)	7.31(2)	0.735	626.8	Hendricks et al. (1932)
$Pb_{10}(PO_4)_6Cl_2$	9.993(2)	7.334(6)	0.734	634.3	Hashimoto and Matsumoto (1998)
$Pb_{10}(PO_4)_6Cl_2$	9.9981(8)	7.344(1)	0.735	635.8	Akao et al. (1989)
$Pb_{10}(PO_4)_6F_2$	9.7547(4)	7.2832(2)	0.747	600.2	Kim et al. (2000)
$Pb_{10}(PO_4)_6F_2$	9.777	7.310	0.748	605.1	Grisafe and Hummel (1970a)
$Pb_{10}(PO_4)_6F_2$	9.760(8)	7.300(8)	0.748	602.2	Belokoneva et al. (1982)
$\square Pb_9(PO_4)_6\square_2$	9.826(4)	7.357(3)	0.749	615.2	Hata et al. (1980)
$Pb_{10}(PO_4)_6O$	9.826	2x7.431	2x0.756	2x621.3	Engel et al. (1975b)
$Pb_{10}(PO_4)_6O\square$	9.84	2x7.43	2x0.755	2x623.0	Wondratschek (1963)
$Pb_{10}(PO_4)_6S\square$	9.45(8)	6.84	0.724	529.0	Trombe and Montel (1975)
$Pb_{10}(PO_4)_4(GeO_4)_2$	9.891(3)	7.338(3)	0.742	621.7	Schwarz (1968)
$Pb_8Bi_2(PO_4)_4(SiO_4)_2$	9.76	7.26	0.744	598.9	Wondratschek (1963)
$Pb_6Bi_2Tl(PO_4)_4(SiO_4)$	9.78	7.34	0.750	608.0	Wondratschek (1963)
$Pb_4Bi_3Na_3(PO_4)_6F_2$	9.653(2)	7.149(2)	0.741	576.9	Mayer and Semadja (1983)
$Pb_6Bi_2Na_2(PO_4)_6F_2$	9.690(2)	7.183(2)	0.741	584.1	Mayer and Semadja (1983)

Table A1 continued.

Composition	*a* (Å)	*c* (Å)	*c/a*	*Volume* (Å^3)	*Reference*
$Pb_8BiNa(PO_4)_6F_2$	9.732(2)	7.246(2)	0.742	594.3	Mayer and Semadja (1983)
$Pb_6Bi_2Na_2(PO_4)_6Cl_2$	9.849(2)	7.195(2)	0.731	604.4	Mayer and Semadja (1983)
$Pb_8BiNa(PO_4)_6Cl_2$	9.888(2)	7.217(2)	0.730	611.1	Mayer and Semadja (1983)
$Pb_6Ca_2Li_2(PO_4)_6$	9.6790(15)	7.1130(7)	0.735	577.1	Naddari et al. (2002)
$Pb_8Na_2(PO_4)_6$	9.722(2)	7.193(2)	0.740	588.8	Mayer and Semadja (1983)
$Pb_9Na(PO_4)_6$	9.77	7.26	0.743	600.1	Wondratschek (1963)
$Pb_6Na_3Bi(PO_4)_6$	9.689(2)	7.154(2)	0.738	581.6	Mayer and Semadja (1983)
$Pb_4Na_4Bi_2(PO_4)_6$	9.657(2)	7.079(2)	0.733	571.7	Mayer and Semadja (1983)
$Pb_6KNa_2Bi(PO_4)_6$	9.725(2)	7.146(2)	0.735	585.3	Mayer and Semadja (1983)
$Pb_{10}(PO_4)_4(SiO_4)_2$	9.804	7.327	0.748	609.9	Schwarz (1967a)
$Pb_{10}(PO_4)_4(SiO_4)_2$	9.794	7.307	0.746	606.9	Engel et al. (1975b)
$Pb_8Ca_2(PO_4)_4(SiO_4)_2$	9.734	7.203	0.740	591.5	Engel et al. (1975b)
$Pb_6Ca_4(PO_4)_4(SiO_4)_2$	9.666	7.070	0.731	572.1	Engel et al. (1975b)
$Pb_4Ca_6(PO_4)_4(SiO_4)_2$	9.567	7.047	0.737	558.5	Engel et al. (1975b)
$Pb_6K_4(PO_4)_4(SeO_4)_2$	9.843	7.336	0.745	615.5	Schwarz (1967a)
$Pb_6K_4(PO_4)_4(SO_4)_2$	9.839	7.335	0.746	614.9	Schwarz (1967a)
$Pb_{0.57}Ca_{9.43}(PO_4)_6F_2$	9.7825(3)	7.0318(2)	0.719	582.8	Dong and White (2004b)
$Pb_{1.33}Ca_{8.67}(PO_4)_6F_2$	9.8208(6)	7.0521(5)	0.718	589.0	Dong and White (2004b)
$Pb_{1.76}Ca_{8.24}(PO_4)_6F_2$	9.8441(5)	7.0635(5)	0.718	592.8	Dong and White (2004b)
$Pb_{3.01}Ca_{6.99}(PO_4)_6F_2$	9.9175(7)	7.1154(6)	0.717	606.1	Dong and White (2004b)
$Pb_{3.06}Ca_{6.94}(PO_4)_6F_2$	9.9174(4)	7.1199(3)	0.718	606.5	Dong and White (2004b)
$Pb_{3.82}Ca_{6.18}(PO_4)_6F_2$	9.9559(2)	7.1508(2)	0.718	613.8	Dong and White (2004b)
$Pb_{4.42}Ca_{5.58}(PO_4)_6F_2$	9.9856(2)	7.1825(1)	0.719	620.2	Dong and White (2004b)
$Pb_{5.55}Ca_{4.45}(PO_4)_6F_2$	10.0233(2)	7.2410(2)	0.722	630.0	Dong and White (2004b)
$Pb_{7.00}Ca_{3.00}(PO_4)_6F_2$	10.0531(1)	7.3033(1)	0.726	639.2	Dong and White (2004b)
$PbCa_9(PO_4)_6(OH)_2$	9.468	6.925	0.731	537.6	Engel et al. (1975b)
$Pb_2Ca_8(PO_4)_6(OH)_2$	9.521	6.976	0.733	547.6	Engel et al. (1975b)
$Pb_4Ca_6(PO_4)_6(OH)_2$	9.619	7.056	0.734	565.4	Engel et al. (1975b)
$Pb_5Ca_5(PO_4)_6(OH)_2$	9.653	7.091	0.735	572.2	Engel et al. (1975b)
$Pb_6Ca_4(PO_4)_6(OH)_2$	9.691	7.130	0.736	579.9	Engel et al. (1975b)
$Pb_7Ca_3(PO_4)_6(OH)_2$	9.718	7.210	0.742	589.7	Engel et al. (1975b)
$Pb_8Ca_2(PO_4)_6(OH)_2$	9.780	7.298	0.746	604.5	Engel et al. (1975b)
$Pb_2Ca_8(PO_4)_6(O,(OH)_2)$	9.496	6.978	0.735	544.9	Engel et al. (1975b)
$Pb_6Ca_4(PO_4)_6(O,(OH)_2)$	9.668	7.116	0.736	576.0	Engel et al. (1975b)

Table A1 continued.

Composition	*a* (Å)	*c* (Å)	*c/a*	*Volume* (Å^3)	*Reference*
$Pb_8K_2(PO_4)_6$	9.827(1)	7.304(1)	0.743	610.8	Mathew et al. (1980)
$Pb_8Na_2(PO_4)_6$	9.7249(8)	7.190(1)	0.739	588.9	El Koumiri et al. (2000)
$Pb_8Na_2(PO_4)_6$	9.734	7.200	0.740	590.8	Engel et al. (1975a)
$Pb_8Na_2(PO_4)_2(SiO_4)_2(SO_4)_2$	9.79	7.29	0.744	605.1	Wondratschek (1963)
$Pb_4Ca_4Na_2(PO_4)_6$	9.595	7.025	0.732	560.1	Engel et al. (1975a)
$Pb_6Ca_2Na_2(PO_4)_6$	9.660	7.082	0.733	572.3	Engel et al. (1975a)
$Pb_6Bi_4(SiO_4)_6$	9.75	7.25	0.745	596.9	Wondratschek (1963)
$Pb_2Dy_8(SiO_4)_6O_2$	9.47	6.87	0.725	533.6	Ito (1968)
$Pb_{10}(SiO_4)_3(SO_4)_3F_2$	9.88	7.41	0.750	626.4	Kreidler and Hummel (1970)
$Pb_2Gd_8(SiO_4)_6O_2$	9.54	6.95	0.729	547.8	Ito (1968)
$Pb_2La_8(SiO_4)_6O_2$	9.71	7.20	0.742	587.9	Ito (1968)
$Pb_2Nd_8(SiO_4)_6O_2$	9.65	7.12	0.738	574.2	Ito (1968)
$\square Pb_3Pr_6(SiO_4)_6\square_2$	9.662(1)	7.162(1)	0.741	579.0	Grisafe and Hummel (1970b)
$Pb_2Sm_8(SiO_4)_6O_2$	9.58	7.06	0.737	561.1	Ito (1968)
$Pb_2Y_8(SiO_4)_6O_2$	9.42	6.80	0.722	522.6	Ito (1968)
$Pb_4Ce_6(SiO_4)_6(OH)_2$	9.77	7.19	0.736	594.4	Ito (1968)
$Pb_4Dy_6(SiO_4)_6(OH)_2$	9.70	6.90	0.711	562.2	Ito (1968)
$Pb_4Er_6(SiO_4)_6(OH)_2$	9.68	6.84	0.707	555.1	Ito (1968)
$Pb_4Gd_6(SiO_4)_6(OH)_2$	9.72	6.99	0.719	571.9	Ito (1968)
$Pb_4La_6(SiO_4)_6(OH)_2$	9.80	7.26	0.741	603.8	Ito (1968)
$Pb_4Lu_6(SiO_4)_6(OH)_2$	9.64	6.75	0.700	543.2	Ito (1968)
$Pb_4Nd_6(SiO_4)_6(OH)_2$	9.76	7.13	0.731	588.2	Ito (1968)
$Pb_4Sm_6(SiO_4)_6(OH)_2$	9.74	7.05	0.724	579.2	Ito (1968)
$Pb_4Y_6(SiO_4)_6(OH)_2$	9.68	6.86	0.709	556.7	Ito (1968)
$Pb_{10}(SO_4)_2(GeO_4)_4$	10.058(4)	7.416(1)	0.737	649.7	Engel and Deppisch (1988)
$Pb_{10}(SO_4)_3(GeO_4)_3F_2$	10.032(3)	7.450(3)	0.743	649.3	Schwarz (1967b)
$Pb_{10}(SO_4)_3(SiO_4)_3F_2$	9.890(3)	7.424(3)	0.751	628.9	Schwarz (1967b)
$Pb_4Na_6(SO_4)_6F_2$	9.63	7.11	0.738	571.0	Kreidler and Hummel (1970)
$Pb_8Na_2(VO_4)_6$	10.059	7.330	0.729	642.3	Sirotinkin et al. (1989)
$Pb_{10}(VO_4)_6(OH)_2$	10.165(2)	7.463(2)	0.734	667.8	Engel (1970)
$Pb_{10}(VO_4)_6Cl_2$	10.317(3)	7.338(3)	0.711	676.4	Dai and Hughes (1989)
$Pr_{10}(VO_4)_6F_2$	10.113	7.375	0.729	653.2	Grisafe and Hummel (1970a)
$Pb_{10}(VO_4)_6F_2$	10.11	7.34	0.726	649.7	Kreidler and Hummel (1970)
$Pb_{9.85}(VO_4)_6I_{1.7}$	10.442(5)	7.467(3)	0.715	705.1	Audubert et al. (1999)

Table A1 continued.

Composition	*a* (Å)	*c* (Å)	*c/a*	*Volume* (Å^3)	*Reference*
$Pr_{9.33}\square_{0.67}(SiO_4)_6O_2$	9.607	7.073	0.736	565.3	Felsche (1972)
$Pr_3Ba_4Na_3(PO_4)_6F_2$	9.813	7.300	0.744	608.8	Mayer et al. (1974)
$\square_2Pr_8(SiO_4)_6\square_2$	9.613(2)	7.068(2)	0.735	565.6	Grisafe and Hummel (1970b)
$Sm_3Ba_4Na_3(PO_4)_6F_2$	9.759	7.243	0.742	597.4	Mayer et al. (1974)
$Sm_{9.33}^{\dagger}{}_{0.67}(SiO_4)_6O_2$	9.493	6.946	0.732	542.0	Felsche (1972)
$Sm_{10}(SiO_4)_6O_2$	9.4959(10)	7.0361(7)	0.741	549.5	Morgan et al. (2002)
$\square_{0.67}Sm_{9.33}(SiO_4)_6\square_2$	9.33	6.85	0.743	516.4	Kuzmin and Belov (1965)
$\square_2Sm_8(SiO_4)_6\square_2$	9.497(3)	6.949(2)	0.732	542.8	McCarthy et al. (1967)
$Sr_{10}(AsO_4)_6CO_3$	10.212	7.392	0.724	667.6	Roux and Bonel (1977)
$Sr_{10}(AsO_4)_6F_2$	9.99	7.40	0.741	639.6	Kreidler and Hummel (1970)
$Sr_{10}(AsO_4)_6Cl_2$	10.12	7.50	0.741	665.2	Klement and Harth (1961)
$Sr_{10}(AsO_4)_4(SO_4)_2S_2$	10.161	7.411	0.729	662.6	Schiff- Francois et al. (1979)
$Sr_{10}(CrO_4)_3(GeO_4)_3F_2$	10.002(3)	7.454(3)	0.745	645.8	Schwarz (1967a)
$Sr_{10}(CrO_4)_3(SiO_4)_3F_2$	9.900(3)	7.409(3)	0.748	628.9	Schwarz (1967a)
$Sr_{10}(CrO_4)_6(OH)_2$	9.98	7.40	0.741	638.3	Banks and Jaunarajs (1965)
$Sr_{10}(CrO_4)_6Cl_2$	10.149	7.333	0.723	654.1	Wilhemi and Jonsson (1965)
$Sr_{10}(CrO_4)_6F_2$	9.956(1)	7.437(1)	0.747	638.4	Herdtweck (1991)
$Sr_{10}(PO_4)_6(OH)_2$	9.745(1)	7.265(1)	0.746	597.5	Sudarsanan and Young (1972)
$Sr_{10}(PO_4)_6O_{0.9}(OH)_{0.2}\square_{0.9}$	9.710	7.279	0.750	594.3	Trombe and Montel (1978)
$Sr_{10}(PO_4)_6Br_2$	9.9641(1)	7.2070(1)	0.723	619.7	Nötzold and Wulff (1998)
$Sr_{10}(PO_4)_6Cl_2$	9.8777(1)	7.1892(1)	0.728	607.5	Nötzold et al. (1994)
$Sr_{10}(PO_4)_6Cl_2$	9.859(1)	7.206(2)	0.731	606.6	Sudarsanan and Young (1980)
$Sr_{10}(PO_4)_6F_2$	9.719	7.276	0.749	595.2	Akhavan-Niaki (1961)
$Sr_{10}(PO_4)_6F_2$	9.720(3)	7.289(3)	0.750	596.3	Schwarz (1967b)
$Sr_{10}(PO_4)_6F_2$	9.717	7.284	0.750	595.6	Grisafe and Hummel (1970a)
$Sr_{10}(PO_4)_6F_2$	9.776(2)	7.270(2)	0.744	601.7	Mayer and Semadja (1983)
$Sr_{10}(PO_4)_6CO_3$	9.882	7.239	0.733	612.2	Nadal et al. (1971)
$Sr_{5.08}Ba_{4.9}Eu_{0.02}(PO_4)_6Cl_2$	10.0265(2)	7.4099(2)	0.739	645.1	Nötzold and Wulff (1996)
$Sr_{3.98}Ba_{6.00}Eu_{0.02}(PO_4)_6Cl_2$	10.0699(1)	7.4599(1)	0.741	655.1	Nötzold and Wulff (1996)
$Sr_8BiNa(PO_4)_6F_2$	9.733(2)	7.290(2)	0.749	598.1	Mayer and Semadja (1983)
$Sr_6Bi_2Na_2(PO_4)_6F_2$	9.670(2)	7.246(2)	0.749	586.8	Mayer and Semadja (1983)
$Sr_{9.98}Eu_{0.02}(PO_4)_6F_2$	9.8775(3)	7.1893(1)	0.728	607.5	Nötzold and Wulff (1996)
$Sr_{9.92}Nd_{0.05}(PO_4)_6F_2$	9.7156(4)	7.2810(3)	0.749	595.2	Corker et al. (1995)
$Sr_{1.0}Pb_{9.0}(PO4)_6F_2$	9.8725(8)	7.3497(5)	0.744	620.4	Badraoui et al. (2002b)

Table A1 continued.

Composition	*a* (Å)	*c* (Å)	*c/a*	*Volume* (Å^3)	*Reference*
$Sr_{2.0}Pb_{8.0}(PO4)_6F_2$	9.8681(9)	7.3616(5)	0.746	620.8	Badraoui et al. (2002b)
$Sr_{4.0}Pb_{6.0}(PO4)_6F_2$	9.8625(7)	7.3414(8)	0.744	618.4	Badraoui et al. (2002b)
$Sr_{4.9}Pb_{5.1}(PO_4)_6F_2$	9.8572(7)	7.3352(7)	0.744	617.2	Badraoui et al. (2002b)
$Sr_{6.9}Pb_{3.1}(PO4)_6F_2$	9.8121(5)	7.3203(6)	0.746	610.4	Badraoui et al. (2002b)
$Sr_{8.9}Pb_{1.1}(PO4)_6F_2$	9.7736(9)	7.2958(4)	0.746	603.5	Badraoui et al. (2002b)
$Sr_{10}(P_{0.70}Mn_{0.30}O_4)_6F_2$	9.746	7.308	0.750	601.1	Dardenne et al. (1999)
$Sr_{10}(P_{0.80}Mn_{0.20}O_4)_6F_2$	9.747	7.307	0.750	601.2	Dardenne et al. (1999)
$Sr_{10}(P_{0.90}Mn_{0.10}O_4)_6F_2$	9.736	7.301	0.750	599.3	Dardenne et al. (1999)
$Sr_{10}(P_{0.95}Mn_{0.05}O_4)_6F_2$	9.722	7.289	0.750	596.6	Dardenne et al. (1999)
$Sr_{10}(P_{0.98}Mn_{0.02}O_4)_6F_2$	9.731	7.294	0.750	598.2	Dardenne et al. (1999)
$Sr_{10}(P_{0.999}Mn_{0.001}O_4)_6F_2$	9.719	9.287	0.956	759.7	Dardenne et al. (1999)
$Sr_{10}(P_{0.99}Mn_{0.01}O_4)_6F_2$	9.733	7.290	0.749	598.1	Dardenne et al. (1999)
$Sr_{10}(PO_4)_4(GeO_4)_2$	9.827	7.340	0.747	613.9	Schwarz (1968)
$Sr_{10}(PO_4)_4(SiO_4)_2$	9.765	7.316	0.749	604.1	Schwarz (1968)
$Sr_{10}(PO_4)_4(SO_4)(SiO_4)F_2$	9.744	7.305	0.750	600.6	Schwarz (1967b)
$Sr_{10}(PO_4)_2(SO_4)_2(SiO_4)_2F_2$	9.787	7.330	0.749	608.0	Schwarz (1967b)
$Sr_{10}(SO_4)_3(GeO_4)_3F_2$	9.905	7.392	0.746	628.1	Schwarz (1967b)
$Sr_{10}(SO_4)_3(SiO_4)_3F_2$	9.796	7.343	0.750	610.2	Schwarz (1967b)
$Sr_2Dy_8(SiO_4)_6O_2$	9.42	6.90	0.732	530.3	Ito (1968)
$Sr_2Er_8(SiO_4)_6O_2$	9.36	6.81	0.728	516.7	Ito (1968)
$Sr_2Gd_8(SiO_4)_6O_2$	9.47	6.97	0.736	541.3	Ito (1968)
$Sr_2La_8(SiO_4)_6O_2$	9.69	7.22	0.745	587.1	Ito (1968)
$\square Sr_3La_6(SiO_4)_6\square_2$	9.710	7.244	0.746	591.5	Schwarz (1967c)
$Sr_2Nd_8(SiO_4)_6O_2$	9.57	7.09	0.741	562.3	Ito (1968)
$\square Sr_3Pr_6(SiO_4)_6\square_2$	9.611(2)	7.144(2)	0.743	571.5	Grisafe and Hummel (1970b)
$Sr_2Sm_8(SiO_4)_6O_2$	9.51	7.02	0.738	549.8	Ito (1968)
$Sr_2Y_8(SiO_4)_6O_2$	9.38	6.86	0.731	522.7	Ito (1968)
$Sr_4Ce_6(SiO_4)_6(OH)_2$	9.67	7.14	0.738	578.2	Ito (1968)
$Sr_4Dy_6(SiO_4)_6(OH)_2$	9.43	6.92	0.734	532.9	Ito (1968)
$Sr_4Er_6(SiO_4)_6(OH)_2$	9.42	6.83	0.725	524.9	Ito (1968)
$Sr_4Gd_6(SiO_4)_6(OH)_2$	9.53	7.00	0.735	550.6	Ito (1968)
$Sr_4Ho_6(SiO_4)_6(OH)_2$	9.42	6.91	0.734	531.0	Ito (1968)
$Sr_4La_6(SiO_4)_6(OH)_2$	9.71	7.23	0.745	590.3	Ito (1968)
$Sr_4Lu_6(SiO_4)_6(OH)_2$	9.50	6.79	0.715	530.7	Ito (1968)

Table A1 continued.

Composition	*a* (Å)	*c* (Å)	*c/a*	*Volume* (Å^3)	*Reference*
$Sr_4Nd_6(SiO_4)_6(OH)_2$	9.62	7.10	0.738	569.0	Ito (1968)
$Sr_4Sm_6(SiO_4)_6(OH)_2$	9.6	7.05	0.734	562.7	Ito (1968)
$Sr_4Y_6(SiO_4)_6(OH)_2$	9.52	6.91	0.726	542.4	Ito (1968)
$Sr_{10}(VO_4)_6Cl_2$	10.21	7.30	0.715	659.0	Kreidler and Hummel (1970)
$Sr_{10}(VO_4)_6F_2$	10.006	7.430	0.743	644.2	Grisafe and Hummel (1970a)
$Sr_{10}(VO_4)_6F_2$	10.01	7.43	0.742	644.7	Kreidler and Hummel (1970)
$Sr_{10}(V_{0.98}Mn_{0.02}O_4)_6F_2$	10.02	7.44	0.743	646.9	Dardenne et al. (1999)
$Sr_{10}(VO_4)_6(CuO)_2$	10.126(1)	7.415(1)	0.732	658.4	Carrillo-Cabrera and von Schnering (1999)
$Sr_{10}(VO_4)_6(CuO_2)_{2/3}$	9.7815(4)	7.3018(4)	0.746	605.0	Kazin et al. (2003)
$Sr_{9.82}Nd_{0.12}(VO_4)_6F_2$	10.0077(6)	7.4342(8)	0.743	644.8	Corker et al. (1995)
$Tb_{9.33}\square_{0.67}(SiO_4)_6O_2$	9.401	6.825	0.726	522.4	Felsche (1972)
$Tm_{9.33}\square_{0.67}(SiO_4)_6O_2$	9.300	6.666	0.717	499.3	Felsche (1972)
$Y_2Ca_6Na_2(PO_4)_6F_2$	9.358	6.866	0.734	520.7	Mayer et al. (1974)
$Y_3Ca_4Na_3(PO_4)_6F_2$	9.344	7.845	0.840	593.2	Mayer et al. (1974)
$Y_4Ca_2Na_4(PO_4)_6F_2$	9.313	7.81	0.839	586.6	Mayer et al. (1974)
$(Y_4Mg)Si_3O_{13}$	9.298(2)	6.635(1)	0.714	496.8	Suwa et al. (1968)
$(Y_{3.73}Mg_{1.31})Si_{3.05}O_{13}$	9.312	6.638	0.713	498.5	Suwa et al. (1968)
$(Y_{3.30}Mg_{1.33})Si_{3.36}O_{13}$	9.306	6.632	0.713	497.4	Suwa et al. (1968)
$Y_{10}Si_4B_2O_{26}$	9.15	6.75	0.738	489.4	Ito (1968)
$Yb_{9.33}\square_{0.67}(SiO_4)_6O_2$	9.275	6.636	0.715	494.4	Felsche (1972)

Table A2. Cell parameters for apatites reported with $P6_3$, $P\bar{3}$ or $P\bar{6}$ symmetry.

Composition	*S.G.*	*a* (Å)	*c* (Å)	*c/a*	*Volume* (Å^3)	*Reference*
$Ba_{10}(CrO_4)_6(OH)_2$	$P6_3$	10.428	7.89	0.757	743.0	Banks and Jaunarajs (1965)
$Ba_{10}[(Ge,C)(O,OH)_4]_6(OH)_2$	$P6_3$	10.207(3)	7.734(2)	0.758	697.8	Malinovskii et al. (1975)
$Ba_{10}(PO_4)_6(OH)_2$	$P6_3$	10.1904(7)	7.721(2)	0.758	694.4	Bondareva and Malinovskii (1986)
$Bi_2Ca_8(VO_4)_6O_2$	$P6_3$	9.819(2)	7.033(2)	0.716	587.2	Huang and Sleight (1993)
$Ca_{10}(PO_4)_6S\square$	$P6_3$	9.455	8.84	0.935	684.4	Suitch et al. (1986)
$Ca_2Sr_2Ca_6(PO_4)_6F_2$	$P6_3$	9.485	7.000	0.738	545.4	Khomyakov et al. (1997)
$(Ca_{4.3}Ce_{5.7})(SiO_4)_6(F)(OH)$	$P6_3$	9.58	6.98	0.729	554.8	Noe et al. (1993)
$Ca_8Bi_2(VO_4)_6O_2$	$P6_3$	9.819(2)	7.033(2)	0.716	587.2	Huang and Sleight (1993)

Table A2 continued.

Composition	*S.G.*	*a* (Å)	*c* (Å)	*c/a*	*Volume* (Å^3)	*Reference*
$Cd_{10}(PO_4)_6(OH)_2$ (superstructure)	$P6_3$	16.199	6.648	0.820	1510.8	Hata and Marumo (1983)
$K_6Sn_4(SO_4)_6Cl_2$	$P6_3$	10.230(20)	7.560(20)	0.739	685.2	Howie et al. (1973)
$K_6Sn_4(SO_4)_6Cl_2$	$P6_3$	10.183(6)	7.540(2)	0.740	677.2	Donaldson and Grimes (1984)
$K_6Sn_4(SO_4)_6Br_2$	$P6_3$	10.280(20)	7.670(20)	0.746	701.9	Howie et al. (1973)
$K_6Sn_4(SO_4)_6Br_2$	$P6_3$	10.256(2)	7.582(4)	0.739	690.7	Donaldson and Grimes (1984)
$La_2Ca_8(PO_4)_6O_2$	$P6_3$	9.463(8)	6.92(1)	0.731	536.7	Buvaneswari and Varadaraju (2000)
$La_2Sr_8(PO_4)_6O_2$	$P6_3$	9.71(1)	7.30(1)	0.752	596.1	Buvaneswari and Varadaraju (2000)
$La_6Ca_{3.5}(SiO_4)_6(H_2O)F$	$P6_3$	9.664(3)	7.090(1)	0.734	573.4	Kalsbeek et al. (1990)
$Na_{0.97}Ca_{1.40}La_{2.20}Ce_{3.69}Pr_{0.32}Nd_{0.80}[(Si_{5.69}P_{0.31})_4]_6(OH,F)$	$P6_3$	9.664(3)	7.090(1)	0.734	573.4	Kalsbeek et al. (1990)
$Na_{6.39}Ca_{3.61}(SO_4)_6Cl_{1.61}$	$P6_3$	9.542	6.843	0.717	539.6	Piotrowskii et al. (2002a)
$Na_6Pb_4(SO_4)_6Cl_2$	$P6_3$	9.810	7.140	0.728	595.1	Schneider (1967)
$Pb_5GeV_{12}O_{12}$	$P6_3$	10.097	7.396	0.732	653.0	Ivanov and Zavodnik (1989)
$Sm_{10}(SiO_4)_6N_2$	$P6_3$	9.517(6)	6.981(4)	0.734	540.5	Gaude et al. (1975)
$(Sm_8Cr_2)(SiO_4)_6N_2$	$P6_3$	9.469(5)	6.890(4)	0.728	534.9	Maunaye et al. (1976)
$Sr_{10}(CrO_4)_6Cl_2$	$P6_3$	10.125	7.328	0.724	650.6	Banks and Jaunarajs (1965)
$Sr_6Ca_4(PO_4)_6F_2$	$P6_3$	9.63	7.22	0.750	579.9	Klevtsova (1964)
$Sr_{7.3}Ca_{2.7}(PO_4)_6F_2$	$P6_3$	9.565(8)	7.115(3)	0.744	563.7	Pushcharovskii et al. (1987)
$Sr_{10}(SiO_4)_3(CrO_4)_3F_2$	$P6_3$	9.9	7.409	0.748	628.9	Schwarz (1967b)
$Ba_4Nd_3Na_3(PO_4)_6F_2$	$P\bar{3}$	9.786(2)	7.281(1)	0.744	603.9	Mathew et al. (1979), Mayer et al. (1974)
$Ca_{10}(PO_4)_6[(CO_3)_x(OH)_{2-2x}]$, $(x \geq 0.5)$	$P\bar{3}$	9.5211(3)	6.8725(2)	0.722	539.5	Fleet and Liu (2003)
$Na_2Ce_2Sr_6(PO_4)_6(OH)_2$	$P\bar{3}$	9.620	7.120	0.740	570.6	Klevtsova and Borisov (1964)
$Na_2Cr_4Sr_2Ce_2(PO_4)_6F_2$	$P\bar{3}$	9.51	7.01	0.737	549.0	Khomyakov et al. (1996)
$Na_{0.5}Ca_{0.3}Ce_{1.00}Sr_{2.95}(PO_4)_6(OH)_2$	$P\bar{3}$	9.692(3)	7.201(1)	0.743	585.8	Nadezhina et al. (1987)
$Na_{1.960}La_{1.998}Sr_{5.508}Ba_{0.24}Ca_{0.12}(PO_4)_6OH_2$	$P\bar{3}$	9.664	7.182	0.743	580.9	Kabalov et al. (1997)
$Nd_3Ba_4Na_3(PO_4)_6F_2$	$P\bar{3}$	9.786	7.281	0.744	603.9	Mayer et al. (1975)
$Sr_6Na_2Ce_2(PO_4)_6(OH)_2$	$P\bar{3}$	9.664	7.182	0.743	580.9	Borodin and Kazakova (1954)
$Sr_6Na_2La_2(PO_4)_6(OH)_2$	$P\bar{3}$	9.647	7.170	0.743	577.9	Pekov et al. (1996)
$Sr_{9.402}Na_{0.209}(PO_4)_6B_{0.996}O_2$	$P\bar{3}$	9.734(4)	7.279(2)	0.748	597.3	Calvo et al. (1975)
$Ba_6La_2Na_2(PO_4)_6F_2$	$P\bar{6}$	9.9392(4)	7.4419(5)	0.749	636.7	Mathew et al. (1979)
$Ca_{10}(PO_4)_6O$	$P\bar{6}$	9.432	6.881	0.730	530.1	Alberius-Henning et al. (1999b)
$Ca_{9.55}((PO_4)_{5.52}(CO_3)_{0.48})(CO_3)_{1.157}$	$P\bar{6}$	9.480(3)	6.898(1)	0.728	536.9	Suetsugu et al. (2000)
$Na_{6.9}Ca_{3.1}(SO_4)_6OH_{1.1}$	$P\bar{6}$	9.4434(13)	6.8855(14)	0.729	531.8	Piotrowski et al. (2002b)
$Na_6Pb_4(SO_4)_6Cl_2$	$P\bar{6}$	9.815	7.105	0.724	592.8	Perret and Bouillet (1975)
$Nd_2Ba_6Na_2(PO_4)_6F_2$	$P\bar{6}$	9.910	7.399	0.747	629.3	Mayer et al. (1975)

Table A3. Cell parameters for monoclinic apatites reported with $P2_1/m$, $P2_1/b$ or $P2_1$ symmetry.

Composition	*S.G.*	*a* (Å)	*b* (Å)	*c* (Å)	γ	*Reference*
$(Ca_{8.40}Sr_{1.61})(AsO_4)_{2.58}(PO_4)_{3.42}F_{0.69}(OH)_{1.31}$	$P2_1/m$	9.594(2)	9.597(2)	6.975(2)	120.0	Hughes and Drexler (1991)
$Ca_8Sr_2(PO_4)_6(OH)_2$	$P2_1/m$	9.594(2)	9.597(2)	6.975(2)	120.0	Hughes and Drexler (1991)
$Ca_{10}(SiO_4)_3(SO_4)_3(F_{0.16}Cl_{0.48}(OH)_{1.36})$	$P2_1/m$	9.476(2)	9.508(2)	6.919(1)	119.5	Sudarsaran (1980)
$Ca_{10}(VO_4)_6F_2$	$P2_1/m$	9.737	9.7358	7.00572	120.002	Dong and White (2004b)
$Na_6Pb_4(SO_4)_6Cl_2$	$P2_1/m$	19.62	9.81	7.14	120.0	Schneider (1967)
$Ca_{9.97}(PO_4)_6Cl_{1.94}$ (superstructure)	$P2_1/b$	9.632(7)	19.226(20)	6.776(5)	120.01	Bauer and Klee (1993)
$Ca_{9.983}(PO_4)_6Cl_{1.966}$	$P2_1/b$	9.643(5)	19.279(10)	6.766(3)	120.01	Bauer and Klee (1993)
$Ca_{9.9}(PO_4)_{5.98}Cl_{1.84}$	$P2_1/b$	9.426(3)	18.856(5)	6.887(1)	119.97	Ikoma et al. (1999)
$Ca_{10}(PO_4)_6Cl_2$	$P2_1/b$	9.628(5)	19.256(10)	6.764(5)	120.0	Mackie et al. (1972)
$Pb_{10}(AsO_4)_6Cl_2$	$P2_1/b$	10.189	20.372	7.456	119.0	Dai et al. (1991)
$(Ca_{4.30}Ce_{5.70})(SiO_4)_6(F_{1.0}(OH)_{1.0})$	$P2_1$	9.58	9.590	6.980	120.1	Noe et al. (1993)
$Ca_{10}(Si_{3.14}S_{2.94}C_{0.08}P_{0.02})O_{24}((O\ H)_{1.12}Cl_{0.316}F_{0.05})$	$P2_1$	9.526(2)	9.506(4)	6.922(1)	120.0	Organova et al. (1994)
$(Na_{1.46}La_{8.55})(SiO_4)_6(F_{0.9}O_{0.11})$	$P2_1$	9.678	9.682	7.1363	120.0	Hughes et al. (1992)

Table A4. Cell parameters for apatites reported with $P6_3cm$ and *Pnma* symmetry.

Composition	*S.G.*	*a* (Å)	*b* (Å)	*c* (Å)	*Reference*
$Ba_{10}(ReO_5)_6Cl_2$	$P6_3cm$	10.935(7)	-	7.795(5)	Besse et al. (1979)
$Ba_{10}(ReO_5)_6Cl_2$	$P6_3cm$	10.926(1)	-	7.7816(8)	Schriewer and Jeitschko (1993)
$Ba_{10}(ReO_5)_6Br_2$	$P6_3cm$	10.967(7)	-	7.790(4)	Baud et al. (1979)
$Ba_{10}(ReO_5)_6I_2$	$P6_3cm$	10.932(7)	-	7.776(5)	Baud et al. (1979)
$Ba_{10}(ReO_5)_6F_2$	$P6_3cm$	10.830(2)	-	7.855(3)	Baud et al. (1980)
$Ba_{10}(ReO_5)_6CO_3$[†]	$P6_3cm$	10.938(1)	-	7.788(3)	Baud et al. (1980)
$Ba_{10}(ReO_5)_6(O_2)_2$	$P6_3cm$	10.912(2)	-	7.774(3)	Besse et al. (1980)
$Na_6Pb_4(SO_4)_6F_2$	$P6_3cm$	9.630	-	7.110	Kreidler and Hummel (1970)
$Sr_{10}(ReO_5)_6Cl_2$	*Pnma*	7.4380(9)	18.434(2)	10.563(2)	Schriewer and Jeitschko (1993)
$Sr_{10}(ReO_5)_6Br_2$	*Pnma*	7.4341(9)	18.478(3)	10.576(2)	Schriewer and Jeitschko (1993)
$Sr_{10}(ReO_5)_6I_2$	*Pnma*	7.473(2)	18.646(5)	10.700(3)	Schriewer and Jeitschko (1993)

APPENDIX B – APATITE SYNTHESIS METHODS

Table B1. Solid state route

Table B2. Hydrothermal route

Table B3. Soft chemistry route

Table B4. Sol-gel route

Table B1. Solid state route for apatite synthesis.

Composition	*Synthesis Procedure*	*Reference*
$Ba_{10}(AsO_4)_4(SO_4)_2S_2$	Stoichiometric amounts of $BaSO_4$, As_2O_5 and BaS were heated at 1400°C under Ar-atmosphere for 3 h.	Schiff-Francois et al. (1979)
$Ba_{10}(CrO_4)_6(OH)_2$	$Ba_3(CrO_4)_2$ was mixed with $Ba(OH)_2$ and fired at 820°C in air, then at 980°C in N_2 atmosphere.	Banks and Jaunarajs (1965)
$Ba_{10}(CrO_4)_6Cl_2$	Stoichiometric mixture of $Ba(OH)_2$, Cr_2O_3, and $BaCl_2$ was fired at 820°C in air for 4 h.	Banks and Jaunarajs (1965)
$Ba_{10}(CrO_4)_6Cl_2$	$Ba_3(CrO_4)_2$ melts were mixed with an excess of $BaCl_2$ at 1000–1200°C in Ar atmosphere. The excess chlorides were extracted with H_2O.	Wilhelmi and Jonsson (1965)
$Ba_{10}(CrO_4)_6F_2$	Stoichiometric quantities of $Ba(OH)_2$, Cr_2O_3, and BaF_2 were mixed and fired at 800°C in air, followed by ignition at 890°C in a N_2 atmosphere containing H_2O vapor.	Banks and Jaunarajs (1965)
$Ba_{10}(MnO_4)_6Cl_2$	Stoichiometric amounts of K_2HPO_4, $BaCl_2$, BaO_2, Mn_2O_3 were ground and sintered at 850°C.	Reinen et al. (1986)
$Ba_{10}(MnO_4)_6F_2$	Stoichiometric mixtures of $BaCO_3$, Mn_2O_3 and NH_4F were pressed into pellets and repeatedly heated for 12 h at 1250°C in air.	Dardenne et al. (1999)
$Ba_{10}(PO_4)_6Cl_2$	Single crystals were grown by reaction of $BaCl_2.2H_2O$ and K_2HPO_4 in distilled water at 473 K for 2 weeks.	Hata et al. (1979)
$Ba_{10}(PO_4)_6F_2$	A mixture of $BaHPO_4$, BaO and BaF_2 were heated at 1100°C for 4–24 h.	Mathew et al. (1979); Mayer et al. (1974)
$Ba_{10}(PO_4)_6CO_3$	$Ba_{10}(PO_4)_6(OH)_2$ was fired at 900°C in a CO_2 atmosphere.	Mohensi-Koutchesfehani (1961)
$Ba_{10}(PO_4)_6(Cu_{0.30}O_{0.86}H_y)_2$	A mixture of $BaCO_3$, $NH_4H_2PO_4$ and CuO was calcined at 600–800°C for 0.5 h, and then further annealed at 1100°C for 24 h.	Karpov et al. (2003)
$Ba_{10}(PO_4)_{6-x}(CrO_4)_xF_2$ (x = 1.2, 2.4, 3.6, 4.8, 6.0)	Starting mixtures were fired in nitrogen atmosphere at 1000°C for 10 h.	Grisafe and Hummel (1970a)

Table B1 continued.

Composition	*Synthesis Procedure*	*Reference*
$Ba_{10}(PO_4)_{6-x}(MnO_4)_xF_2$ (x = 0.6, 1.2, 2.4, 3.6, 4.8, 6.0)	Respective starting materials were fired in oxygen atmosphere at 1000–1025°C for 10 h.	Grisafe and Hummel (1970a)
$Ba_{10}(PO_4)_{6-x}(MnO_4)_xCl_2$ (x = 0.6, 1.2, 2.4, 3.6, 4.8, 6.0)		Grisafe and Hummel (1970a)
$Ba_{10}(PO_4)_{6-x}(SbO_4)_xCl_2$ ($x \leq 1.2$)	Starting mixtures were fired in air at 950°C for 8 h.	Grisafe and Hummel (1970a)
$Ba_{10}(PO_4)_{6-x}(SbO_4)_xF_2$ ($x \leq 0.6$)	Starting mixtures were fired in air at 1000°C for 10 h.	Grisafe and Hummel (1970a)
$Ba_{10}(PO_4)_{6-x}(VO_4)_xF_2$ (x = 1.2, 2.4, 3.6, 4.8, 6.0)	Starting mixtures were fired in air at 1000°C for 8 h.	Grisafe and Hummel (1970a)
$Ba_{10}(P_{1-x}Mn_xO_4)_6F_2$ (x = 0, 0.001, 0.01, 0.02, 0.033, 0.05, 0.1, 0.2, 0.3, 0.5, 0.6, 0.8, 1)	Stoichiometric amounts of $BaCO_3$, NH_4HPO_4/Mn_2O_3, and NH_4F were pressed into pellets and heated for 12 h at 1250°C in air (for $x \leq 0.3$) and at 1000°C in an oxygen stream (for $x > 0.3$).	Dardenne et al. (1999)
$Ba_{10-x}Eu_x(PO_4)_6F_2$ ($0.05 \leq x \leq 0.5$) $Ba_{10-x}Eu_x(PO_4)_6Br_2$ ($0.05 \leq x \leq 0.5$) $Ba_{10-x}Eu_x(PO_4)_6Cl_2$ ($0.05 \leq x \leq 0.5$)	$BaHPO_4$, $BaCO_3$, $NH_4F/NH_4Br/BaCl_2{\cdot}2H_2O$ and Eu_2O_3 were mixed proportionately and heated at 1100°C for 2 h in a reducing atmosphere (either N_2 plus H_2 or CO gas produced by burning activated charcoal).	Kottaisamy et al. (1994)
$Ba_6La_2Na_2(PO_4)_6F_2$ $Ba_4Nd_3Na_3(PO_4)_6F_2$	$BaHPO_4$, BaF_2, La_2O_3 and Nd_3PO_4 were stoichiometrically mixed and heated at 1100°C for 4–24 h.	Mathew et al. (1979); Mayer et al. (1974)
$Ba_{10}(ReO_5)_6Br_2$ $Ba_{10}(ReO_5)_6I_2$	Single crystal were obtained by heating Re and BaX_2 (X = Br, I) in air at 700-800°C.	Baud et al. (1979)
$Ba_{10}(ReO_5)_6Cl_2$	Annealed the powders of alkaline-earth metaperrhenates $Ba(ReO_4)_2.H_2O$ in vacuum-sealed tubes with an excess of $BaCl_2{\cdot}H_2O$ at 800°C.	Besse et al. (1979); Schriewer and Jeitschko (1993)
$Ba_{10}(ReO_5)_6CO_3\square$ $Ba_5(ReO_5)_3F$	Single crystals were obtained by heating a mixture of Re+BeF_2 or Re+$BaCO_3$ at 700°C in air, followed by slow cooling to room temperature at 4°C/min.	Baud et al. (1980)
$Ba_{10}(ReO_5)_6(O_2)_2$	Single crystal was obtained by heating Re, BaO_2 at 900°C in an oxygen atmosphere.	Besse et al. (1980)

Table B1 continued.

Composition	*Synthesis Procedure*	*Reference*
$Ba_2La_8(SiO_4)_6O_2$	A stoichiometric mixtures of $BaCO_3$, amorphous SiO_2 and La_2O_3 was calcined at 1400°C for 2 h.	Takeda et al. (2000)
$\square Ba_5Nd_4(SiO_4)_4(PO_4)_2\square_2$	Stoichiometric amounts of metal carbonates or oxides, diammonium hydrogen phosphate and silicic acid were mortared in acetone. Dried sample was placed in Pt or silica crucible and heated to 600–650°C, remixed and reheated to 1350°C for 16 h.	Grisafe and Hummel (1970b)
$Ba_2Ln_8(SiO_4)_6O_2$ (Ln = La, Nd, Sm)	High temperature solid-state reaction of stoichiometric mixtures made from respective oxides of lanthanides, chlorides or hydroxides of alkaline earth metals, cadmium sulfate, manganese chloride, and potassium silicate at 1200°C in air.	Ito (1968)
$Ba_{10}(VO_4)_{6-x}(CrO_4)_xF_2$ (x = 1.2, 2.4, 3.6, 4.8, 6.0)	Starting mixtures were fired in N_2 atmosphere at 1000°C for 10 h.	Grisafe and Hummel (1970a)
$Ba_{10}(VO_4)_{6-x}(MnO_4)_xF_2$ (x = 0.6, 1.2, 2.4, 3.6, 4.8, 6.0) $Ba_{10}(VO_4)_{6-x}(MnO_4)_xCl_2$ (x = 0.6, 1.2, 2.4, 3.6, 4.8, 6.0)	Respective starting materials were fired in an O_2 atmosphere at 975–1000°C for 10 h.	Grisafe and Hummel (1970a)
$Ba_{10}(V_{1-x}P_xO_4)_6F_2$ (x = 0, 0.02, 0.2, 0.6, 1)	Stoichiometric amounts of $BaCO_3$, V_2O_5/NH_4HPO_4, and NH_4F were pressed into pellets and heated for 12 h at 1000ºC in an oxygen stream.	Dardenne et al. (1999)
$Ba_{10}(VO_4)_{6-x}(SbO_4)_xCl_2$ ($x \leq 1.2$)	Starting mixtures were fired in air at 950°C for 8 h.	Grisafe and Hummel (1970a)
$Ba_{10}(VO_4)_{6-x}(SbO_4)_xF_2$ ($x \leq 0.6$)	Starting mixtures were fired in air at 1000°C for 10 h.	Grisafe and Hummel (1970a)
$Bi_2Ca_8(PO_4)_6O_2$ $Bi_2Ca_6Sr_2(PO_4)_6O_2$ $Bi_2Ca_4Sr_4(PO_4)_6O_2$ $Bi_2Ca_2Sr_6(PO_4)_6O_2$ $Bi_2Sr_8(PO_4)_6O_2$	Stoichiometric quantities of $NH_4H_2PO_4$, Bi_2O_3, $CaCO_3$ and/or $SrCO_3$ were initially heated at 300°C for 6 h to eliminate H_2O and NH_3, and then further heated at 700°C for 12 h and at 950°C for 24 h. Powders were then pelletized and sintered at 1100°C.	Buvaneswari and Varadaraju (2000)

Table B1 continued.

Composition	*Synthesis Procedure*	*Reference*
$Bi_2Ca_8(VO_4)_6O_2$	Single crystals were grown by mixing Bi_2O_3, CaO, and V_2O_5 at 700–1240°C for a total of 22 h.	Huang and Sleight (1993)
$Ca_{10}(AsO_4)_6Cl_2$	Crystals were grown via a eutectic flux of 31% $CaCl_2$ and 69% NaCl (m.p. 773 K) from a reaction mixture of As_2O_3, CuO and Cu_2O in a fused-silica ampoule. The reactants were heated at 973 K for 6 days before being slowly cooled to room temperature.	Wardojo and Hwu (1996)
$Ca_{10}(AsO_4)_6CO_3$	Sintered stoichiometric mixture of $Ca_3(PO_4)_2$ and $CaCO_3$ at 900°C in CO_2 atmosphere.	Roux and Bonel (1977)
$Ca_{10}(CrO_4)_6(OH)_2$	Partial oxidation of a mixture of CaO and Cr_2O_3 in humid air at 900°C.	Wilhelmi and Jonsson (1965)
$Ca_{10}(CrO_4)_6(OH)_2$	$CaCrO_4{\cdot}2H_2O$ and $Ca(OH)_2$ were mixed stoichiometrically and fired at 900°C for 12 h in a flow of Ar humidified at room temperature.	Yasuda and Hishinuma (1995)
$Ca_{10}(CrO_4)_6Cl_2$ $Ca_{10}(CrO_4)_6F_2$	$CaCO_3$, CrO_3 and $CaCl_2/CaF_2$ were stoichiometrically mixed and calcined at 900°C in air, followed by ignition at 950°C in a N_2 atmosphere.	Banks and Jaunarajs (1965)
$Ca_4La_6(GeO_4)_6(OH)_2$	A stoichiometric mixture of CaO, La_2O_3 and GeO_2 was fired at 1350°C for 1 h in air.	Cockbain and Smith (1967)
$Ca_{10}(PO_4)_6Br_2$	Crystals were grown by slowly cooling a mixture of powdered bromapatite and $CaBr_2$ in an HBr atmosphere at 1073 K.	Elliot et al. (1981)
$Ca_{10}(PO_4)_6Br_2$	$Ca_{10}(PO_4)_6(OH)_2$ was reacted with CH_2Br_2 under oxygen flushing at 800°C for 2 h.	Kim et al. (2000)
$Ca_{10}(PO_4)_6Cl_2$	$CaCl_2$ and $Ca_3(PO_4)_2$ were mixed in a stoichiometric ratio and fused in a platinum crucible.	Hendricks et al. (1932)
$Ca_{10}(PO_4)_6Cl_2$	Single crystals were prepared by annealing Ca_2PO_4Cl in argon at 1200°C for several hours, followed by rapid cooling. Rapid cooling is required to prevent reconversion to Ca_2PO_4Cl.	Prener (1971)
$Ca_{10}(PO_4)_6Cl_2$	Crystals were grown from solutions of the apatite in fused $CaCl_2$.	Mackie et al. (1972)

Table B1 continued.

Composition	*Synthesis Procedure*	*Reference*
$Ca_{10}(PO_4)_6CO_3$	$Ca_{10}(PO_4)_6(OH)_2$ was treated with dry CO_2 at 1170 K for several days.	Elliot et al. (1980)
$Ca_{10}(PO_4)_6F_2$	$Ca_3(PO_4)_2$ and CaF_2 were mixed and calcined in the range 350-1250°C for 0.5–24 h.	Kreidler and Hummel (1970)
$Ca_{10}(PO_4)_6F_2$	$Ca_4(PO_4)_2O$ and CaF_2 were mixed and calcined at 900°C for several hours.	Elliot (1994); Wallaeys (1952)
$Ca_{10}(PO_4)_6F_2$	Crystals were grown by the Czochralski method in an Ar atmosphere from a seed crystal pulled from an induction heated Ir-crucible at rates of 3–5 mm h^{-1} and rotations of 30–100 rpm.	Mazelsky et al. (1968)
$Ca_{10-x}(PO_4)_6Cl_{2-2x}\square_{2x}$ ($x = 0.03$)	Crystals were grown from a flux of molten $CaCl_2$.	Bauer and Klee (1993)
$Ca_{10}(PO_4)_6[(CO_3)_x(OH)_{2-2x}]$ ($x \geq 0.5$)	Single crystals were prepared by direct reaction of stoichiometric amounts of $Ca_2P_2O_7$, CaO and $CaCO_3$ in the ratio 3:3:1 at a pressure of 2 Gpa and at 1400–1500°C.	Fleet and Liu (2003)
$Ca_{10}(PO_4)_6Cu_{0.54}O_{1.72}H_{2y}$	$CaCO_3$, $NH_4H_2PO_4$ and CuO were mixed and calcined from 600–800°C for 0.5 h, then further annealed at 1100°C for 24 h.	Karpov et al. (2003)
$Ca_{10}(PO_4)_{6-x}(CrO_4)_xF_2$ ($x \leq 4.8$)	Respective starting materials were fired in a nitrogen atmosphere at 1000°C for 10 h.	Grisafe and Hummel (1970a)
$Ca_{10-x}(PO_4)_{6-x}(HPO_4)_x(OH)_{2-x}$ ($0 \leq x \leq 1$)	H_3PO_4 was added to $(CH_3COO)_2Ca{\cdot}xH_2O$ with Ca/P=1.5, 1.55, 1.6 and 1.67 for 2 h. NH_3 was used to keep the solution at pH 10. After filtering, the mixture was dried at 100°C overnight.	Liou et al. (2004)
$Ca_{10}(PO_4)_6(NCN)$	Hydroxyapatite was subjected to a nitrogen atmosphere. At 600°C, nitrogen flow was replaced by ammonia and the temperature raised from 800 to 1300°C over 16 h.	Habelitz et al. (1999)
$Ca_{10}(PO_4)_6O_{0.75}(OH)_{0.5}\square_{0.75}$	Peroxiapatites are formed by thermal treatment of calcium hydroxyapatite at 900ºC under pure O_2. In order to eliminate traces of water, the stream of oxygen has been allowed to run through a coil cooled by carbon dioxide-ice before reaching the product.	Trombe and Montel (1978)
$Ca_{10}(PO_4)_6S\square$	$Ca_3(PO_4)_2$ was mixed with an excess of CaS and heated at 950°C under vacuum.	Trombe and Montel (1975)

Table B1 continued.

Composition	*Synthesis Procedure*	*Reference*
$Ca_{10}(P_{1-x}Mn_xO_4)_6F_2$ ($0.001 \le x \le 0.02$)	$CaCO_3$, NH_4HPO_4/Mn_2O_3, and NH_4F were mixed in stoichiometric amounts, pressed into pellets and heated for 12 h at 1250°C in air (for $x \le 0.3$) and 1000°C in an oxygen stream (for $x > 0.3$).	Dardenne et al. (1999)
$Ca_{10-2x}BixNa_x(PO_4)_6F_2$ (x = 1, 2, 3)	Stoichiometric amounts of $Ca_3(PO_4)_2$, CaF_2, $NH_4H_2PO_4$, NaF, $Na_3PO_4{\cdot}12H_2O$ and $Bi(NO_3)_3.5H_2O$ were mixed together and heated at 1100°C for 24–48 hrs in a closed gold or Pt-crucible.	Mayer and Semadja (1983)
$Ca_{10-x}Cox(PO_4)_6F_2$ (x = 0.45, 0.9, 1.8 and 2.7) $Ca_{10-x}Cox(PO_4)_6Cl_2$ (x = 0.45, 0.9, 1.8 and 2.7)	Stoichiometric amounts of metal carbonates or oxides and diammonium hydrogen phosphate and/or silicic acid were mixed and dried in sealed platinum crucibles and heated at 975°C for 8 h.	Grisafe and Hummel (1970b)
$Ca_{10-x}Eu_x(PO_4)_6F_2$ ($0.05 \le x \le 0.5$) $Ca_{10-x}Eu_x(PO_4)_6Br_2$ ($0.05 \le x \le 0.5$) $Ca_{10-x}Eu_x(PO_4)_6Cl_2$ ($0.05 \le x \le 0.5$)	$CaHPO_4$, $CaCO_3$, $CaF_2/NH_4Br/NH_4Cl$ and Eu_2O_3 were mixed proportionately and heated at 1100°C for 2 h in a reducing atmosphere (either N_2 plus H_2 or CO gas produced by burning activated charcoal).	Kottaisamy et al. (1994)
$Ca_{10-x}Eu_x(PO_4)_6O_{1+x/2}\square_{1-x/2}$ ($0.05 \le x \le 2$)	A mixture of dry β-calcium pyrophosphate, Ca-carbonate and Eu-oxide were fired at 1350°C in air. The samples were annealed in vacuum at 900°C until a single-phase oxyapatite was obtained.	Piriou et al. (1987)
$Ca_{10-2x}Na_xTb_x(PO_4)_6F_2$ ($0 \le x \le 2$)	Solid-state reactions between a stoichiometric mixture of $Ca_3(PO_4)_2$, NaF, $TbPO_4$ and CaF_2 at 1060ºC for 15 h under argon.	Tachihante et al. (1993)
$Ca_{10-x}Nix(PO_4)_6Cl_2$ (x = 0.2, 0.5 and 1.0)	Stoichiometric amounts of metal carbonates or oxides and diammonium hydrogen phosphate and/or silicic acid were mixed and dried in covered crucibles and heated at 800°C for 4 h.	Grisafe and Hummel (1970b)
$Ca_8RE_2(PO_4)_6O_2$ (RE = La, Pr, Nd)	Stoichiometric amounts of metal carbonates or oxides and diammonium hydrogen phosphate were mortared in acetone. Dried sample was placed in Pt or silica crucible and heated to 600–650°C, remixed and reheated at 1320°C for 72 h.	Grisafe and Hummel (1970b)
$Ca_{10-x}Sb_x(PO_4)_6F_2$ (x = 0.2, 0.3)	CaO, CaF_2, $Ca_2P_2O_7$ and $CaSb_2O_6$ were stoichiometrically mixed and fired at 1473 K for 2.5 h in air.	De Boer et al. (1991)

Table B1 continued.

Composition	*Synthesis Procedure*	*Reference*
$Ca_6Sm_2Na_2(PO_4)_6F_2$	Crystals were obtained by mixing $CaCO_3$, $(NH_4)_2HPO_4$, Sm_2O_3, and NaF and heating at 400°C for 4 h, then at 1200°C for 1 h.	Toumi et al. (2000)
$Ca_{10-x}Sr_x(PO_4)_6Cl_2$ ($0.23 \le x \le 4.85$)	Single crystals were prepared by standard flux-growth techniques. The starting material was calcium chlorapatite mixed with $CaCl_2$ and $SrCl_2$. The mixture was placed in a lightly covered Pt-crucible and heated in a N_2 atmosphere at 1553 K for 24 h. The furnace was cooled at a rate of 30 K/day to 1333 K and then shut off.	Sudarsanan and Young (1980)
$Ca_9Nd(PO_4)_5(SiO_4)F_{1.5}O_{0.25}$	Stoichiometric mixtures of CaF_2, P_2O_5, $CaCO_3$, Nd_2O_3 and SiO_2 were heated at 1973 K over a period of 2 h followed by cooling at 50 K min^{-1}.	Boyer et al. (1998)
$(Ca_{9.02}Nd_{0.98})[(PO_4)_{5.1}(SiO_4)_{0.9}]F_{1.53}O_{0.27}$	Single crystals were obtained from a stoichiometric mixture of CaF_2, P_2O_5, $CaCO_3$, Nd_2O_3 and SiO_2 with rapid heating to 1973 K and kept there for 2 h.	Boyer et al. (1998)
$Ca_{10}(PO_4)_{6-x}(VO_4)_xF_2$ ($x \le 4.8$)	Respective starting materials were fired in air at 1000°C for 10 h.	Grisafe and Hummel (1970a)
$Ca_{3.05}Ce_{2.38}Fe_{0.25}Gd_{5.37}Si_{4.88}O_{26}$ $Ce_{1.45}Zr_{0.78}Fe_{0.14}Nd_{2.15}Eu_{0.50}Si_{6.02}O_{26}$	Synthesized by inductive melting of an oxide mixture in a cold crucible.	Utsunomiya et al. (2003)
$Ca_2La_8(SiO_4)_6O_2$	Single crystals grown from stoichiometric melt.	Wang and Weber (1999)
$Ca_2Ln_8(SiO_4)_6O_2$ (Ln = La, Nd, Sm, Gd, Dy, Y, Er, Lu)	Solid-state reaction of stoichiometric mixtures made from respective oxides of lanthanides, chlorides or hydroxides of alkaline earth metals, cadmium sulfate, manganese chloride, and potassium silicate at 1200°C in air.	Ito (1968)
$Ca_{10-x}La_x(SiO_4)_x(PO_4)_{6-x}F_2$ ($0 \le x \le 6$) $Ca_{10-x}La_x(SiO_4)_x(PO_4)_{6-x}O\square$ $0 \le x \le 6$)	Stoichiometric amounts of La_2O_3, CaF_2, SiO_2, $Ca_2P_2O_7$ and $CaCO_3$ were mixed and sintered at 1100–1400°C.	Boyer et al. (1997)
$Ca_2Nd_8(SiO_4)_6O_2$	Appropriate amounts of Nd_2O_3, CaO were dissolved in 35% nitric acid and the resulting solution was added to an ammonia stabilized silicate solution containing the desired amount of SiO_2. The solution was evaporated to dryness and heated to 500°C for 2 hr. Pressed into pellets and fired at 1250°C for 24 h.	Fahey et al. (1985)

Table B1 continued.

Composition	*Synthesis Procedure*	*Reference*
$Ca_2Pu_8(SiO_4)_6O_2$ $Ca_2Gd_7A(SiO_4)_6O_2$ (A = U, Hf) $Ca_3Gd_6Hf(SiO_4)_6O_2$	Aqueous metal nitrate solutions were mixed with colloidal silica and were calcined at 1350°C for 20 h.	Vance et al. (2003)
$Ca_{5.43}La_{3.22}(SiO_4)_{1.68}(PO_4)_{4.32}O_{0.411}$ $Ca_5La_{4.49}(SiO_4)_{2.8}(PO_4)_{3.2}O_{1.23}$ $Ca_{4.15}La_{5.38}(SiO_4)_{3.74}(PO_4)_{2.26}O_{1.31}$ $CaLa_{8.66}(SiO_4)_6O_2$	Stoichiometric mixtures of $CaCO_3$, La_2O_3, SiO_2, and $(NH_4)_2HPO_4$ were fired at 1200–1400°C for 12 h.	El Ouenzerfi (2003)
$Ca_6Th_4(SiO_4)_6O_2$	Stoichiometric mixtures of ThO_2, $CaCO_3$ and SiO_2 were calcined at 1400ºC.	Engel (1978)
$Ca_{10}(VO_4)_6F_2$ $Ca_{10}(VO_4)_6Cl_2$	$Ca_3(VO_4)_2$ was mixed with CaF_2 or $CaCl_2$ and fired at 970°C for 1 h.	Kreidler and Hummel (1970)
$Ca_{10-x}La_x(VO_4)_6O_{1+x/2}\square_{1-x/2}$ ($0 \le x \le 2$)	Single crystals were grown by the Czochralski method.	Benmoussa et al. (2000)
$Ca_{10}(V_{1-x}Mn_xO_4)_6F_2$ ($x = 0.02$)	$CaCO_3$, V_2O_5/Mn_2O_3, and NH_4F were stoichiometrically mixed, pressed into pellets and heated for 12 h at 1000°C in an O_2 stream.	Dardenne et al. (1999)
$Ca_8Bi_2(VO_4)_6O_2$	A stoichiometric mixture of Bi_2O_3, CaO, and V_2O_5 was first heated at 700°C for 12 h and then at 950°C for 20 h. It was further heated to 1240°C and held at this temperature for 5min, followed by cooling to 1200°C at a rate of 15 °C/h, held there for 1 h, cooled to 1150°C at a rate of 3°C/h, then cooled to 600°C at 15 °C/h, and finally cooled to room temperature.	Huang and Sleight (1993)
$Cd_{10}(AsO_4)_6Br_2$ $Cd_{10}(AsO_4)_6I_2$ $Cd_{9.84}(AsO_4)_6Br_{3.04}$	Single crystals were grown from $Cd_3(MO_4)_2$ and an excess of CdX_2 (M = As, V, or P and X = Br or I).	Sudarsanan et al. (1977) Wilson et al. (1977)
$Cd_{10}(PO_4)_6Br_2$ $Cd_{10}(PO_4)_6Cl_2$	Crystals were grown from the melt in Pt crucibles charged with $Cd_3(PO_4)_2$ and an excess of $CdBr_2$ or $CdCl_2$. Crucibles were not perfectly closed against air.	Sudarsanan et al. (1977)

Table B1 continued.

Composition	*Synthesis Procedure*	*Reference*
$Cd_2La_8(SiO_4)_6O_2$	Solid-state reaction of stoichiometric mixtures made from respective oxides of lanthanides, chlorides or hydroxides of alkaline earth metals, cadmium sulfate, manganese chloride, and potassium silicate at 1200°C in air.	Ito (1968)
$Cd_9Nd(PO_4)_5(SiO_4)F_2$	Stoichiometric amounts of Nd_2O_3, CaF_2, SiO_2, CaP_2O_7 and $CaCO_3$ were mixed and sintered at 1400°C for 6 h in air.	Bregiroux et al. (2003)
$Cd_{10}(VO_4)_6Br_2$ $Cd_{10}(VO_4)_6I_2$	Crystals were grown from melt in platinum crucibles charged with $Cd_3(VO_4)_2$ and an excess of $CdBr_2$ or CdI_2. The crucibles were not perfectly closed against air.	Sudarsanan et al. (1977)
$Eu_{10}(PO_4)_6Cl_2$ $Eu_{10}(PO_4)_6F_2$	$Eu_3(PO_4)_2$, which was prepared by the reduction of $EuPO_4$ by metallic Eu, was mixed with $EuCl_2$ or EuF_2 in vitreosil tubes at 1000°C for 24 h.	Mayer et al. (1975)
$Eu_{10-x}Ba_x(PO_4)_6F_2$ ($0 \le x \le 10$) $Eu_{10-x}Ba_x(PO_4)_6Cl_2$ ($0 \le x \le 10$)	Solid solutions were prepared by reacting the fluoride and chloride apatites of Ba with that of Eu(II) at 1000°C for 24 h.	Mayer et al. (1975)
$Eu_{10-x}Ca_x(PO_4)_6F_2$ ($0 \le x \le 10$)	$Eu_3(PO_4)_2$, which was prepared by the reduction of $EuPO_4$ by metallic Eu, was mixed with $Ca(PO_4)_2$ and EuF_2, and the reactions performed in vitreosil tubes, evacuated and sealed off. This was fired at 1000°C for 24 h.	Mayer et al. (1975)
$Eu_xCa_{10-2x}Na_x(PO_4)_6F_2$ ($2 \le x \le 4$)	$Eu_3(PO_4)_2$ was prepared by heating $(NH_4)_2HPO_4$ and Eu_2O_3 at 500°C for 2–3 h, grinding the mixture, and reheating at 1100°C for 4-12 h. $Eu_3(PO_4)_2$, Na_3PO_4, $Ca_3(PO_4)_2$, CaF_2 were then mixed in stoichiometric ratios and fired at 1100°C for 4–24 h.	Mayer et al. (1974)
$K_2La_2Ba_6(PO_4)_6Z_2$ (Z = F, Cl)	Stoichiometric amounts of metal carbonates or oxides and diammonium hydrogen phosphate were mortared in acetone. The dried sample was placed in Pt or silica crucible and heated to 600–650°C, remixed and reheated to 950°C for 8 h.	Grisafe and Hummel (1970b)
$K_6Ca_4(SO_4)_6F_2$	Single crystals were obtained by firing stoichiometric mixtures of $CaSO_4$, K_2SO_4 and CaF_2 together with 3% excess CaF_2 and K_2SO_4 at 960°C for 17 h followed by quenching with water.	Fayos et al. (1987)
$K_8Na_2(VO_4)_6$	Stoichiometric quantities of sodium and potassium carbonates, and NH_4VO_3 were mixed and annealed at 600°C for 48 h.	Sirotinkin et al. (1989)

Table B1 continued.

Composition	*Synthesis Procedure*	*Reference*
$K_2La_2Ba_6(VO_4)_6Z_2$ (Z = F, Cl)	Stoichiometric amounts of metal carbonates or oxides and ammonium metavanadate were mortared in acetone. Dried sample was placed in Pt or silica crucible and heated to 600–650°C, remixed and reheated to 950°C for 8 h.	Grisafe and Hummel (1970b)
$La_{9.33}(GeO_4)_6O_2$	Stoichiometric amounts of La_2O_3 and GeO_2 were ground and sintered below 1100°C in air for 24 h followed by sintering at 1000–1250°C for 2 days.	Berastegui et al. (2002)
$La_2Ca_8(PO_4)_6O_2$ $La_2Sr_8(PO_4)_6O_2$	$CaCO_3$/ $SrCO_3$, La_2O_3 and $NH_4H_2PO_4$ mixed stoichiometrically and heated at 300–1100°C for a total of 42 h.	Buvaneswari and Varadaraju (2000)
$La_{9.33}(SiO_4)_6O_2$	Stoichiometric mixtures of La_2O_3 and SiO_2 were fired at 1200–1400°C for 12 h.	El Ouenzerfi (2003)
$La_{9.33+x/3}Si_{6-x}Ga_xO_2$ ($0 \le x \le 2$)	Stoichiometric amounts of La_2O_3, Ga_2O_3 and SiO_2 were ground and heated to 1300°C for 16 h. It was then reground and reheated to 1350°C for 16 h.	Sansom et al. (2004)
$Li_2La_2R_6(PO_4)_6F_2$ (R = Ca, Sr, Ba)	Stoichiometric amounts of metal carbonates or oxides and diammonium hydrogen phosphate were mortared in acetone. Dried sample was placed in Pt or silica crucible and heated to 600–650°C, remixed and reheated to 800 and 900°C each for 6 h.	Grisafe and Hummel (1970b)
$Li_2La_2Pb_6(PO_4)_6F_2$	Stoichiometric amounts of metal carbonates or oxides and diammonium hydrogen phosphate were mortared in acetone. Dried sample was placed in Pt or silica crucible and heated to 600–650°C, remixed and reheated to 850°C for 3 h.	Grisafe and Hummel (1970b)
$LiY_9(SiO_4)_6O_2$	Solid-state reaction of the respective oxides of lanthanides, Mg-nitrate, Li-carbonate, K-silicate and Na-silicate at 1050°C in air.	Ito (1968)
$LiY_9(SiO_4)_6O_2$	Single crystals were obtained by mixing Li_2CO_3, Y_2O_3 and SiO_2 (in proportions corresponding to the chemical composition of $LiYSi_2O_6$) and Li_2MoO_4 (high-temperature solvent 1:10 ratio). The mixture was placed in a Pt-crucible heated slowly to 1573 K, maintained at this temperature for 24 h and then cooled slowly (2 K/h) to 673 K.	Redhammer et al. (2003)

Table B1 continued.

Composition	*Synthesis Procedure*	*Reference*
$LiRE_9[SiO_4]_6O_2$ (RE = La→Lu)	Pellets containing the corresponding oxide/salt mixtures $7RE_2O_3{\cdot}9SiO_2$, $Li_2CO_3{\cdot}9RE_2O_3{\cdot}12SiO_2$ were annealed at different T in the range 1000–1900°C for 24 h after pre-sintering at 900°C.	Felsche (1972)
$Ln_xM_{10-2x}Na_x(PO_4)_6F_2$ (Ln = La, Pr, Nd, Sm, Eu, Dy, Er, Lu, and Y; M = Sr, and Ba)	Starting materials used were $SrHPO_4$/$BaHPO_4$, the fluorides of Sr and Ba, oxides and phosphates of the rare earths (Ln = La, Pr, Nd, Sm, Eu, Dy, Er, Lu, and Y) and Na_3PO_4. $LnPO_4$ were prepared by heating $(NH_4)_2HPO_4$ and Ln_2O_3 at 500°C for 2–3 h, and reheating at 1100°C for 4–12 h. Stoichiometric mixtures were sintered at 1100°C for 4–24 h.	Mayer et al. (1974)
$Mg_2La_8(SiO_4)_6O_2$ (Ln = La, Nd, Sm, Gd, Dy, Y, Er)	Solid-state reaction of the respective oxides of lanthanides, Mg-nitrate, Li-carbonate, K-silicate and Na-silicate at 1050°C in air.	Ito (1968)
$Mn_{10}(PO_4)_6Cl_2$	$Mn_3(PO_4)_2$ and $MnCl_2$ were mixed and put in a sealed silica tube at 1000°C for several hours.	Klement and Haselbeck (1965)
$Mn_2Ln_8(SiO_4)_6O_2$ (Ln = La, Nd, Sm, Gd, Dy, Y, Er)	High temperature solid-state reaction of stoichiometric mixtures made from respective oxides of lanthanides, chlorides or hydroxides of alkaline earth metals, Cd-sulfate, Mn-chloride, and K-silicate at 1200°C in air.	Ito (1968)
$Na_6Pb_4(BeF_4)_6F_2$ $Na_6Ca_4(BeF_4)_6F_2$	Stoichiometric amounts of Na_2BeF_4, $(NH_4)_2BeF_4$, PbF_2 and $CaCO_3$ in Pt-crucible were mixed and fired at 400–600°C in N atmosphere.	Engel (1978)
$NaLa_9(GeO_4)_6O_2$	Sintering Na_2CO_3, La_2O_3 and GeO_2 at 1173 K for 6 h and then at 1373 K for 1 h. Crystals grown by both high temperature flux and melt system.	Takahashi et al. (1998)
$Na_2RE_2Ca_6(PO_4)_6Cl_2$ (RE = La, Pr, Nd) $Na_2RE_2Ca_6(PO_4)_6F_2$ (RE = La, Pr, Nd) $Na_2La_2Sr_6(PO_4)_6F_2$ $Na_2La_2Sr_6(PO_4)_6Cl_2$ $Na_2La_2Ba_6(PO_4)_6Cl_2$ $Na_xLa_xBa_{10-x}(PO_4)_6F_2$ (x = 1, 2, 3)	Stoichiometric amounts of metal carbonates or oxides and diammonium hydrogen phosphate were mortared in acetone. Dried sample was placed in Pt or silica crucible and heated to 600–650°C, remixed and reheated to 1000°C for 8 h.	Grisafe and Hummel (1970b)

Table B1 continued.

Composition	*Synthesis Procedure*	*Reference*
$NaRE_9[SiO_4]$ (RE = La→Lu)	Pellets containing the corresponding oxide/salt mixtures $7RE_2O_3{\cdot}9SiO_2$ and $Na_2CO_3{\cdot}9RE_2O_3{\cdot}12SiO_2$ were annealed at different temperatures in the range of 1000–1900°C for 24 h after pre-sintering at 900°C.	Felsche (1972)
$Na_2RE_2Pb_6(PO_4)_6Z_2$ (RE = La, Pr, Nd; Z = F, Cl)	Stoichiometric amounts of metal carbonates or oxides and diammonium hydrogen phosphate were mortared in acetone. Dried sample was placed in Pt or silica crucible and heated to 600–650°C, remixed and reheated to 850°C for 6 h.	Grisafe and Hummel (1970b)
$(Na_{1.46}La_{8.55})(SiO_4)_6(F_{0.9}O_{0.11})$	Single crystals were grown by slow cooling and evaporation of a NaF flux at 1350°C to 900°C.	Hughes et al. (1992)
$NaLn_9(SiO_4)_6O_2$ (Ln = La, Y)	Solid-state reaction of the respective oxides of lanthanides, Mg-nitrate, Li-carbonate, K-silicate and Na-silicate at 1050°C in air.	Ito (1968)
$(Na,Th,La)_{10}(SiO_4)_6O_2$	Solid-state reaction of the respective oxides of lanthanides, Mg-nitrate, Li-carbonate, K-silicate and Na-silicate at 1050°C in air.	Ito (1968)
$NaY_9(SiO_4)_6O_2$	Crystals were obtained by mixing Na_2CO_3, Y_2O_3 and SiO_2 (in proportions to the chemical composition of $NaYSi_2O_6$) and Na_2MoO_4 (high-temperature solvent 1:10 ratio). The mixture was placed in a Pt-crucible heated slowly to 1473 K, maintained at this temperature for 24 h and then cooled slowly (2 K/h) to 673 K.	Redhammer et al. (2003)
$NaY_9(SiO_4)_6O_2$	Single crystals were grown by melting respective starting materials at 1748 K and quenched to yield a glass which was subsequently annealed in air at 1538 K for 12 h.	Gunawardane et al.(1982)
$Na_{6.35}Ca_{3.65}(SO_4)_6F_{1.65}$ $Na_{6.39}Ca_{3.61}(SO_4)_6Cl_{1.61}$	Stoichiometric mixtures of $CaSO_4{\cdot}2H_2O$, Na_2SO_4, CaF_2 or $CaCl_2$ were heated in covered corundum crucibles at 740°C for 10 h and subsequently cooled to 100°C with 4 °C/h.	Piotrowski et al. (2002a)
$Na_6Cd_4(SO_4)Cl_2$ $Na_6Pb_4(SO_4)_6Cl_2$	Solid state reaction of NaCl, Na_2SO_4, $CdSO_4/PbSO_4$ at 500°C.	Perret and Bouillet (1975)
$Na_6Pb_4(SO_4)_6F_2$	Stoichiometric mixtures of NaF_2 were heated with a pre-reacted intermediate at 570°C for 2 h. The intermediate was formed by sintering the starting metal carbonates/sulfates at 500–1000°C for 15 h.	Kreidler and Hummel (1970)

Table B1 continued.

Composition	*Synthesis Procedure*	*Reference*
$Nd_xCa_{10-2x}Na_x(PO_4)_6F_2$ ($2 \le x \le 4$)	$Nd_3(PO_4)_2$ was prepared by heating $(NH_4)_2HPO_4$ and Nd_2O_3 at 500°C for 2–3 h, grinding the mixture, and reheating at 1100°C for 4–12 h. $Nd_3(PO_4)_2$, Na_3PO_4, $Ca_3(PO_4)_2$ and CaF_2 were then mixed in stoichiometric ratios and fired at 1100°C for 4–24 h.	Mayer et al. (1974)
$Nd_{9.33}(SiO_4)_6O_2$	Stoichiometric mixture of Pr_6O_{11}, Sm_2O_3, and SiO_2 was calcined at 1200–1600°C for 10–20 h in air.	Higuchi et al. (2000)
$Nd_8Mn_2(SiO_4)_6O_2$	Single crystals prepared from stoichiometric sintering of Nd_2O_3, $MnCO_3$ and SiO_2 at 950°C for 48 h using a Bi_2O_3 flux in closed Cu-tubes.	Kluver and Mueller-Busch-baum (1995)
$Pb_6K_4(AsO_4)_4(SO_4)_2$	Solid-state reaction of stoichiometric mixture of $Pb_3(X^VO_4)_2$, $K_2X^{VI}O_4$ (X^V = As; X^{VI} = S) at 550–1000°C.	Schwarz (1967b)
$Pb_9K_2(AsO_4)_5(SiO_4)$	Solid-state reaction of a stoichiometric mixture of PbO, $NaNO_3$, $NH_4H_2AsO_4$ and SiO_2 was fired at 1000–1400°C.	Wondratschek (1963)
$Pb_{10}(CrO_4)_2(GeO_4)_4$	Solid-state reaction of PbO, GeO_2 and $PbCrO_4$ at 730–830°C.	Engel and Deppisch (1988)
$Pb_{10}(GeO_4)_2(VO_4)_2$	Yellow monocrystals were obtained from the melt of the starting materials.	Ivanov and Zavodnik (1989); Ivanov (1990)
$Pb_8Bi_2(PO_4)_4(SiO_4)_2$ $Pb_6Bi_2Tl(PO_4)_4(SiO_4)$	Solid-state reaction of a stoichiometric mixture of PbO, $NH_4H_2PO_4$, Bi_2O_3, SiO_2 (and Tl_2CO_3) was fired at 1000–1400°C.	Wondratschek (1963)
$Pb_6Ca_2Li_2(PO_4)_6$	Single crystals were grown by mixing Li_2CO_3, $(NH_4)_2HPO_4$, $CaCO_3$ and PbO between 800–900°C in air for 24 h.	Naddari et al. (2002)
$Pb_6Ca_2Na_2(PO_4)_6$	Na_2CO_3, $(NH_4)_2HPO_4$, $CaCO_3$ and PbO powders were stoichiometrically mixed and heated at 1073 K in air for 12 h and at 1173 K for 12 h.	Naddari et al. (2003)
$Pb_8K_2(PO_4)_6$	Powders and single crystals of $Pb_8K_2(PO_4)_6$ were prepared by mixing $Pb_3(PO_4)_2$, KPO_3, and PbO at 600–700°C for 48 h.	Mathew et al. (1980)

Table B1 continued.

Composition	*Synthesis Procedure*	*Reference*
$Pb_8La_2(PO_4)_6O_2$	Stoichiometric amounts of metal carbonates or oxides and diammonium hydrogen phosphate were mortared in acetone. Dried sample was placed in Pt or silica crucible and heated to 600–650°C, remixed and reheated at 1000°C for 10 h.	Grisafe and Hummel (1970b)
$Pb_{10}(PO_4)_{6-x}(VO_4)_xF_2$ (x = 1.2, 2.4, 3.6, 4.8, 6.0)	Starting mixtures were fired in air at 800°C for 4 h.	Grisafe and Hummel (1970a)
$Pb_{10-x}Nix(PO_4)_6F_2$ (x = 0.2, 0.5 and 1.0)	Stoichiometric amounts of metal carbonates or oxides and diammonium hydrogen phosphate and/or silicic acid were mixed and dried in covered crucibles and heated at 800°C for 4 h.	Grisafe and Hummel (1970b)
$Pb_6K_4(PO_4)_4(SO_4)_2$ $Pb_6K_4(PO_4)_4(SeO_4)_2$	Solid-state reaction of stoichiometric mixtures of $Pb_3(X^VO_4)_2$, $K_2X^{VI}O_4$ (X^V = P; X^{VI} = S, Se) at 550–1000°C.	Schwarz (1967b)
$Pb_9Na(PO_4)_5(SiO_4)$ $Pb_8Na_2(PO_4)_2(SiO_4)(SO_4)$	Solid-state reaction of a stoichiometric mixture of PbO, $NaNO_3$, $NH_4H_2PO_4$, SiO_2 (and $(NH_4)_2SO_4$) at 1000–1400°C.	Wondratschek (1963)
$Pb_{10-2x}BixNa_x(PO_4)_6F_2$ (x =1, 2, 3)	Stoichiometric amounts of $Pb_3(PO_4)_2$, $NH_4H_2PO_4$, NaF, $Na_3PO_4{\cdot}12H_2O$ and $Bi(NO_3)_3{\cdot}5H_2O$ were mixed together and heated in a closed Au- or Pt-tube at 900°C for 24–24 h.	Mayer and Semadja (1983)
$Pb_{10-2x}BixNa_x(PO_4)_6Cl_2$ (x =1, 2)	Stoichiometric amounts of $Pb_3(PO_4)_2$, $NH_4H_2PO_4$, NaCl, $Na_3PO_4{\cdot}12H_2O$ and $Bi(NO_3)_3{\cdot}5H_2O$ were mixed together and heated in closed Au or Pt tube at 600°C for 24–48 h.	Mayer and Semadja (1983)
$Pb_{10-(2x+2)}Na_{x+2}Bix(PO_4)_6$ (x = 0, 1, 2)	Stoichiometric amounts of $Pb_3(PO_4)_2$, $NH_4H_2PO_4$, $Na_3PO_4{\cdot}12H_2O$ and $Bi(NO_3)_3{\cdot}5H_2O$ were mixed together and heated in closed Au or Pt-tube at 900°C for 24–48 h.	Mayer and Semadja (1983)
$Pb_8La_2(SiO_4)_2(PO_4)_4Z_2$ (Z = F, Cl)	Stoichiometric amounts of metal carbonates or oxides and diammonium hydrogen phosphate and silicic acid were mortared in acetone. Dried sample was placed in Pt or silica crucible and heated to 600–650°C, remixed and reheated to 875°C for 12 h.	Grisafe and Hummel (1970b)

Table B1 continued.

Composition	*Synthesis Procedure*	*Reference*
$\square Pb_5Nd_4(SiO_4)_4(PO_4)_2\square_2$	Stoichiometric amounts of metal carbonates or oxides, diammonium hydrogen phosphate and silicic acid were mortared in acetone. Dried sample was placed in Pt or silica crucible and heated to 600–650°C, remixed and reheated at 1000°C for 12 h.	Grisafe and Hummel (1970b)
$Pb_6Bi_4(SiO_4)_6$	Solid-state reaction of a stoichiometric mixture of PbO, Bi_2O_3 and SiO_2 at 1000–1400°C.	Wondratschek (1963)
$Pb_4La_6(SiO_4)_6F_2$	Stoichiometric amounts of metal carbonates or oxides and silicic acid were mortared in acetone. Dried sample was placed in Pt or silica crucible and heated to 600–650°C, remixed and reheated to 950°C for 12 h.	Grisafe and Hummel (1970b)
$Pb_2Ln_8(SiO_4)_6O_2$ (Ln = La, Nd, Sm, Gd, Dy, Y)	Solid-state reaction of respective oxides of lanthanides, Pb-nitrate and K-silicate at 900°C in air.	Ito (1968)
$\square PbLa_8(SiO_4)_6F_2$	Stoichiometric amounts of metal carbonates or oxides and silicic acid were mortared in acetone. Dried sample was placed in Pt or silica crucible and heated to 600–650°C, remixed and reheated to 1000°C for 16 h.	Grisafe and Hummel (1970b)
$Pb_4Nd_6(SiO_4)_6O\square$	Stoichiometric amounts of metal carbonates or oxides and silicic acid were mixed. Dried sample was placed in Pt or silica crucible and heated to 600–650°C, remixed and reheated at 1000°C for 10 h.	Grisafe and Hummel (1970b)
$\square Pb_3RE_6(SiO_4)_6\square_2$ (RE = La, Pr, Nd)	Stoichiometric amounts of metal carbonates or oxides and silicic acid were mixed. Dried sample was placed in Pt or silica crucible and heated to 600–650°C, remixed and reheated at 1000°C for 10 h.	Grisafe and Hummel (1970b)
$Pb_{10}(SO_4)_2(GeO_4)_4$	Solid-state reaction of PbO, GeO_2 and $PbSO_4$ at 730–830°C.	Engel and Deppisch (1988)
$Pb_{10}(VO_4)_6Cl_2$	$Pb_3(VO_4)_2$ and $PbCl_2$ were mixed and fired at 550°C for 1 h.	Kreidler and Hummel (1970)
$Pb_{9.85}(VO_4)_6I_{1.7}$	Single crystal was grown from a melt of $Pb_3(VO_4)_2$ and PbI_2 in stoichiometric amounts at 773–1073 K.	Audubert et al. (1999)

Table B1 continued.

Composition	*Synthesis Procedure*	*Reference*
$Pb_8Na_2(VO_4)_6$	Stoichiometric quantities of Na_2CO_3, PbO and NH_4VO_3 were mixed and annealed at 600°C for 48 h.	Sirotinkin et al. (1989)
$(Pb_xCa_{10-x})(VO_4)_6F_{2\delta}$ $(0 < x < 9)$	CaO, PbO, V_2O_5 and CaF_2 were mixed in a stoichiometric ratio and fired at 1073 K for 4 weeks.	Dong and White (2004a)
$Pr_{9.33}(SiO_4)_6O_2$	Stoichiometric mixture of Pr_6O_{11} and SiO_2 was calcined at 1200–1600°C for 10–20 h in air.	Higuchi et al. (2000)
$R_4Nd_6(SiO_4)_6O\square$ (R = Ca, Sr, Ba)	Stoichiometric amounts of metal carbonates or oxides and silicic acid were mixed. Dried sample was placed in Pt or silica crucible and heated to 600–650°C, remixed and reheated to 1350°C for 16 h.	Grisafe and Hummel (1970b)
$\square R_5Nd_4(SiO_4)_4(PO_4)_2\square_2$ (R = Ca, Sr)	Stoichiometric amounts of metal carbonates or oxides, diammonium hydrogen phosphate and silicic acid were mortared in acetone. Dried sample was placed in Pt or silica crucible and heated to 600–650°C, remixed and reheated to 1350°C for 16 h.	Grisafe and Hummel (1970b)
$R_8La_2(SiO_4)_2(PO_4)_4Z_2$ (R = Ca, Sr, Ba ; Z = F, Cl)	Stoichiometric amounts of metal carbonates or oxides and diammonium hydrogen phosphate and silicic acid were mortared in acetone. Dried sample was placed in Pt or silica crucible and heated to 600–650°C, remixed and reheated to 1000°C for 18 h.	Grisafe and Hummel (1970b)
$R_4La_6(SiO_4)_6(PO_4)_4F_2$ (R = Ca, Sr, Ba)	Stoichiometric amounts of metal carbonates or oxides and diammonium hydrogen phosphate and silicic acid were mortared in acetone. Dried sample was placed in Pt or silica crucible and heated to 600–650°C, remixed and reheated to 1100°C for 12 h.	Grisafe and Hummel (1970b)
$\square RLa_8(SiO_4)_6F_2$ (R = Ca, Sr, Ba)	Stoichiometric amounts of metal carbonates or oxides and silicic acid were mixed. Dried sample was placed in Pt or silica crucible and heated to 600–650°C, remixed and reheated to 1000°C for 16h.	Grisafe and Hummel (1970b)
$\square R_3RE_6(SiO_4)_6\square_2$ (R= Ca, Sr, Ba ;RE = La, Pr, Nd)	Stoichiometric amounts of metal carbonates or oxides and silicic acid were mixed. Dried sample was placed in Pt crucible, heated to 600–650°C, remixed and reheated to 1350–1400°C for 36 h.	Grisafe and Hummel (1970b)

Table B1 continued.

Composition	*Synthesis Procedure*	*Reference*
$RE_{9.33}\square_{0.67}[SiO_4]_6O_2$ (RE= La→Lu)	Pellets containing the corresponding oxide/salt mixtures $7RE_20_3.9Si0_2$, were annealed at different temperatures in the range 1000–1900°C for 24 h after pre-sintering at 900°C.	Felsche (1972)
$\square_2RE_8(SiO_4)_6\square_2$ (RE = La, Pr, Nd, Sm, Eu)	Stoichiometric amounts of metal carbonates or oxides and silicic acid were mixed. Dried sample was placed in Pt or silica crucible and heated to 600–650°C, remixed and reheated to 1350–1400°C for 72 h.	Grisafe and Hummel (1970b)
$Sm_{10}Si_6N_2O_{24}$	Stoichiometric amounts of Sm_2O_3, Si_3N_4 and SiO_2 were heated at 1250°C for 36 h in a sealed Ni-tube sealed under a N_2 atmosphere.	Gaude et al. (1975)
$Sm_{9.33}(SiO_4)_6O_2$	Stoichiometric mixture of Sm_2O_3 and SiO_2 was calcined at 1200–1600°C for 10–20 h in air.	Higuchi et al. (2000)
$Sm_{10}(SiO_4)_6O_2$	Elemental Samarium was heated in an evacuated fused-silica tube at 1223 K for 4 days, cooled to 773 K over 4 days, and then cooled to room temperature over 1.5 days. Partial attack was observed on the walls of the silica tube, on which were deposited dark-red needle-shaped crystals.	Morgan et al. (2002)
$(Sm_8Cr_2)(SiO_4)_6N_2$	Powders were prepared by heating $8Sm_2O_3$–$2Cr_2O_3$–$1Si_3N_4$–$9SiO_2$ at 1250°C in a sealed nickel tube.	Maunaye et al. (1976)
$Sr_{10}(AsO_4)_4(SO_4)_2S_2$	Stoichiometric amounts of $SrSO_4$, As_2O_5 and SrS were heated at 1400°C under argon atmosphere for 3 h.	Schiff-Francois et al. (1979)
$Sr_{10}(CrO_4)_6Cl_2$	Stoichiometric mixture of $Sr(OH)_2{\cdot}8H_2O$, Cr_2O_3 and $SrCl_2{\cdot}.6H_2O$ was heated in air at 845°C for 5 h.	Mueller-Buschbaum and Sander (1978)
$Sr_{10}(CrO_4)_6Cl_2$	Stoichiometric mixture of $Sr(OH)_2{\cdot}8H_2O$, Cr_2O_3 and $SrCl_2{\cdot}6H_2O$ was heated in air at 845°C for 5 h, then in N_2 atmosphere at 920°C for 5 h.	Banks and Jaunarajs (1965)
$Sr_{10}(CrO_4)_6Cl_2$	$Sr_3(CrO_4)_2$ melts were put in an excess of $SrCl_2$ at 1000–1200°C in argon. The excess chlorides were extracted with H_2O.	Wilhelmi and Jonsson (1965)

Table B1 continued.

Composition	*Synthesis Procedure*	*Reference*
$Sr_{10}(CrO_4)_6F_2$	Stoichiometric mixture of $SrCO_3$, SrF_2 and Cr_2O_3 was heated in a corundum crucible at 1400 K in a dry N_2 atmosphere.	Herdtweck (1991)
$Sr_{10}(CrO_4)_6(OH)_2$	$Sr(OH)_2.8H_2O$ was mixed with Cr_2O_3 and heated in air at 845°C for 5 h, then in N_2 atmosphere at 920°C for a further 5 h.	Banks and Jaunarajs (1965)
$Sr_{10}(CrO_4)_3(SiO_4)_3F_2$	$PbCrO_4$, Pb_2SiO_4 and PbF_2 were stoichiometrically mixed and heated at 500–600°C for 24–48 h in a N_2 atmosphere.	Schwarz (1967a)
$Sr_{10}(PO_4)_6Br_2$	After a mixture of $SrHPO_4$ and $SrCO_3$ was fired for 0.5 h at 800°C, dehydrated $SrBr_2$ was added and the combined mixture fired for 90 min at 1180°C.	Nötzold and Wulff (1998)
$Sr_{10}(PO_4)_6Cl_2$	$SrHPO_4$, $SrCO_3$ and $SrCl_2{\cdot}6H_2O$ were mixed and heated at temperatures ranging from 25 to 1200°C for a few hours.	Nötzold et al. (1994)
$Sr_{10}(PO_4)_6Cl_2$	Single crystals were prepared by mixing $SrCl_2$ with $Sr_{10}(PO_4)_6OH_2$ and heating to 1280°C for 24 h.	Sudarsanan and Young (1974)
$Sr_{10}(PO_4)_6F_2$	$Sr_3(PO_4)_2$ and SrF_2 were mixed and fired for 0.5 h at 1230°C.	Kreidler and Hummel (1970)
$Sr_{10}(PO_4)_6CO_3$	A stream of CO_2 was added to strontium hydroxyapatite.	Nadal et al. (1971)
$Sr_{10}(PO_4)_6(CuO)_2$	$SrCO_3$, $NH_4H_2PO_4$ and CuO were mixed stoichiometrically and heated stepwise at 400, 600 and 850°C for 32 h, then pressed into pellets and annealed in air at 1100°C for 24 h.	Kazin et al. (2003)
$Sr_{10}(PO_4)_{6-x}(CrO_4)_xF_2$ (x = 1.2, 2.4, 3.6, 4.8, 6.0)	Starting mixtures were fired in a nitrogen atmosphere at 1000°C for 10 h.	Grisafe and Hummel (1970a)
$Sr_{10}(PO_4)_4(GeO_4)_2\square_2$	Solid-state reaction of stoichiometric amounts of $Sr_3(PO_4)_2$, Sr_2GeO_4 at 1200°C in air.	Schwarz (1968)
$Sr_{10}(PO_4)_6O_{0.9}(OH)_{0.2}\square_{0.9}$	Peroxiapatites are formed by thermal treatment of strontium hydroxyapatite at 900°C, under pure O_2. In order to eliminate traces of water, the stream of oxygen was allowed to run through a coil cooled by carbon dioxide-ice, before reaching the product.	Trombe and Montel (1978)

Table B1 continued.

Composition	*Synthesis Procedure*	*Reference*
$Sr_{10}(PO_4)_6F_2$ $Sr_8BiNa(PO_4)_6F_2$ $Sr_6Bi_2Na_2(PO_4)_6F_2$	Stoichiometric amounts of $SrCO_3$, $NH_4H_2PO_4$, SrF_2, (and $NaF/Na_3PO_4{\cdot}12H_2O/Bi(NO_3)_3{\cdot}5H_2O$) were mixed together and heated at 1100°C for 24–48 h in a closed Au- or Pt-crucible.	Mayer and Semadja (1983)
$Sr_{5-x-y}Ba_xEu_y(PO_4)_3Cl$ ($0 \le x \le 4.99$, $0 \le y \le 0.05$)	Starting mixtures were fired at 700°C and 1050°C in a N_2/H_2 atmosphere. H_3BO_3 with an excess of $SrCl_2$ and/or $BaCl_2$ as flux.	Nötzold and Wulff (1996)
$Sr_{10-x}Cox(PO_4)_6F_2$ ($x = 0.45$, 0.9, 1.8, and 2.7) $Sr_{10-x}Cox(PO_4)_6F_2$ ($x = 0.45$, 0.9, 1.8, and 2.7)	Stoichiometric amounts of metal carbonates or oxides and diammonium hydrogen phosphate and/or silicic acid were mixed and dried in sealed platinum crucibles and heated at 975°C for 8 h.	Grisafe and Hummel (1970b)
$Sr_{10-x}Eu_x(PO_4)_6F_2$ ($0.05 \le x \le 0.5$) $Sr_{10-x}Eu_x(PO_4)_6Br_2$ ($0.05 \le x \le 0.5$) $Sr_{10-x}Eu_x(PO_4)_6Cl_2$ ($0.05 \le x \le 0.5$)	$SrHPO_4$, $SrCO_3$, $NH_4F/NH_4Br/SrCl_2{\cdot}6H_2O$ and Eu_2O_3 were mixed proportionately and heated at 1100°C for 2 h in a reducing atmosphere (either N_2 plus H_2 or CO gas).	Kottaisamy et al. (1994)
$Sr_{9.402}Na_{0.209}(PO_4)_6B_{1.992}$	Crystals were grown in a Pt-crucible from a mixture of $(NH_4)_2HPO_4$, $SrCO_3$ and $Na_2B_4O_7{\cdot}10H_2O$ (2:3:6) at 1450°C.	Calvo et al. (1975)
$Sr_{10-x}Nix(PO_4)_6F_2$ ($x = 0.2$, 0.5 and 1.0)	Stoichiometric amounts of metal carbonates or oxides and diammonium hydrogen phosphate and/or silicic acid were mixed and heated at 800°C for 4 h in covered crucibles.	Grisafe and Hummel (1970b)
$Sr_{10}(P_{1-x}Mn_xO_4)_6F_2$ ($x = 0.01$, 0.1, 0.2, 0.3)	$SrCO_3$, NH_4HPO_4/Mn_2O_3, and NH_4F were stoichiometrically mixed, pressed into pellets and repeatedly heated for 12 h at 1250ºC in air (for $x \le 0.3$) and at 1000°C in an O_2 stream (for $x > 0.3$).	Dardenne et al. (1999)
$Sr_{10}(PO_4)_6O$	$Sr_{10}(PO_4)_6(OH)_2$ was heated at 1000°C for 2 days under pure O_2. To eliminate traces of H_2O, the stream of oxygen was run through a coil cooled by CO_2-ice before reaching the product.	Trombe and Montel (1978)
$Sr_{10}(PO_4)_{6-x}(VO_4)_xF_2$ ($x = 1.2$, 2.4, 3.6, 4.8, 6.0)	Starting mixtures were fired in air at 1000°C for 8 h.	Grisafe and Hummel (1970a)
$Sr_{9.92}Nd_{0.05}(PO_4)_6F_2$	Crystals were grown by the Czochralski method.	Corker (1995)

Table B1 continued.

Composition	*Synthesis Procedure*	*Reference*
$Sr_8RE_2(PO_4)_6O_2$ (RE = La, Pr, Nd)	Stoichiometric amounts of metal carbonates or oxides and diammonium hydrogen phosphate were mortared in acetone. Dried sample was placed in Pt or silica crucible and heated to 600–650°C, remixed and reheated at 1350°C for 72 h.	Grisafe and Hummel (1970b)
$Sr_{10}(ReO_5)_6X_2$ (X= Cl, Br, I)	Powders of respective alkaline-earth metaperrhenates $M(ReO_4)_2{\cdot}H_2O$ were annealed with an excess of corresponding alkaline-earth halides at 500–800°C.	Schriewer and Jeitschko (1993)
$Sr_{10}(SiO_4)_3(CrO_4)_3F_2$	Solid-state reaction of $SrCrO_4$, Sr_2SiO_4, SrF_2 (3:3:1) at 1000°C for 18 h in O_2.	Schwarz (1967a)
$Sr_2Ln_8(SiO_4)_6O_2$ (Ln =La, Nd, Sm, Gd, Dy, Y, Er)	Solid-state reaction of stoichiometric mixtures made from respective oxides of lanthanides, chlorides or hydroxides of alkaline earth metals, cadmium sulfate, manganese chloride, and potassium silicate at 1200°C in air.	Ito (1968)
$Sr_{10}(SO_4)_3(GeO_4)_3F_2$	Solid-state reaction of $SrSO_4$, Sr_2GeO_4, SrF_2 (3:3:1) at 1000°C for 23 h in air.	Schwarz (1967a)
$Sr_{10}(VO_4)_6F_2$	Crystals were grown by the Czochralski method.	Corker et al. (1995)
$Sr_{10}(VO_4)_6(CuO)_2$	Solid-state reactions of $SrCO_3$, V_2O_5 and CuO were carried out in air at 1173–1740 K for a total of 59 h.	Carrillo-Cabrera and von Schnering (1999)
$Sr_{10}(VO_4)_{6-x}(CrO_4)_xF_2$ (x = 1.2, 2.4, 3.6, 4.8, 6.0)	Starting mixtures were fired in nitrogen atmosphere at 1000°C for 10 h.	Grisafe and Hummel (1970a)
$Sr_{9.818}Nd_{0.122}(V_{0.972}O_4)_6F_{1.96}$	Crystals were grown by the Czochralski method.	Corker et al. (1995)
$Sr_{10}(V_{1-x}Mn_xO_4)_6F_2$ (x = 0.02)	$SrCO_3$, V_2O_5/Mn_2O_3, and NH_4F were mixed in stoichiometric amounts, pressed into pellets and heated for 12 h at 1000°C in an oxygen stream.	Dardenne et al. (1999)
$Y_xCa_{10-2x}Na_x(PO_4)_6F_2$ ($2 \le x \le 4$)	$Y_3(PO_4)_2$ was prepared by heating $(NH_4)_2HPO_4$ and Y_2O_3 at 500°C for 2–3 h, grinding the mixture, and reheating at 1100°C for 4–12 h. $Y_3(PO_4)_2$, Na_3PO_4, $Ca_3(PO_4)_2$, CaF_2 were then mixed in stoichiometric ratios and fired at 1100°C for 4–24 h.	Mayer et al. (1974)
$(Y_4Mg)Si_3O_{13}$ $(Y_{3.73}Mg_{1.31})Si_{3.05}O_{13}$ $(Y_{3.30}Mg_{1.33})Si_{3.36}O_{13}$	Stoichiometric amounts of yttria, silica and magnesia were mixed in ethanol using an agate mortar pestle and heated at 1200°C for 2 h. It was then reground, pelletized and heated at 1450–1550°C for several hours.	Suwa et al. (1968)

Table B2. Hydrothermal route for apatite synthesis.

Composition	*Synthesis Procedure*	*Reference*
$Ba_{10}(PO_4)_6(OH)_2$	Crystals were obtained from hydrothermal treatment of a Na_2O, BaO–Lu_2O_3, P_2O_5, H_2O mixture (500°C and P of ~1 kbar).	Bondareva and Malinovskii (1986)
$Ba_4Ln_6(SiO_4)_6(OH)_2$ (Ln = Nd, Sm, Gd, Dy)	Hydrothermal treatment at 650°C and 2 kbars of gels made from respective oxides of lanthanides, chlorides or hydroxides of alkaline earth metals, Cd-sulfate, Mn-chloride, K-silicate and Na-silicate.	Ito (1968)
$Ca_{10}(CrO_4)_6(OH)_2$	Hydrothermal treatment of $Ca_3(CrO_4)_2$ and CaO saturated steam pressures at 200–300°C for 2–5 days.	Banks and Jaunarajs (1965)
$Ca_{10}(PO_4)_6(OH)_2$	Hydrothermal reaction of $Ca(NO_3)_2$ and $(NH_4)_2HPO_4$ at 100–200°C, 1–2 Mpa.	Yoshimura and Suda (1994)
$Ca_{10}(PO_4)_6O$	$Ca_{10}(PO_4)_6(OH)_2$ was prepared under hydrothermal conditions at 523 K for 7 days using stoichiometric amounts of $Ca(NO_3)_2$ and $(NH_4)_2HPO_4$. The dehydration product under high vacuum and beam irradiation is $Ca_{10}(PO_4)_6O$.	Alberius-Henning et al. (1999b)
$Ca_2Na_2La_6Si_4P_2O_{24}(OH)_2$	Hydrothermal reaction of Ca-nitrate, Y-oxide, La-oxide, ammonium dihydrogen phosphate, K-silicate and Na-silicate at 550°C at 2 kbar.	Ito (1968)
$Ca_{9.50}(NH_4)_{0.10}(PO_4)_{5.05}(CO_3)_{0.95}(OH)_2$	$CaCO_3$ was reacted with $NH_4H_2PO_4$ solution under hydrothermal conditions at 250°C and 1 kbar for 10 days. A small amount of NH_4OH was added to the starting solution to bring the pH value to 9.	Ivanova et al. (2001)
$Ca_{9.42}Sr_{0.18}H_{0.8}(PO_4)_6(OH)_2$	Crystals were grown hydrothermally from Ca and Sr hydrogenphoshates by gradual heating from 493–603 K with 40.2 MPa at pH 2.	Kikuchi et al. (1994)
$CaY_9Si_5BO_{26}$	Hydrothermal reaction of Ca/Mn-nitrate, Y-oxide, K-silicate and boric acid at 1150°C, 1 bar.	Ito (1968)
$Ca_4La_6Si_4P_2O_{26}$	Hydrothermal reaction of Ca-nitrate, Y-oxide, ammonium dihydrogen phosphate and K-silicate at 1200°C, 1 bar.	Ito (1968)

Table B2 continued.

Composition	*Synthesis Procedure*	*Reference*
$Ca_4Ln_6(SiO_4)_6(OH)_2$ (Ln = La, Ce, Nd, Sm, Gd, Dy, Y, Er, Lu)	Hydrothermal treatment at 650°C and 2 kbars of gels made from respective oxides of lanthanides, chlorides or hydroxides of alkaline earth metals, Cd-sulfate, Mn-chloride, K-silicate and Na-silicate.	Ito (1968)
$Ca_4Na_2La_4Si_2P_4O_{24}(OH)_2$	Hydrothermal reaction of Ca-nitrate, Y-oxide, La-oxide, ammonium dihydrogen phosphate, potassium silicate and sodium silicate at 550°C, 2 kbar.	Ito (1968)
$Ca_4Y_6Si_4P_2O_{26}$ $Ca_6La_4Si_2P_4O_{26}$ $Ca_6Y_4Si_2P_4O_{26}$	Hydrothermal reaction of Ca-nitrate, Y-oxide, ammonium dihydrogen phosphate and potassium silicate at 1200°C, 1bar.	Ito (1968)
$Ca_6Y_4Si_4P_2O_{24}(OH)_2$	Hydrothermal reaction of Ca-nitrate, Y-oxide, La-oxide, ammonium dihydrogen phosphate, K-silicate and Na-silicate at 550°C, 2 kbar.	Ito (1968)
$Ca_8Y_2Si_2P_4O_{24}(OH)_2$	Hydrothermal reaction of calcium nitrate, yttrium oxide, ammonium dihydrogen phosphate and potassium silicate at 500°C, 2 kbar.	Ito (1968)
$Ca_{10}(VO_4)_6(OH)_2$	Oxide phases of vanadium underwent hydrothermal treatment.	Kutoglu (1974); Kutoglu and Schulien (1972)
$Cd_{10}(PO_4)_6(OH)_2$ ($P6_3$ - superstructure)	Hydrothermal treatment of $Cd_5H_2(PO_4)_4{\cdot}4H_2O$ at 200°C for 2 weeks in the pH range 2.5–7.0.	Hata and Marumo (1983)
$Cd_{10}(PO_4)_6(OH)_2$ ($P6_3/m$)	Hydrothermal reaction of $Cd_3H_2(PO_4)_4{\cdot}4H_2O$, controlled by H_3PO_4 solution, at 200°C for 2 weeks in pH range 2.8–3.3.	Hata et al. (1978)
$Cd_4La_6(SiO_4)_6(OH)_2$	Hydrothermal treatment at 650°C and 2 kbars of gels made from respective oxides of lanthanides, chlorides or hydroxides of alkaline earth metals, Cd-sulfate, Mn-chloride, K-silicate and Na-silicate.	Ito (1968)
$KNd_9(SiO_4)_6O_2$	Hydrothermal synthesis from stoichiometric amounts of K_2O, Nd_2O_3, SiO_2 and H_2O.	Pushcharovskii et al. (1978)
$Mg_4La_6(SiO_4)_6(OH)_2$	Hydrothermal treatment at 650°C and 2 kbars of gels made from respective oxides of lanthanides, chlorides or hydroxides of alkaline earth metals, Cd-sulfate, Mn-chloride, K-silicate and Na-silicate.	Ito (1968)

Table B2 continued.

Composition	*Synthesis Procedure*	*Reference*
$MgY_9Si_5BO_{26}$	Hydrothermal reaction of Ca/Mg-nitrate, Y-oxide, K-silicate and boric acid at 1150°C, 1 bar.	Ito (1968)
$Mn_{10}(PO_4)_6Cl_{1.8}(OH)_{0.2}$	Hydrothermal treatment of $Mn_3(PO_4)_2$, $MnCl_2{\cdot}4H_2O$ and H_2O mixture at 425°C.	Engel et al. (1975a)
$Mn_4Ln_6(SiO_4)_6(OH)_2$ (Ln = La, Nd, Sm, Gd, Dy, Y, Er)	Hydrothermal treatment at 650°C and 2 kbars of gels made from respective oxides of lanthanides, chlorides or hydroxides of alkaline earth metals, Cd-sulfate, Mn-chloride, K-silicate and Na-silicate.	Ito (1968)
$Na_2Ln_8(SiO_4)_6(OH)_2$ (Ln = La,Y)	Hydrothermal treatment at 650°C and 2 kbars of gels made from respective oxides of lanthanides, chlorides or hydroxides of alkaline earth metals, Cd-sulfate, Mn-chloride, K-silicate and Na-silicate.	Ito (1968)
$Na_{6.9}Ca_{3.1}(SO_4)_6OH_{1.1}$	Stoichiometric mixtures of Na_2SO_4, $CaSO_4$, and $Ca(OH)_2$ were heated under hydrothermal conditions and carried out at 250°C for 14 days.	Piotrowski et al. (2002b)
$Pb_{10}(AsO_4)_6(OH)_2$	Hydrothermal synthesis using stoichiometric powders of PbO and As_2O_5 with water at 425°C.	Engel (1970)
$\square Pb_9(PO_4)_6\square_2$	Hydrothermal reaction of $Pb(CH_3COO)_2{\cdot}3H_2O$ and K_2HPO_4 at 473 K for 1 week. This hydroxyapatite was fused at 1363 K and cooled to room temperature, yielding single crystals of $Pb_3(PO_4)_2$.	Hata et al. (1980)
$Pb_{10}(PO_4)_6F_2$	A mixture of PbO, P_2O_5, KF, H_2O was heated in a hydrothermal system at 1200°C.	Belokoneva et al. (1982)
$Pb_2^{4+}Pb_4^{2+}Y_4Si_6O_{26}$ $Pb_2^{4+}Pb_8^{2+}P_4Si_2O_{26}$ $Pb_3^{4+}Pb_5^{2+}Y_2Si_6O_{26}$ $Pb^{4+}Pb_3^{2+}Y_6Si_6O_{26}$	Hydrothermal reaction of Pb-nitrate, Y-oxide, K-silicate at 900°C, 1 bar.	Ito (1968)
$Pb_4Ln_6(SiO_4)_6(OH)_2$ (Ln = La, Ce, Nd, Sm, Gd, Dy, Y, Er, Lu)	Hydrothermal treatment at 450°C and 2 kbars of gels made from respective oxides of lanthanides, Pb-nitrate and K-silicate.	Ito (1968)

Table B2 continued.

Composition	*Synthesis Procedure*	*Reference*
$Pb_{10}(VO_4)_6(OH)_2$	PbO was firstly reacted with V_2O_5. Resulting $Pb_{10}(VO_4)_6O$ was treated hydrothermally with H_2O at 425°C.	Engel (1970)
$Sr_4Ln_6(SiO_4)_6(OH)_2$ (Ln = La, Ce, Nd, Sm, Gd, Dy, Y, Ho, Er, Lu)	Hydrothermal treatment at 650°C and 2 kbars of gels made from respective oxides of lanthanides, chlorides or hydroxides of alkaline earth metals, Cd-sulfate, Mn-chloride, K-silicate and Na-silicate.	Ito (1968)
$Y_{10}Si_4B_2O_{26}$	Hydrothermal reaction of Ca/Mg-nitrate, Y-oxide, K-silicate and boric acid at 1150°C, 1 bar.	Ito (1968)

Table B3. Soft chemistry route for apatite synthesis.

Composition	*Synthesis Procedure*	*Reference*
$Ca_{10}(PO_4)_6(OH)_2$	$Ca(OH)_2$ mixed with H_3PO_4 at 100°C/2 h then calcined at 850°C/24 h.	Bigi et al. (1991)
$Ca_{10}(PO_4)_6(OH)_2$	$Ca(NO_3)_2{\cdot}4H_2O$ and $(NH_4)_2HPO_4$ were dissolved in H_2O. 25 vol% NH_4OH solution was added and heated to 65°C for 1.5 h, then further heated to boiling for 2 h. Solution was then cooled and allowed to precipitate overnight.	Engin and Tas (2000)
$Ca_{10}(PO_4)_6(OH)_2$	$Ca(OH)_2$ and H_3PO_4 were mixed and aged for 3 days, with the final pH 7.5. Resulting hydroxyapatite suspension was freeze-dried and heated in air at 1473 K for 1 h.	Ikoma et al. (1999)
$Ca_{10}(PO_4)_6OH_{2-x}F_x$ $(0.02 \le x \le 2)$	Varying amounts of NaF was added to $Ca(NO_3)$ $4H_2O$ and $(NH_4)_2HPO_4$ with stirring in N_2 atmosphere. pH was adjusted using NH_4OH.	Bertoni et al. (1998)
$Ca_{10}(PO_4)_6(OH)_{2-x}F_x$ $(0 < x < 1)$	Ca-acetate and orthophosphoric acid were used as starting materials for Ca and P precursors. Na-fluoride (1, 3, 5 mol%) was added to the Ca precursor solution and precipitates filtered after 24 h of hydrolysis. Calcination was carried out at 900°C for 12 h.	Manjubala et al. (2001)

Table B3 continued.

Composition	*Synthesis Procedure*	*Reference*
$Ca_{10-x}Ag_x(PO_4)_6(OH)_{2-x}\square_x$ ($0 < x < 0.55$)	Apatite was precipitated from a solution of Na_2HPO_4 and a mixture of $Ca(NO_3)_2{\cdot}4H_2O$ and $AgNO_3$ in stoichiometric proportions.	Badrour et al. (1998)
$Ca_{10-x}Cd_x(PO_4)_6(OH)_2$ ($0 \le x \le 10$)	A double decomposition method is used in a boiling aqueous medium.	Nounah and Lacout (1993)
$Ca_{10-x}Cd_x(PO_4)_6(OH)_2$ ($x = 0.70, 0.73, 0.76$)	Ca-hydroxyapatite was introduced into Cd-nitrate solution of known concentrations. The solution was shaken at 20°C for 2 days.	JeanJean et al. (1996a,b)
$Ca_{10-x}Cd_x(PO_4)_6F_2$ ($0 \le x \le 6$)	A double decomposition method was used in a boiling aqueous medium in the presence of a large excess of fluoride ions.	Nounah and Lacout (1993)
$Ca_{9.1}Na_{0.5}(PO_4)_{4.7}(HPO_4)_{1.3}.2.9H_2O$ $Ca_{9.1}Na_{0.5}(PO_4)_6(OH)_{0.7}.4.2H_2O$ $Ca_{9.8}Na_{0.06}(PO_4)_{5.6}(HPO_4)_{0.4}.0.84H_2O$ $Ca_{9.8}Na_{0.06}(PO_4)_6(OH)_{1.6}.1.2H_2O$	Cd-nitrate was dissolved in H_2O and pH adjusted to 5 with HNO_3. Cal-hydroxyapatite was introduced and suspensions shaken at 20°C from 1 min to 10 days.	Mandjiny et al. (1998)
$Ca_{10-x}Na_{2x/3}(PO_4)_{6-x}(CO_3)_x(H_2O)_x(OH)_{2-x/3}$ ($0 \le x \le 3$)	Stoichiometric amounts of $Ca(CH_3COO)_2$ solution was added to Na_2HPO_4 and $NaHCO_3$ solutions at 95°C over 3 h. The solution was maintained at 91-95°C for 5 days, filtered, washed and dried at 80°C overnight.	Wilson et al. (2004)
$Ca_9Na_{0.5}(PO_4)_{4.5}(CO_3)_{1.5}(OH)_2$	An aqueous solution of $Ca(NO_3)_2{\cdot}4H_2O$ containing 0.027mol of Ca^{2+} ions was added dropwise (187.5 µl s^{-1}) using a peristaltic pump into a solution of ammonium phosphate and ammonium carbonate (0.018mol of PO_4^{3-} and 0.036 mol CO_3^{2-}) and kept at 80°C. The precipitate was filtered when hot, washed with distilled water and dried at 70°C for 15 h in oven and then heated at 400°C in air for 24 h.	El Feki et al. (1999)
$Ca_{10-x}Pb_x(PO_4)_6(OH)_2$ ($0 < x < 10$)	Solutions of $Ca(NO_3)_2{\cdot}4H_2O$ and $Pb(NO_3)_2$, were added separately to $(NH_4)_2HPO_4$ and mixed in stoichiometric amounts. The pH was adjusted by addition of NH_3.	Andres-Verges et al. (1983)
$[Ca_{10-x}Y_x](PO_4)_6[(OH)_{2-x}O_2$ ($x \le 2$)	Apatites were synthesized by aqueous solutions and sintered at 1000°C in a mulitte tube under steam flow.	Owada et al. (1989)

Table B3 continued.

Composition	*Synthesis Procedure*	*Reference*
$Ca_{10}(PO_4)_{6-x}(VO_4)_x(OH)_2$ (x = 0.3, 1.5, 3.0, 4.5, 6.0)	A double precipitation of phosphate and vanadate anions through stoichiometric addition of ammoniacal solutions of phosphate and vanadate to Ca-nitrate, refluxing near boiling point. The precipitate was dried at 100°C for 24 h and then calcined at 900°C for 3 h under inert atmosphere.	Boechat et al. (2000)
$Cd_{10-x}Pb_x(PO_4)_6(OH)_2$ ($0 \le x \le 10$)	A double decomposition method was used, where stoichiometric Cd-nitrate and Pb-acetate, were added to disodium hydrogen phosphate and heated at 100°C under nitrogen for 2 h. Ammonia was then added to maintain pH at 11 and the mixture filtered and dried at 110°C for 24 h.	Badroui et al. (2002a)
$Eu_{10}(AsO_4)_6(OH)_2$	Boiling $EuSO_4$ under Ar atmosphere with a solution containing an excess of Na_2HAsO_4 and NaOH. It was then filtered, washed with acetone and stored in dessicator to avoid oxidation. $EuSO_4$ was prepared by dissolving Eu_2O_3 in HCl and passing the solution through Jones reductor in to 8 N H_2SO_4.	Mayer et al. (1975)
$K_6Sn_4(SO_4)_6Cl_2$ $K_6Sn_4(SO_4)_6Br_2$	Acid solution of Zn(II) sulphate (33%) was mixed with H_2SO_4 (0.5 M) and an appropriate volume of a saturated solution of potassium salt in distilled water, and set aside at 5°C overnight. The crystals were recovered by filtration and vacuum drying.	Howie et al. (1973)
$K_6Sn_4(SO_4)_6Cl_2$ $K_6Sn_4(SO_4)_6Br_2$	Colorless acicular crystals were formed from a mixture of K-acetate and the appropriate Zn(II) halide, in the molar ratio 5:1, heated in the minimum amount of H_2SO_4 (2 mol dm^{-3}). The crystals were recovered by filtration and vacuum drying.	Donaldson and Grimes (1984)
$Mg_xCa_{10-x}(PO_4)_6(OH)_2$ ($1 \le x \le 3$)	$Ca(NO_3)$ $4H_2O$ and $Mg(NO_3)_2{\cdot}6H_2O$ were added in appropriate amounts to $(NH_4)_2HPO_4$ with stirring in N_2 atmosphere. pH was adjusted with NH_4OH.	Bigi et al. (1996)
$Pb_{10}(PO_4)_6(OH)_2$	Lead oxynitrate, $Pb_6O_5(NO_3)_2$, was treated with phosphoric acid at 100°C, and the pH raised with NH_4OH under heating and stirring for 2 h. Product was dried at 100°C for 15 h.	Kim et al. (2000); Robin and Theólier (1956); Newkirk and Hughes (1969); Bigi et al. (1991)
$Pb_{10}(PO_4)_6(OH)_2$	Hot aqueous solutions of Pb(II) acetate trihydrate was mixed with disodium hydrogenphosphate and dried at 100°C for 24 h.	Brückner et al. (1995)

Table B3 continued.

Composition	*Synthesis Procedure*	*Reference*
$Pb_{10}(PO_4)_6Br_2$ $Pb_{10}(PO_4)_6Cl_2$ $Pb_{10}(PO_4)_6F_2$	Pb-oxynitrate, was treated with phosphoric acid at 100°C, and pH raised with NH_3Br/NH_3Cl/NH_3F under heating and stirring for 2 h. Product was dried at 100°C for 15 h.	Kim et al. (2000); Robin and Theólier (1956); Newkirk and Hughes (1969); Bigi et al. (1991)
$Sr_{10}(AsO_4)_6CO_3$	The arsenate was prepared by double decomposition between aqueous solutions of ammonium arsenate and Sr-nitrate. The precipitate tri Sr-arsenate was dried and calcined at 900°C in CO_2 at 60 bars pressure.	Hitmi et al. (1986)
$Sr_{10}(PO_4)_6(OH)_2$	Hot $(NH_4)_2HPO_4$ was added to $Sr(NO_3)_2{\cdot}4H_2O$ and mixed. 25 vol% NH_4OH solution was added and heated to 95°C for 6 h. Solution was then cooled and allowed to precipitate overnight. The precipitate was filtered and dried at 110°C, then calcined at 950°C for 4 h.	Collin (1959)
$Sr_{10-x}Ca_x(PO_4)_6(OH)_2$ $(0 \le x \le 10)$	Ethylenediamine was added to required amounts of Ca- and Sr-nitrate. Hot ammonium phosphate solution was added dropwise. The precipitate and solution was maintained at 95°C for 6 h, and the precipitate allowed settling overnight. The supernatant was pulled off by an aspirator and washed until pH was 7. The precipitate was filtered, dried at 110°C, and heated to 950°C for 4 h.	Collin (1959)
$Sr_{9.5}Eu_{0.5}(PO_4)_6(OH)_2$	Sr-nitrate is mixed with Eu-nitrate solution (7.3 ml, 5 mol% Eu) and heated at 90°C. Ammonia was added until pH reaches 8. $(NH_4)_2HPO_4$ (2.04 g in 200 ml H_2O) is added drop-wise under stirring and the precipitate digested at 90°C for 6 h and dried at 110°C. It is then sintered at 950°C for 2 h in a reducing atmosphere.	Kottaisamy et al. (1994)
$Sr_{10-x}Pb_x(PO_4)_6(OH)_2$ $(0 < x < 10)$	A double decomposition method was used, where $(NH_4)H_2(PO_4)$ was added dropwise to stoichiometric mixture of $Pb(CH_3COO)_2.3H_2O$, $Sr(NO_3)_2$ and $(NH_4)H_2(PO_4)$ solutions and heated at boiling under N_2 stream. It was dried at 100°C for 12 h and calcined at 600°C for 4 h.	Badraoui et al. (2002b)

Table B4. Sol-gel route for apatite synthesis.

Composition	*Synthesis Procedure*	*Reference*
$Ca_{10}(PO_4)_6(OH)_2$	0.03 mol of triethylphosphite was hydrolyzed for 24 h with distilled water (molar ratio of water to phosphite is 8) under vigorous stirring. 0.05 mol of Ca-nitrate was dissolved first in 25 ml of distilled water and added dropwise into the hydrolyzed phosphite sol. The mixed sol solution was then continuously agitated for additional 3 min and kept static (aging) at 45°C and subjected to thermal treatment at 80°C for 16 h until a white, dried gel was obtained. The dried gels were further calcined at 200°C, 300°C for 2h and at 400°C, 500°C for 10 min (10°C/min).	Liu et al. (2002)
$La_{10}(Si_{3.96}B_{1.98}O_4)_6O_2$	A sol was prepared from $La(NO_3)_3{\cdot}6H_2O$, H_3BO_3, tetraethylorthosilicate, ethanol and glycerol (pH~0.5–1.0, adjusted by dil.HNO_3), converted to gel and heated in air at 1100°C for 3 h.	Mazza et al. (2000)
La10(SiO4)6O3 La9.33(SiO4)6O2	Sol-gel prepared from tetraethoxysilane (TEOS) and La_2O_3 and sintered at 800°C for 6 h.	Tao and Irvine (2001)
$La_{10}Si_4B_2O_{26}$	A sol was prepared from $La(NO_3)_3{\cdot}6H_2O$, H_3BO_3, tetraethylorthosilicate and glycerol; converted to gel and heated in air at 1100°C for 3 h.	Mazza et al. (2000)
$La_{9.33}Si_6O_{26}$	A sol was prepared from $La(NO_3)_3{\cdot}6H_2O$, H_3BO_3, tetraethylorthosilicate and glycerol; converted to gel and heated in air at 1100°C for 3 h.	Mazza et al. (2000)
$La_{9.66}Si_5BO_{26}$	A sol was prepared from $La(NO_3)_3{\cdot}6H_2O$, H_3BO_3, tetraethylorthosilicate and glycerol; converted to gel and heated in air at 1100°C for 3 h.	Mazza et al. (2000)
$Y_4(SiO_4)_3$ $Y_4Fe_{0.2}(SiO_4)_3O_{0.2}$	A gel was prepared from a sol prepared from an ethanol-water mixture of $Y(NO_3)_3{\cdot}5H_2O$, $Fe(NO_3)_3{\cdot}9H_2O$, tetraethylorthosilicate at 80°C and calcined at 1650–1700°C.	Parmentier et al. (2001)